5-2017

Cyclin B1 mediates the effect of UCHL1 in promoting cell cycle progression in uterine papillary serous carcinoma

Suet Ying Kwan

Recommended Citation

CYCLIN B1 MEDIATES THE EFFECT OF UCHL1 IN PROMOTING CELL CYCLE

PROGRESSION IN UTERINE PAPILLARY SEROUS CARCINOMA

by

Suet Ying Kwan, BSc

APPROVED:

_____
Karen H. Lu, M.D.
Advisory Professor

_____
Russell R. Broaddus, M.D., Ph.D.

_____
Wenliang Li, Ph.D.

_____
Samuel C. Mok, Ph.D.

_____
Kwong-Kwok Wong, Ph.D.

APPROVED:

_____

Dean, The University of Texas
MD Anderson Cancer Center UTHealth Graduate School of Biomedical Sciences

CYCLIN B1 MEDIATES THE EFFECT OF UCHL1 IN PROMOTING CELL CYCLE

PROGRESSION IN UTERINE PAPILLARY SEROUS CARCINOMA

A

DISSERTATION

Presented to the Faculty of

The University of Texas

MD Anderson Cancer Center UTHealth

Graduate School of Biomedical Sciences

in Partial Fulfillment

of the Requirements

for the Degree of

DOCTOR OF PHILOSOPHY

by

Suet Ying Kwan, BSc

Houston, Texas

May 2017

DEDICATION

This thesis is dedicated to my family: mum, dad, Suet Yan, Rita Urlanda and Benjy;

and to Christopher Nguyen, Lorraine Fung, Kenneth Hui and Daniel Man

for their unconditional friendship and support.

In loving memory of my grandparents.

ACKNOWLEDGEMENTS

I would like to express my sincere gratitude to my advisor Dr. Karen Lu for her expert advice and encouragement, and for reminding me to always look at the bigger picture. I would also like to thank the rest of my thesis committee, Dr. Samuel Mok, Dr. Russell Broaddus, Dr. Wenliang Li and Dr. Kwong Kwok Wong, for providing me with their precious insight. In particular, I am grateful to Dr. Samuel Mok for his guidance, which has been crucial for helping me navigate the intricacies of a dissertation; Dr. Russell Broaddus for asking the difficult yet imperative questions; Dr. Wenliang Li for allowing me to rotate in his laboratory in my first year in graduate school when I still had a lot to learn; and Dr. Kwong Kwok Wong for sparking my interest in the use of bioinformatics to answer important clinical questions.

I am thankful to Dr. Rosemarie Schmandt and Dr. Melinda Yates for their helpful feedback on the project. I would also like to thank the past and present members of my research group and neighboring labs, Joseph Celestino, Tri Nguyen, Dr. Qian Zhang, Dr. Connie Teodoro, Dr. YunYun Jiang, Dr. Suet Yan Kwan, Dr. Daisy Izaguirre, Dr. Yvonne Tsang, Dr. Chilam Au-Yeung, Dr. Tsz-Lun Yeung, and Dr. Jessica Bowser, for their expertise and endless support. My gratitude also goes to Stacie Gallardo, Lydia Soto, and Heetae Kim, who have allowed my research to progress smoothly; and Carol Johnston, the North Campus Flow Cytometry Core Facility and the shRNA and ORFeome Core for their services. Lastly, I would like to thank the staff members of GSBS for providing assistance, emotional support and free caffeine.

CYCLIN B1 MEDIATES THE EFFECT OF UCHL1 IN PROMOTING CELL CYCLE

PROGRESSION IN UTERINE PAPILLARY SEROUS CARCINOMA

Suet Ying Kwan, BSc

Advisory Professor: Karen H. Lu, M.D.

Uterine papillary serous carcinoma (UPSC) is an aggressive form of endometrial cancer with poor survival rates and a high risk of recurrence. The rarity of UPSC poses challenges to the discovery of novel targeted therapies. Therefore, the purpose of this dissertation was to identify novel therapeutic targets that could aid in the management of UPSC. To do so, we began with the relatively large cohort of UPSC cases in the TCGA data set, which was used to identify differentially expressed genes between UPSC and low-grade endometrioid endometrial carcinoma (EEC) and normal tissue.

We identified Ubiquitin Carboxyl-Terminal Hydrolase L1 (*UCHL1*) to be a gene of interest, as it was significantly upregulated in UPSC and correlated with poorer overall survival. These findings were validated through immunohistochemical analysis of an independent cohort of tumor samples. Due to its role as a deubiquitinating enzyme, we hypothesized that UCHL1 contributes to UPSC tumor progression by modulating the protein stability of target genes.

To test this hypothesis, we first examined the functional role of UCHL1 in UPSC progression. Subsequently, we found that UCHL1 silencing reduced cell proliferation *in vitro* and *in vivo*. The treatment of UPSC-bearing mice with the UCHL1-specific inhibitor LDN-57444 via intraperitoneal injection also reduced tumor growth and increased overall survival times.

Next, we found that the effect of UCHL1 on increased cell proliferation was due to its ability to stabilize cyclin B1 protein, an essential protein in mitotic progression. Specifically, we demonstrated that UCHL1 and cyclin B1 interact with each other in both the cytoplasm and nuclear space prior to mitosis. UCHL1 silencing increased the deubiquitination of cyclin B1, suggesting that UCHL1 counteracts the ubiquitination of cyclin B1 by the anaphase-promoting complex.

Accordingly, UCHL1 silencing slowed the progression of cells into mitosis. Taken together, our

findings indicate that UCHL1 impairs the degradation of cyclin B1, leading to uncontrolled cell cycle

progression. In summary, we have identified UCHL1 as a prognostic marker for UPSC and a viable

therapeutic target.

TABLE OF CONTENTS

LIST OF FIGURES

LIST OF TABLES

CHAPTER 1:

INTRODUCTION

ENDOMETRIAL CANCER

Endometrial cancer (EC) is the most common gynecologic malignancy in the United States. It is estimated that there will be 61,380 new cases and 10,920 deaths in the United States alone in 2017 [1]. Worldwide incidence of EC is steadily rising, with an average annual increase of 2.0% from 2008 to 2011 in the Unites States [2]. This increase is predicted to continue through the next few decades, with 122,000 expected number of cases in the Unites States by 2030 [3]. In spite of this, overall 5-year survival rates have not improved (87% from 1975 to 1977 versus 83% from 2005 to 2011) [2].

The increase in endometrial cancer incidence is attributed to multiple factors. For example, endometrial cancer risk is strongly associated with obesity [4], which is on the rise worldwide [5, 6]. Obesity leads to an imbalance in estrogen/progesterone levels; unopposed excess estrogen and insufficient progesterone is the primary risk factor for the majority of endometrial cancers [7]. Obesity is also linked to other hormonal abnormalities such as hyperinsulinemia, which further increase the risk of endometrial cancer. Other factors contributing to increasing incidence are the advancing age of the population, and a decrease in hormone therapy for menopausal women that counteracts estrogen to relieve symptoms [8].

Histopathological classification of endometrial cancer

Endometrial cancers are categorized into two subtypes based on their histopathology [9]. Type I malignancies comprise approximately 80% of all endometrial cancer cases and are characterized by endometrioid histologic features, low histological grade, limited myometrial spread, and an overall favorable prognosis. In contrast, type II malignancies, which include grade 3 endometrioid carcinoma, uterine papillary serous carcinoma (UPSC) and clear cell carcinoma, are associated with presentation at an older age and a poorer prognosis.

UPSC is the most common non-endometrioid endometrial carcinoma and the most aggressive type II variant: although comprising less than 10% of all endometrial cancers, it accounts for

approximately 40% of deaths [10, 11]. Poor survival outcome is partly due to the high percentage of cases diagnosed at stage III and VI (41.3% as opposed to 13.9% of EEC) [12]. While the risk of metastasis and recurrence in type I cancers can be predicted from the tumor size, grade, and depth of myometrial invasion [13-16], such factors are not predictive for UPSC [17-19]. Disease stage and the presence of extra-uterine disease are risk factors for overall survival [20, 21], but both early- and late-stage UPSC behave aggressively and show a tendency towards lymphovascular invasion, intraperitoneal disease and extra-abdominal spread [22-24].

Pathogenesis of endometrial cancer

The pathogenesis of EEC has been well characterized (Figure 1). Positive estrogen or progestin receptor status is common, and patients present at a relatively young age. Unopposed estrogen stimulation and an early loss of the tumor suppressor *PTEN* give rise to complex atypical hyperplasia, the precursor to most type I carcinomas [25-27]. Mutations in *CTNNB1* and *KRAS*, as well as microsatellite instability arising from defects in DNA mismatch repair, are common additional features [28-30].

In contrast, patients with UPSC present at an older age, and the majority are postmenopausal [31]; therefore, these tumors frequently arise from a background of atrophic endometrium [32, 33] and the majority are estrogen and/or progesterone receptor-negative [34]. Endometrial glandular dysplasia (EmGD) has been described as the putative precancerous lesion [35, 36], with an intermediate level of morphological atypia between normal endometrium and UPSC [37], followed by the development of minimally invasive endometrial intraepithelial carcinoma (EIC), characterized by cells closely resembling UPSC but confined to the surface endometrium [38]. Histological studies have observed frequent co-occurrence of EmGD and EIC with UPSC [20, 21, 32, 39].

TP53 mutation occurs early in carcinogenesis – approximately 80%-90% of UPSCs carry a mutation [40-42]. While type I tumors tend to be diploid, aneuploidy is observed in the majority of

UPSC cases [43, 44]. *HER2/neu* amplification or overexpression has been reported in 15% to 62% of UPSC cases and is correlated with advanced stage and poorer progression-free and overall survival [45-52]. There is also frequent loss of the cell adhesion molecule E-cadherin [53, 54] and upregulation of the tight junction proteins claudin-3 and -4 [55], which may explain the enhanced ability of UPSC tumor cells to detach from the primary tumor. The cell cycle-related proteins, p16 and cyclin E1, are also overexpressed [42, 56-59].

It has been suggested that a minority of non-endometrioid carcinomas can also arise from dedifferentiation of high grade endometrioid carcinomas, due to microsatellite instability and accumulation of mutations such as *TP53* [60-62]. This would explain the frequent presentation of mixed endometrioid and serous histology, and why mixed cases more commonly present in a background of hyperplastic endometrium, while pure serous carcinomas present more in atrophic or weakly proliferative endometrium [33, 63]. Further studies are needed to establish this possible alternative pathogenesis.

Several independent studies have compared the survival outcomes of grade 3 EEC and UPSC, with some finding equally poor survival between the two for both early- and late-stage patients [64, 65], while others have observed poorer survival in UPSC [66-69]. Of these, the largest study of 2316 grade 3 EEC and 1473 UPSC patients indicated a statistically significant difference in survival at each stage [68], suggesting that grade 3 endometrioid carcinomas is of intermediate risk between grade 1 and 2 endometrioid carcinomas and non-endometrioid carcinomas.
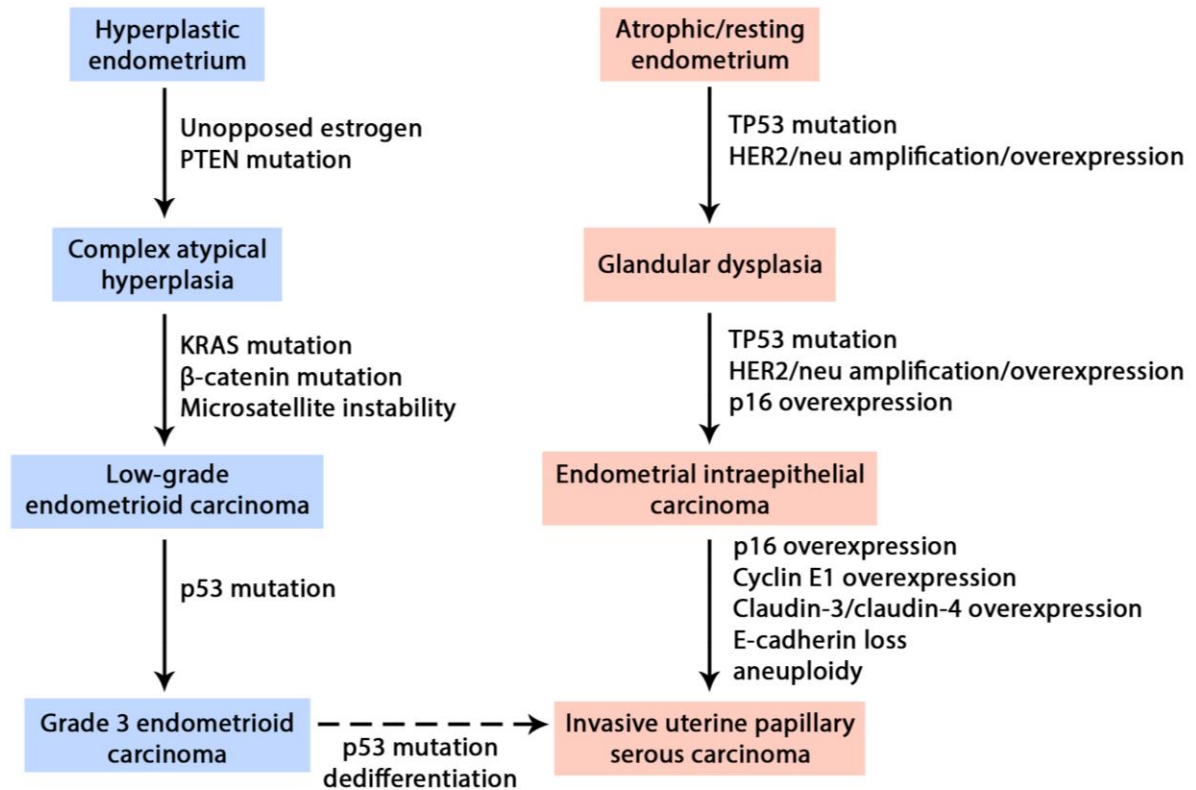
Figure 1. Molecular pathogenesis of endometrioid and serous endometrial cancer.

Molecular classification of endometrial cancer

Classification of endometrial cancer based on histology and cell morphology is unreliable for high-grade tumors, and EEC tumors can be misdiagnosed as papillary serous and vice versa, especially when an ECC tumor displays villoglandular morphology [70, 71]. Therefore, extra criteria for determining risk would improve reliability.

The Nature paper published by the TCGA network on endometrial cancer [72] suggested categorizing endometrial tumors into four novel groups, based on integrated mutational analysis using exome sequencing, copy number alterations, and microsatellite instability (MSI) status of 248 tumor/normal sample pairs: i) POLE ultramutated; ii) MSI-high hypermutated; iii) copy-number low (endometrioid); and iv) copy-number high (serous-like). Unsupervised clustering of multiplatform data (RNA, protein, microRNA expression and DNA methylation) was reported to correlate well with

these four groups. Overall survival outcomes were different between the groups: the POLE ultramutated group exhibited the best prognosis for progression-free survival, while the copy-number high group had the worst prognosis. In accordance with previously established data, the majority of UPSC cases were in the copy-number high group, along with a quarter of all grade 3 EEC. Tumors in this group were characterized by a high number of somatic copy number alterations, as well as a low mutation rate and high frequency of *TP53* mutation. Only two serous cases (pure or mixed) were not in this group, one of which underwent histological re-review based on its *TP53* wild-type status, *KRAS* mutation and high mutation rate, and was subsequently reclassified as grade 3 EEC.

The endometrial tumors were also clustered by individual data sets (mRNA expression, protein expression, miRNA expression and DNA methylation). These results further indicated that a subset of grade 3 EEC are molecularly similar to UPSC, and also revealed that these serous/serous-like tumors have frequent dysregulation of cell cycle proteins, particularly those involved in mitosis. Of note, unsupervised clustering of mRNA profiles identified mitotic, hormonal and immunoreactive clusters. 92% of pure/mixed UPSC tumors and 56% of grade 3 EEC were in the mitotic cluster, characterized by dysregulation of cell cycle genes such as *CCNB2* and *CDK1*, as well as *TP53* mutation. Furthermore, supervised analysis of reverse phase protein array (RPPA) profiles showed that the mitotic cluster had high protein expression of cyclin B1, cyclin E1 and CDK1.

UPSC patterns of spread

The UPSC precursor, endometrial intraepithelial carcinoma (EIC), is characterized by the transformation of atrophic surface epithelium and underlying glands into malignant cells. These cells exhibit anaplastic nuclei and morphology resembling invasive UPSC, but stromal or myometrial invasion is absent [32]. In spite of this, EIC may still be associated with extra-uterine tumor: a study of 40 EIC or UPSC with invasion limited to the endometrium found presence of extra-uterine disease

in 45% of cases [73], while another found extra-uterine disease in 6 out of 9 patients with EIC [74], highlighting the need for complete surgical staging.

As the risk of extra-uterine disease is predicted by depth of myometrial invasion in EEC but not in UPSC, it indicates that the two subtypes have distinct mechanisms of spread. While EEC tumors commonly reach the peritoneal cavity by invasion through the myometrium, UPSC tumors are more likely to metastasize via the lymphatic/vascular system [18]. One additional mechanism of spread for UPSC is the retrograde passage of exfoliated tumor cells through the fallopian tubes and subsequent dissemination into the peritoneal cavity. In one study of patients with extra-uterine disease, 48% did not have lymphatic/vascular disease and 33% did not have myometrial invasion [75]. Ayeni et al. [76] also observed a significantly lower frequency of positive peritoneal cytology in patients with tubal ligation versus those without (18.8% versus 45%), along with an improved overall survival rate in late stage patients with tubal ligation. However, positive peritoneal cytology was not completely eradicated, indicating that EIC and UPSC can utilize one of several methods of spread to reach the peritoneal cavity.

Current treatment strategies for endometrial cancer

Current treatment for endometrial cancer varies according to stage of disease and histological type. Complete surgical staging is recommended for all tumor types, comprising total hysterectomy, bilateral salpingo-oophorectomy and lymph node dissection [77]. Omentectomy and peritoneal washings are also performed, especially in patients with UPSC. Optimal cytoreduction (≤ 1 cm maximum diameter of residual tumor nodules) has been shown to increase median overall survival in both early and late stage UPSC patients [78]. In one study of 79 patients with late stage UPSC, the median overall survival time was 39 months for patients with optimal cytoreduction, which was significantly higher than the 12 month survival time of patients with suboptimal cytoreduction [79].

In addition, since stage and presence of extra-uterine disease are the main prognostic factors, complete surgical staging has prognostic benefit.

Following cytoreductive surgery, adjuvant chemotherapy and radiation therapy is considered for patients with endometrial cancer [80]. Carboplatin and paclitaxel is considered the optimal chemotherapy regimen [81, 82]. Adjuvant chemotherapy has not been proven to improve outcomes for patients with early stage EEC; adjuvant radiation may reduce the risk of local recurrence but does not improve overall survival. Therefore, only 28% of patients with stage I and II disease received adjuvant chemotherapy and/or radiation treatment in 2013 [83]. In contrast, 66% of patients with late stage EEC received adjuvant therapy. Chemotherapy improves outcomes for patients with late-stage EEC and is considered the optimal chemotherapy regimen; the addition of radiation therapy confers additional benefit.

If any UPSC component is present in the tumor, patients are considered high risk regardless of presence of extrauterine disease and are therefore recommended for adjuvant therapy. After cytoreductive surgery, adjuvant chemotherapy appears to confer a survival advantage in both early and late-stage UPSC, while the benefit of adjuvant radiotherapy has yet to be established [10, 78].

With current therapy, the 5-year disease-specific survival for UPSC is approximately 74% and 33% for early-stage and late-stage patients [68, 84], compared to 77% in grade 3 EEC and 89% in low-grade EEC [85]. In light of the poor patient survival rates and high recurrence rates, the development of targeted therapies specific to UPSC pathway aberrations would likely aid in its management [10, 17, 78].

Development of targeted therapeutic strategies for UPSC

Several targets are being investigated for UPSC treatment. For example, due to the frequent amplification and overexpression of HER2/neu in UPSC and other cancers, various anti-HER2 therapies have been developed. The first developed anti-HER2 monoclonal antibody, trastuzumab,

recruits natural killer cells to tumor cells and initiates antibody-dependent cell-mediated cytotoxicity, leading to cell cycle arrest and reduced angiogenesis [86, 87]. Its use has been FDA-approved for HER2-positive breast cancer in combination with chemotherapy, where risk of death in patients with metastatic disease was reduced by 20% in a phase III trial. The EGFR and HER2 small molecule inhibitor, afatinib, has also been FDA-approved as first-line treatment of metastatic non-small cell lung cancer with activating EGFR mutations [88, 89], and as second-line treatment for advanced squamous cell carcinoma of the lung that has progressed after platinum-based chemotherapy [90, 91].

Several clinical trials are investigating the benefit of using HER2 inhibitors in endometrial cancer. Afatinib is being investigated in a phase II study (NCT02491099 [92]) for persistent or recurrent UPSC confirmed to have HER2/neu overexpression. A GOG phase II study (GOG-181B [93]) tested the use of trastuzumab as a single agent in advanced or recurrent HER2-positive endometrial carcinoma. No significant activity was observed; however, only 33 patients were accrued for the trial. Of these, only a third had UPSC histology, and *HER2/neu* amplification was only confirmed in 55.5% of patients [94]. A current phase II study (NCT01367002 [95]) is investigating the use of carboplatin and paclitaxel with or without trastuzumab in patients with advanced or recurrent UPSC confirmed to have HER2 overexpression through IHC or fluorescence in situ hybridization.

The differences in initial clinical response to trastuzumab observed in clinical trials with endometrial cancer compared to breast cancer may be explained by a significantly higher frequency of expression of the p95HER2 mutant in UPSC and grade 3 EEC than in breast cancer cases [96]. This truncated form of the protein lacks the trastuzumab-binding extracellular domain; subsequently, its expression has been associated with trastuzumab resistance and poor progression-free and overall survival in breast cancer [97, 98].

As the PIK3CA/AKT/mTOR pathway is downstream of HER2 and *PIK3CA* mutation/amplification has been observed in almost half of all UPSC cases [42], several phase I and II clinical trials are ongoing to evaluate the use of PI3KCA, AKT, and mTOR inhibitors in *HER2/neu-*

amplified UPSC [99]. Concurrent inhibition of this pathway may reduce the resistance to HER2-targeted therapies [100].

The pro-angiogenic vascular endothelial growth factor (*VEGF*) has been associated with increasing grade, lymphovascular invasion and spread, and p53 upregulation in endometrial cancer [101, 102]. A previous phase II study (GOG-229E [103]) investigated the use of Bevacizumab, the monoclonal antibody against all isoforms of VEGF, in recurrent endometrial cancer. 27% of the patients had UPSC tumors. A 13.5% clinical response rate was observed following 3 weeks of treatment: 100% and 50% of those with complete and partial response were patients with UPSC. Currently, another phase II study (NCT00513786 [104]) is evaluating the benefit of Bevacizumab in combination with carboplatin and paclitaxel in advanced endometrial cancer.

THE UBIQUITIN-PROTEASOME SYSTEM

The ubiquitin-proteasome system is the major intracellular pathway through which normal and misfolded/damaged proteins are degraded. Proteins are marked for degradation by the tagging of ubiquitin, a highly conserved 76 amino-acid polypeptide; substrate proteins are then recognized by the 26S proteasome. The process of ubiquitin conjugation to substrates is facilitated by the sequential activity of three major classes of enzymes. Ubiquitin-activating enzymes (E1) activate ubiquitin in an ATP-dependent process before transferring it to ubiquitin-conjugating enzymes (E2). Ubiquitin-protein ligases (E3) recognize substrate proteins both normal and damaged, and catalyzes the transfer of activated ubiquitin from the E2 enzyme to a lysine residue or N-terminal amino acid of the target protein [105-107].

Ubiquitin can be conjugated as a monomer or form polyubiquitin chains; all seven lysine residues in the ubiquitin protein can be conjugated to additional ubiquitin molecules, forming different polyubiquitin chains that lead to distinct downstream effects [108]. A chain of four or more ubiquitin proteins linked via lysine 48 (K48-linked ubiquitination) is the canonical signal for

degradation by the 26S proteasome. In addition to polyubiquitination, proteins can also be conjugated to a single ubiquitin (monoubiquitination) or be conjugated to multiple ubiquitin monomers at different sites within the protein (multi-monoubiquitination) [109].

As the conjugation of ubiquitin is reversible, ubiquitin can be removed from substrates, or processed from ubiquitin chains back to monomers by deubiquitinating enzymes (DUBs). In addition, small ubiquitin adducts form during the ubiquitination and proteolytic process, which must be processed by DUBs for free ubiquitin monomers to be regenerated [110]. At least 98 DUBs exist, which are classified into six groups [111].

UCHL1

UCHL1 is a DUB in the family of ubiquitin carboxyl-terminal hydrolases [112]. The most understood function of UCHL1 in normal tissue is what characterizes members of its protein family: the enzyme acts specifically on ubiquitin adducts, where its deubiquitinating activity catalyzes hydrolysis at the C-terminal glycine of ubiquitin to generate ubiquitin monomers [113-115].

UCHL1 is one of the most abundant proteins in the brain, where it is localized to neurons and ganglia. In rats, UCHL1 mRNA and protein was detected strongly in the brain and moderately in the testis by northern blot and western blot analysis; expression was undetectable in the heart, lung, pancreas, small intestine, liver, kidney, spleen and adrenal tissue [116]. In human, rat and guinea-pig samples, protein expression as detected by polyclonal and monoclonal antibodies was restricted to the central and peripheral nervous system, and in neuroendocrine cells. In addition, strong to moderate immunohistochemical staining was observed in the germ cells and Leydig cells of the testis; in the ova, theca externa and theca interna of the corpus luteum; and in the distal tubular epithelium and calyceal urothelium [117]. UCHL1 protein was undetectable in the pancreas. Expression is predominantly in the cytoplasm, with 5% of UCHL1-positive neuronal and neuroendocrine cells displaying concurrent nuclear staining.

Dysregulation of UCHL1 in cancer

The *UCHL1* I93M mutation is associated with Parkinson's disease [118, 119]. However, mutations or amplification have not been reported in cancer; rather, UCHL1 expression is dysregulated mainly by aberrant gene methylation in a multitude of cancer types. Hypermethylation and/or loss of expression of UCHL1 has been reported in melanoma, colorectal, prostate, breast, ovarian, nasopharyngeal and renal cancer [120-127]. On the other hand, UCHL1 hypomethylation and/or overexpression has been observed in lymphoma, gallbladder, prostate, gastric and colorectal cancer compared to normal tissue [128-132].

A long non-coding UCHL1 antisense RNA (*UCHL1-AS1*) has been identified, which initiates transcription within the second intron of *UCHL1* and overlaps with the beginning of the *UCHL1* gene [133]. *UCHL1-AS1* increases UCHL1 protein levels by promoting translation of its mRNA. In mouse tissue, *UCHL1-AS1* was highly expressed in the ventral mid-brain and moderately expressed in the colon, but expression was negative in other normal tissue samples, including the uterus.

Promotion of UCHL1 degradation by the E3-ubiquitin ligase, parkin (*PARK2*), has also been reported. Parkin mediated the K63-linked ubiquitination of UCHL1 both *in vitro* and in mouse brain extracts, leading to degradation through the autophagy-lysosome pathway [134]. The *PARK2* gene is frequently inactivated in various cancers through mutation, copy number loss, or promoter hypermethylation [135]; however, its protein levels have not been studied in endometrial cancer.

Both oncogenic and tumor suppressive functions of UCHL1 have been described. Correlation of high expression with worse clinical prognosis in melanoma, breast, lung, colorectal and pancreatic ductal tumors suggests that UCHL1 contributes to tumorigenesis in these cancers [136-139]. In addition, transgenic mice overexpressing UCHL1 under a ubiquitous promoter developed spontaneous lipomas, lymphomas and lung adenomas [132]. Further studies in immortalized human B-cell lines showed that UCHL1 promoted cell proliferation and survival. UCHL1 also promoted cell invasion and motility in lung, colorectal and prostate cancer cells [140, 141]. Expression of wild-type UCHL1, but not the catalytically inactive UCHL1 C90S mutant, induced epithelial-to-mesenchymal

transition of normal prostatic epithelial cells [142], and UCHL1 silencing in a metastatic prostate cancer cell line induced mesenchymal-to-epithelial transition.

Contrary to reports of UCHL1 overexpression, silencing of UCHL1 has also been reported in breast carcinoma cell lines compared to normal breast tissue and mammary epithelial cells [143], nasopharyngeal carcinoma cells [124], melanoma [120], and prostate cancer [127]. However, the role of UCHL1 as a potential tumor suppressor has mostly been inferred from *in vitro* studies, rather than by survival analysis of patient data. *In vitro*, reintroduction of UCHL1 suppressed colony formation and proliferation through G0/G1 cell cycle arrest and apoptosis in breast carcinoma cell lines [143]; induced apoptosis in nasopharyngeal cell lines [124]; and reduced proliferation and anchorage-independent growth in prostate cancer cells [127].

Mechanisms of action of UCHL1

The mechanism through which UCHL1 contributes to tumorigenesis has not been fully elucidated. As a deubiquitinating enzyme from the family of ubiquitin carboxyl-terminal hydrolases [112], UCHL1 has been shown to affect the stability and/or activity of various cancer-related proteins involved in cell cycle regulation, as well as cancer cell survival, metastasis and angiogenesis.

UCHL1 and cell cycle progression

UCHL1 is able to regulate cell cycle progression by its interaction with p53, p27 and cyclin-dependent kinases. In the *TP53*-mutant nasopharyngeal cell lines HONE1 and CNE1, UCHL1 formed a complex with p53, MDM2 and p14^{ARF}. Furthermore, it stabilized p53 protein by reducing the ubiquitination of p53 and p14^{ARF} while increasing the ubiquitination of MDM2, the E3 ubiquitin ligase that typically targets p53 for degradation [124]. Overexpression of UCHL1 also induced p53 protein accumulation and loss of MDM2 in *TP53*-mutant MDA-MB-231 [143], LNCaP [127], and HCT116 cells [144], as well as the *TP53*-wild type EC109 cells [144, 145].

In a yeast two-hybrid screen, JAB1 was identified as an interacting partner of UCHL1 [112]. UCHL1 was found to colocalize and interact with JAB1, enhancing its role in promoting nuclear export and degradation of p27. p27 is a tumor suppressor that inhibits cell cycle progression by preventing the activation of cyclin E-CDK2, cyclin D-CDK4 and cyclin D-CDK6 [146]. UCHL1 has also been shown to interact with and promote the kinase activity of CDK1, 4, and 5 in a cell-free assay independent of its deubiquitinating activity; this effect was also seen for CDK4 and CDK5 *in vitro*, as UCHL1 overexpression increased phosphorylation of their downstream targets, Rb and p27 [147].

Other putative UCHL1 targets

UCHL1 may enhance tumor cell survival by regulating the mTOR/AKT pathway. UCHL1 promoted AKT signaling by downregulating its negative regulator PHLPP1 [132]. In addition, PHLPP1 translation is enhanced by mTOR complex 1 activity; UCHL1 destabilized mTOR complex 1, suggesting another mechanism through which AKT signaling is promoted [148].

UCHL1 may also promote angiogenesis: Goto et al. demonstrated a direct interaction between UCHL1 and HIF-1α, preventing VHL-mediated ubiquitination of HIF-1α and promoting HIF-1α protein stability [139].

The effect of UCHL1 on metastasis may be mediated through stabilization of the oncogenic transcription factor, β-catenin, and promotion of β-catenin/TCF signaling [149, 150]. Interestingly, UCHL1 transcription was in turn upregulated by β-catenin/TCF signaling to form a positive feedback loop [149].

In addition to its deubuiquitinating enzyme activity, an ATP-independent E3 ligase ability has been observed *in vitro*, which is dependent on UCHL1 dimerization [151]. Indeed, Karim et al. found that UCHL1 increased K63-linked ubiquitination of TRAF6 [152].

CELL CYCLE PROGRESSION

        In eukaryotic cells, the cell cycle is a unidirectional chain of processes that allows cells to

grow and duplicate. The cycle is split into two major stages: mitosis, where a cell divides into two

daughter cells, and interphase, which allows cells to grow and prepare for the next cycle of cell

division [153-155] (Figure 2).
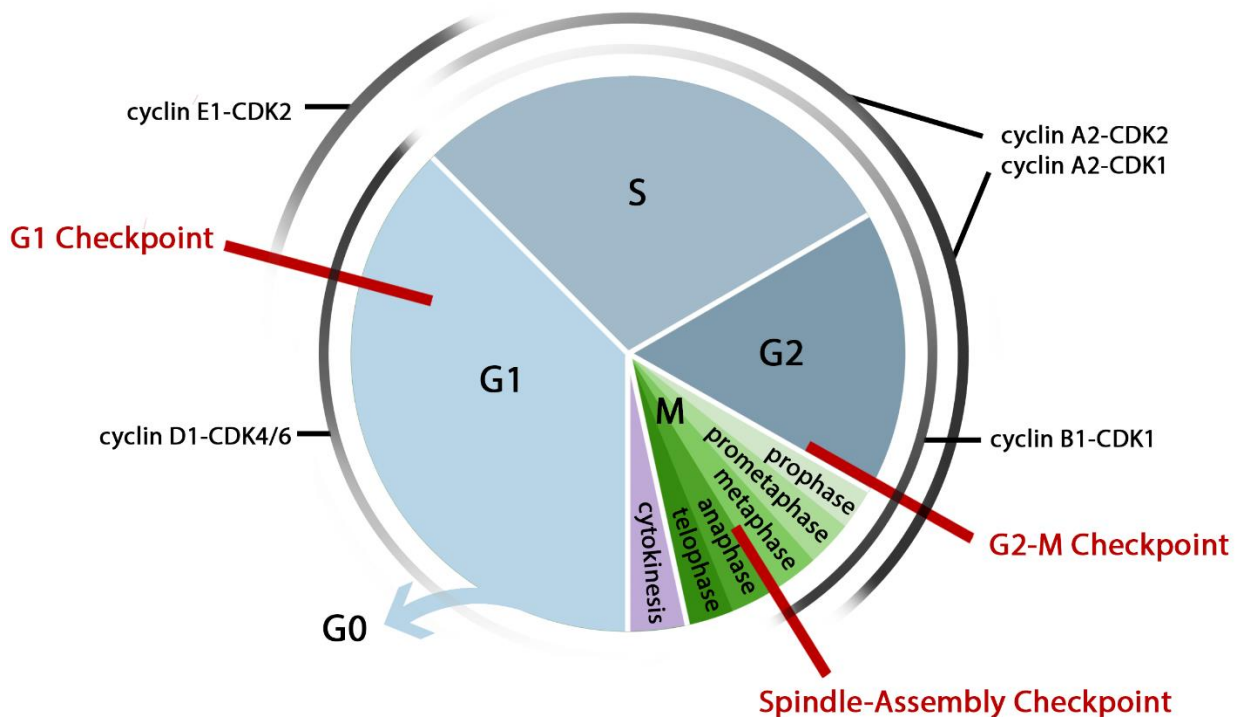
Figure 2. Overview of the cell cycle.

Progression through the cell cycle is mediated by the cyclin-dependent kinases (CDKs), which are

activated when bound to their cyclin partners. While CDK protein levels are constant, transcription

and protein stability of the cyclin proteins fluctuate through the cycle. The G1 and G2-M checkpoints

ensure that cells with DNA damage do not divide, while the spindle-assembly checkpoint delays the

onset of anaphase until the chromatid pairs are correctly aligned. Intensity of black lines indicate the

protein levels of the cyclin proteins and the relative activity level of cyclin-CDK pairs.

Interphase is composed of a DNA synthesis stage (S) sandwiched between two gap phases (G1 and G2). Following the end of mitosis, cells enter G1 and undergo a period of growth and increase in cellular content to prepare for the next round of DNA synthesis. In S phase, cells synthesize a copy of the entire DNA contents in the nucleus, resulting in identical sister chromatids that are bound together by the centromere [156]. The centrosome, i.e. microtubule organizing center, is also replicated. Finally, G2 phase allows cells to prepare for mitosis. Cells may also exit the cell cycle and enter a resting state known as G0 phase, where they do not prepare for DNA replication or cell division.

Following G2, cells enter mitosis, which includes prophase, prometaphase, metaphase, anaphase and telophase (Figure 3). During prophase, the chromosomes condense [157, 158]. In addition, the two centrosomes migrate to opposite ends of the cell. At the end of prophase, nuclear envelope breakdown is initiated in higher eukaryotes and continues into prometaphase. This begins with the disassembly of nuclear pore complexes [159, 160], which is followed by depolymerization of the nuclear lamina [161] and the absorption of the nuclear envelope proteins into the endoplasmic reticulum [162, 163]. Loss of the nuclear envelope allows the microtubules to extend from the cytoplasmic centrosomes into the nuclear space and attach to the kinetochores located on the chromosomal centromeres.

By metaphase, the chromosomes reach their most compact configuration and complete their alignment along the equatorial plane, i.e. metaphase plate, of the cell. In anaphase, the sister chromatids separate, and the daughter chromosomes are pulled towards the centrosomes at opposite ends of the cell [164, 165]. Finally, during telophase, a new nuclear envelope forms around each set of daughter chromosomes, which begin to de-condense. Telophase is followed by cytokinesis, which divides the cytoplasm and completes the division of a cell into two daughter cells [166].
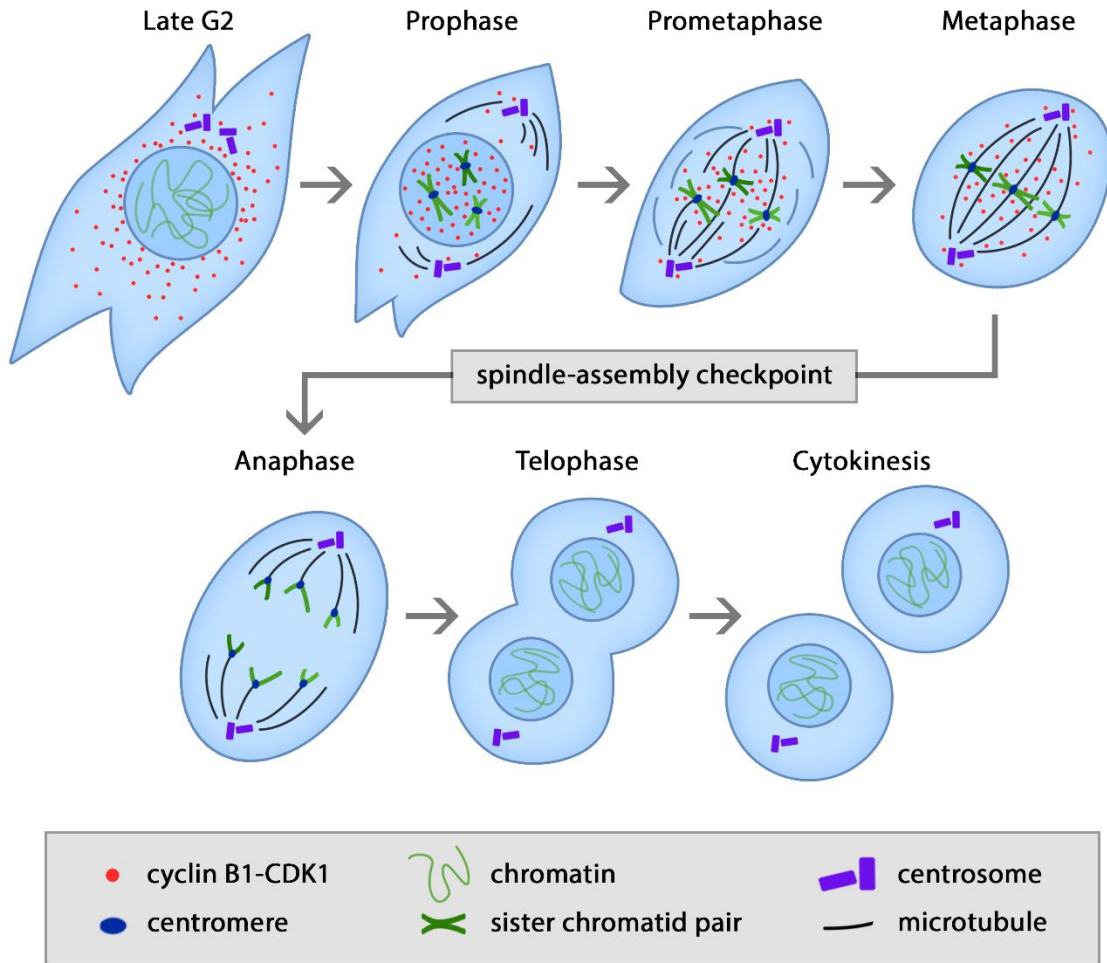
Figure 3. Overview of mitosis and cyclin B1-CDK1 localization.

For simplicity, only three chromatid pairs are shown.

Cyclin-dependent kinases (CDK) and cyclins

The progression of cells through the cell cycle is regulated by cyclin/CDK protein complexes [155]. CDKs are serine/threonine protein kinases that are constitutively expressed, but only activated at specific points in the cell cycle. Their regulation involves phosphorylation at several sites; activation also requires binding to their specific cyclin protein partners. Unlike CDKs, cyclin protein expression fluctuates throughout the cell cycle.

When cells exit the G_0 resting phase and enter G_1, CDK4 and CDK6 complex with cyclin D1 to phosphorylate the transcriptional repressor retinoblastoma protein (pRb), thus releasing the E2F transcription factor from repression [155, 167]. In late G_1, cyclin E-CDK2 continues phosphorylation of Rb, promoting G1-S transition. Cyclin A2-CDK2 is required for DNA replication in the S phase, while cyclin A2-CDK1 promotes G2-M transition. Lastly, cyclin B1 and CDK1 complex together to form the mitosis-promoting factor and induce mitosis [153, 154].

Cyclin B homologs

Five cyclin B homologs have been identified in higher eukaryotes, three of which (B1, B2, B3) are found in human tissue [168]. Of these, cyclin B1 (*CCNB1*) and cyclin B2 (*CCNB2*) exhibit protein accumulation prior to mitosis and interact with CDK1 [169, 170]. Cyclin B1-CDK1 is predominantly cytoplasmic during interphase and translocates to the nucleus at the onset of mitosis. On the other hand, cyclin B2-CDK1 colocalizes to the golgi apparatus during both interphase and mitosis. Thus, Cyclin B1-CDK1 is the primary regulator of mitosis, promoting chromosome condensation, microtubule reorganization and solubilization of the nuclear lamina, while Cyclin B2-CDK1 is restricted to promoting disassembly of the golgi apparatus during mitosis [171]. Indeed, mice that are *CCNB1*-null die *in utero*, while *CCNB2*-null mice develop normally and are fertile, despite a smaller body weight compared to wild-type mice [172]. Cyclin B3 (*CCNB3*) is a nuclear protein that is restricted to the testis in adult tissue; it does not interact with CDK1, but binds to CDK2 and is able to activate it, albeit poorly [173].

Regulation of cyclin B1 expression

Cyclin B1 undergoes strict temporal regulation (Figure 3). Cyclin B1 mRNA transcription and stability increases from late S phase onwards, leading to accumulation of cyclin B1 protein [174].

During metaphase, cyclin B1 is targeted for proteasomal degradation due to ubiquitination by the anaphase-promoting complex (APC), a multi-unit E3 ligase. Cyclin B1 is therefore rapidly degraded during the metaphase-anaphase transition, immediately after inactivation of the spindle-assembly checkpoint, returning to a low level of protein expression that persists through G1 [175-177]. Following mitosis, the APC continues ubiquitination of cyclin B1 throughout G1; APC activity ceases in S phase due to phosphorylation by cyclin A1-CDK2 and interaction with the inhibitory regulator Emi1 [178, 179]. K48-linked ubiquitination is the canonical signal for degradation, but *in vitro* studies have shown that cyclin B1 can also be targeted for degradation by K11- and K63-linked ubiquitination, as well as multi-monoubiquitination [180-182].

CDK1 regulation

CDK1 activity is regulated by cyclin A and cyclin B binding, and by the balance of inhibitory and activating phosphorylation at specific amino acid residues. CDKs and cyclins bind to each other via the cyclin box, a motif found in cyclin proteins that also serves to activate their CDK binding partner [183, 184]. Starting at late S and early G2, cyclin B1 begins binding to CDK1 as it is increasingly expressed, causing accumulation of cyclin B1-CDK1 complexes. These complexes are kept mostly inactive until the end of G2 through phosphorylation at a threonine and tyrosine residue (Thr14/Tyr15), both of which are within the ATP-binding site [183]. Phosphorylation of these residues therefore prevent binding with ATP. WEE1 resides in the nucleus and phosphorylates CDK1 at Tyr15 [185, 186], while MYT1 resides in the golgi apparatus and endoplasmic reticulum, and phosphorylates both residues [187, 188]. In turn, CDK1 is activated when CDC25 phosphatase gradually removes the phosphorylation at these sites [189].

Activation of CDK1 also requires phosphorylation at threonine 161 (Thr161) by the CDK-activating kinase (CAK). This only occurs after CDK1 complexes with cyclin B1, as Thr161 is

inaccessible to CAK when CDK1 is monomeric; binding of CDK1 to cyclin B leads to conformational changes that exposes Thr161 to CAK [190-192].

With gradual Thr14/Tyr15 dephosphorylation and Thr161 phosphorylation through the G2 phase, cyclin B1-CDK1 complexes reach a low level of activation by the end of G_2. In *Xenopus* egg extracts, approximately 30% of maximum activity is reached by the end of G2 [170, 193, 194]. Accumulation of cyclin B1-complex levels reach a threshold by this point, initiating a positive-feedback loop that inhibits WEE1 and activates CDC25, leading to rapid and complete activation of CDK1 [195].

Spatial regulation of the cyclin B1-CDK1 complex

During interphase, the inactive cyclin B1-CDK1 complex is continuously shuttled between the nucleus and cytoplasm; however, it is predominantly cytoplasmic, due to a higher rate of nuclear export versus import. This is mediated by the cytoplasmic retention signal (CRS) within the cyclin B1 protein, which in turn contains the nuclear export signal (NES). The NES binds to the nuclear transport receptor CRM1, which mediates export of the cyclin B1-CDK1 complex from the nucleus [196, 197]. During early prophase the affinity of CRM1 for cyclin B1 is greatly reduced when the CRS is phosphorylated, reducing the export rate and leading to accumulation in the nucleus prior to breakdown of the nuclear envelope [176, 198, 199].

There is partial retention of activated cyclin B1-CDK1 in the cytoplasm, which is needed to activate mitotic processes such as microtubule rearrangement and nuclear envelope breakdown [200]. In addition, a fraction of cyclin B1-CDK1 complexes translocates to the mitochondrial matrix to upregulate mitochondrial respiration and oxygen consumption. The resulting increase in ATP provides the energy needed for successful G2-M transition [201]. It has been suggested that this continuous shuttling between the nucleus and cytoplasm allows the complex to receive integrated input from both compartments before determining if mitosis should proceed; for example, this can

ensure that the DNA damage checkpoint is passed in the nucleus before the complex is activated and initiates mitotic processes in the cytoplasm [196].

After nuclear envelope breakdown, cyclin B1-CDK1 continues its association with the centrosomes [202], microtubules [169] and chromosomes [177, 203] in prometaphase before the spindle-assembly checkpoint is activated at the metaphase-anaphase transition and cyclin B1 is degraded.

Targets of CDK1

CDK1 substrates are phosphorylated at a minimal or complete consensus motif, S/T-P or S/T-P-X-R/K [204, 205]. Over 300 CDK1 substrates have been identified in budding yeast [206]. However, information on CDK1 substrates in vertebrates is currently less established. Recent attempts have been made to identify CDK1 substrates in vertebrates; for example, Petrone et al. performed phosphoproteomics analysis of HeLa cells, using the CDK1 inhibitors Flavopiridol and RO-3306. Inhibition of CDK1 reduced the phosphorylation of 1215 phosphopeptides on 551 proteins [207]. Using chicken DT40 cells, Ohta et al. isolated and analyzed proteins associated with chromosomes during mitosis, identifying 4274 phosphorylation sites in 1014 proteins, of which 350 sites underwent mitosis-specific phosphorylation [208]. Nevertheless, it is known that CDK1 regulates proteins that mediate mitotic processes; the main known substrates in vertebrates will be discussed.

CDK1 initiates chromosome condensation and assembly by phosphorylation of Histone H1 [209, 210], Kif4A [208], topoisomerase IIα [208] and the condensin I [211] and II complexes [212]. To induce nuclear envelope breakdown, CDK1 phosphorylates nucleoporins [213-216], leading to disassembly of nuclear pore complexes and complete nuclear envelope breakdown. In addition, phosphorylation of lamin proteins causes disassembly of the nuclear lamin [217, 218].

Mitosis requires dramatic rearrangement of the microtubule network, leading to formation of the mitotic spindle. CDK1 regulates microtubule dynamics by phosphorylation of tubulin, which polymerizes to form microtubules [219], and microtubule- and tubulin- binding proteins [220, 221]. For correct kinetochore-microtubule attachment [203], CDK1 phosphorylates kinetochore-associated proteins during prometaphase, required for correct attachment of the microtubules to kinetochores. One such substrate at the unattached kinetochore is Cdc20; phosphorylated protein is bound to Mad2, maintaining the APC in an inactive state. After successful attachment, cyclin B1-CDK1 is displaced, Mad2 is no longer bound and is subsequently able to activate the APC [203].

CDK1 also promotes inactivation of itself at the end of mitosis by phosphorylating APC-related proteins, as will be discussed later.

Cyclin B1 in cancer

While normal cells are cyclin B1-negative outside of mitosis, unscheduled cyclin B1 expression in interphase has been observed in cancer cells lines and tumor samples [222-225]; overexpression of cyclin B1 has also been associated with increased mitosis, grade and poorer disease-free survival and/or overall survival [226-228]. In endometrioid endometrial cancer, cyclin B1 levels – as measured by immunohistochemistry – were associated with increasing grade, stage and poorer cancer-specific survival by univariate analysis [229].

The overexpression and/or unscheduled expression of cyclin B1 may be due to aberrant cyclin B1 expression or impaired degradation. Uncontrolled cyclin B1 expression can disrupt control of cell cycle progression. For example, the injection of cyclin B1 mRNA into *Xenopus* embryos shortens the cell cycle length [194, 230]. In addition, overexpression of cyclin B1 can allow cells to overcome G2-M arrest [231, 232].

Cell cycle checkpoints

Several checkpoints exist in the cell cycle (Figure 2). The G_1 checkpoint ensures that there is an absence of DNA damage before proceeding to S phase; the major signaling pathway is the ATM/ATR-CHK2/CHK1-p53/MDM2/p21 pathway [233]. Detection of DNA damage by the ATM and ATR kinases leads to phosphorylation of p53 and its stabilization and accumulation. p53 then induces the transcriptional activity of p21, which inhibits cyclin E-CDK2 to induces G1 arrest [234, 235].

The G2-M checkpoint also ensures that there is no DNA damage or errors in chromosome replication before cells enter mitosis. p38 and/or ATM/ATR are activated [236], which ultimately results in inactivation of cyclin B1-CDK1 activity through several possible mechanisms [235, 237, 238] and G2 arrest. While p53 is critical for mediating the G1 checkpoint, its role in G2-M checkpoint activation is redundant [239, 240]. However, p53 has been shown to suppress cyclin B1 transcription during induction of the G2-M checkpoint, as the cyclin B1 promoter contains a p53-sensitive region [231, 241].

The spindle-assembly checkpoint ensures that the duplicated sister chromatids are equally divided and correctly attached to the microtubules before anaphase begins [242]. As discussed later, the checkpoint proteins maintain APC^{Cdc20} in an inactive state until the checkpoint is overcome. Defects in the spindle-assembly checkpoint contribute to chromosomal instability and subsequent aneuploidy.

The anaphase-promoting complex

The two major E3 ubiquitin ligases involved in the cell cycle are the Skp1/Cullin/F-box (SCF) and the anaphase-promoting complex (APC) [243, 244]. While the SCF acts mostly during the G1-S and G2-M transitions, the APC is essential for metaphase-anaphase transition. The APC is

nuclear during interphase; during mitosis, it associates with proteins involved in the spindle-assembly checkpoint located at kinetochores [245].

The APC complex is composed of at least 11 subunits in vertebrates [244]. Of these, the cullin subunit APC2 and RING-H2 domain subunit APC11 make up the catalytic core, while Cdc20 and Cdh1 are the co-activator subunits that interact with APC at different times in the cycle to mediate the recognition and binding of different substrates [243]. There are several amino acid motifs recognized by the Cdc20 and/or Cdh1. For example, the "destruction box" (D box), first identified in cyclin B proteins [246], is recognized by both Cdc20 and Cdh1, while the KEN box is only recognized by Cdh1 [247]. The KEN box is also present in Cdc20, as Cdc20 itself is an APC[Cdh1] substrate.

The APC is regulated by phosphorylation and interaction with several inhibitor proteins, which ensure that the APC is kept inactive until the spindle-assembly checkpoint is overcome [248]. Therefore, cyclin A and B are allowed to accumulate until the onset of mitosis, and the separation of sister chromatids during APC-induced anaphase does not occur until the chromosomes are correctly aligned at the metaphase plate and attached to the microtubules.

The inhibition of free APC by Emi1 begins in S phase, which prevents APC-Cdc20 binding [249]. Emi1 is degraded during prophase, but inhibition is continued by RASSFA1 until late prometaphase [250]. At this point, the APC is phosphorylated by CDK1 and polo-like kinase 1 [251-253], allowing Cdc20 to bind and initiate degradation of cyclin A and Nek2A at the prometaphase-metaphase transition. These substrates have a modified D box that allows them to be degraded while the APC[Cdc20] is otherwise kept inactive by Mad2-Bub3-BubR1, a complex of spindle-assembly checkpoint proteins associated with unattached kinetochores [243, 254, 255]. Once the chromatids are correctly aligned and checkpoint is overcome, the Mad2-Bub3-BubR1 complex dissociates from APC[Cdc20] to allow its full activity, initiating degradation of cyclin B at the metaphase-anaphase transition [255]. APC[Cdc20] is then ubiquitinated and inactivated by APC[Cdh1], which continues degradation of cyclin B1 from late anaphase through to G1. Finally, Cdh1 is phosphorylated by

24

CDK1 at the G1-S transition [251], causing it to dissociate from APC, which is once again inhibited by Emi1. Cdh1 remains phosphorylated until the next round of mitosis, when APC[Cdc20] begins cyclin B degradation and CDK1 activity begins to decrease [243].

SUMMARY OF PROBLEMS AND HYPOTHESIS

There are currently 7000 or fewer new cases of UPSC per year in the US; as a result, few therapeutic targets are being studied. In addition, conducting studies that focus solely on this rare subtype have been a constant challenge, making it difficult to determine optimal treatment strategies [78]. Most large trials combine all endometrial subtypes, with UPSC making up only a small percentage of cases. The purpose of this study was to identify novel therapeutic targets that could aid in the management of UPSC. As of May 2013, the TCGA dataset for endometrial cancer contained 91 UPSC cases with both clinical and RNA sequencing data. This relatively large sample size allows a meaningful comparison to be made between UPSC and EEC to identify relevant genetic differences.

To determine genetic changes that are responsible for the increased aggressiveness and poorer survival outcomes in UPSC compared to favorable type I tumors, we analyzed the RNA sequencing data from The Cancer Genome Atlas (TCGA) to identify genes differentially expressed between grade 1/2 endometrioid carcinomas and UPSCs. In particular, we identified *UCHL1* as a gene that was more strongly expressed in UPSCs than in endometrioid carcinoma and normal endometrium, and whose expression level was associated with poorer overall survival. These findings were validated through immunohistochemical analysis of an independent cohort of tumor samples.

Based on these findings, and the fact that UCHL1 is a deubiquitinating enzyme known to affect the protein stability of various cancer-related proteins, the hypothesis tested in this dissertation is that UCHL1 contributes to UPSC tumor progression by modulating the protein stability of target genes.

Our specific aims are as follows:

1. To identify important genes of interest in UPSC.

    a. Identify differentially expressed genes between normal endometrial tissue and the different subtypes of endometrial cancer.

    b. Confirm upregulation of UCHL1 in an independent sample cohort.

2. To delineate the functional role of UCHL1 in UPSC tumor progression.

3. To determine the mechanisms through which UCHL1 modulates UPSC tumor progression.

CHAPTER 2:

MATERIALS AND METHODS

TCGA analysis

TCGA data sets

Data was directly downloaded from the TCGA Data Portal. Clinical data was downloaded on May 2013. Patients with stage IIA were converted to I in accordance with the 2009 revisions to the surgical staging system for endometrial carcinoma by the International Federation of Gynecology and Obstetrics (FIGO) [256, 257]. Overall survival duration was inferred from "days to death" since initial diagnosis for deceased patients, whereas overall survival duration for censored patients was derived from "days to last known alive" and "days to last follow-up". Survival data was updated with the additional v1.7 and v2.0 follow-up information as released by the TCGA Data Portal. Level 3 RNAseqV2 data was downloaded on May 2013 and included the global expression profiles of 21 normal, 87 EEC grade 1, 100 EEC grade 2, 161 EEC grade 3, 15 mixed EEC/UPSC and 91 UPSC samples. Normalized RSEM data was used for principal component analysis (PCA), while raw counts were used for Significance Analysis of Microarrays (SAM). Level 3 RPPA data was downloaded on May 2014 and included 171 EEC samples, 3 mixed UPSC/EEC samples, and 22 pure UPSC samples for which concurrent clinical and RNAseqV2 data were available.

Principal component analysis

Level 3 normalized RSEM data for normal, EEC, mixed and pure UPSC samples was used for PCA analysis. The signal-to-noise (SNR) ratio of each gene was calculated by dividing the mean expression value across patients over its standard deviation. The data was then filtered to remove genes with a log10 SNR 2 standard deviations below the mean. The 500 genes with the highest variance were selected for analysis; values were log2 transformed and mean-centered before analysis using the "prcomp" function in R.

Significance Analysis of Microarrays (SAM)

The SAM method for sequencing data (version 4.0; Stanford University Labs) was used to identify differentially expressed (DE) genes between low-grade EEC and pure UPSC. Raw counts from the level 3 data for RNAseqV2 were filtered to remove genes with 10 or less reads across all samples, or genes with an average of 0.5 or less across all samples. The remaining 19093 genes were then converted to integers for analysis. For each comparison, two-class (unpaired) analysis was used, and the number of permutations was set to 100. q-values were obtained for each gene. Genes were considered DE if $q < 0.05$ and the SAM calculated fold change ≥ 2.

Automated log-rank test of genes in the RNA sequencing data set

A two-sample log-rank test for overall survival was calculated for every significant gene identified from the SAM assessment using level 3 normalized RSEM data for all 91 pure UPSC samples (57 initial samples plus an additional 34). Vital status and overall survival time were extracted from clinical data as previously described. For each gene, patients were assigned to one of two groups: below or above the median expression value. A loop in R statistical software (version 2.15.0, R Foundation for Statistical Computing) was used to perform the "survdiff" function from the package "survival" on each gene. The computed p-values were extracted for each gene. Hazard ratio was calculated for each gene (above median/ below median) by $HR = (O_1/E_1)/(O_2/E_2)$, where O_1 and O_2 are the observed number of deaths in the groups below and above the median respectively, and E_1 and E_2 are the expected number of deaths in the groups below and above the median respectively.

Pearson's test of correlation between UCHL1 RNA expression and RPPA data

Of the pure UPSC samples within the RNA sequencing dataset, 22 also had RPPA data available (3 of which were mixed EEC/UPSC). Using these 22 samples, we performed Spearman's test of

correlation to determine the correlation between *UCHL1* RNA expression and each of the 166 protein probes. For probes with p<0.05, Spearman's test was also performed with their RNA expression levels against *UCHL1* RNA expression levels.

Materials

Clinical specimens

All samples and clinical data were collected following approval by the MD Anderson Institutional Review Board. Formalin-fixed, paraffin-embedded sections of UPSC, EEC and normal tissue samples were obtained from The University of Texas MD Anderson Gynecologic Cancer Translational Research Tissue Bank. Normal premenopausal uterine samples were from individuals without cancer, while normal postmenopausal uterine samples were from tissue adjacent to tumor. Prior to the collection of these samples, informed consent had been obtained from patients undergoing primary cytoreductive surgery from 1989 through 2012. Overall survival time was measured from the date of diagnosis onwards.

Cell culture and reagents

Human endometrial carcinoma cell lines ECC1, HEC-1A, HEC-1B, HEC-50, HEC-59, Ishikawa, MFE-296, MFE-280 and RL-952 (ATCC) were cultured in RPMI-1640 supplemented with 2 nM L-glutamine (Invitrogen) and 10% fetal bovine serum. Human UPSC cell lines ARK1 and ARK2 were a kind gift from Dr. Alessandro D. Santin (Yale Cancer Center), and UPSC cell lines ACI-126 and ACI-158 were a kind gift from Dr. John I. Risinger (Michigan State University). All four cell lines were cultured in DMEM supplemented with 1.0 g/L glucose, L-glutamine, sodium pyruvate (Corning Cellgro) and 10% fetal bovine serum. All cell lines were grown at 37℃ in a humidified incubator with 5% CO_2. UCHL1 was transiently silenced by transfection with *Silencer*® select siRNAs (s14616

and s14618, Life Technologies) duplexed with Lipofectamine RNAiMAX (Life Technologies) at a final concentration of 5 nM. Non-targeting *Silencer*® select siRNA was used as a negative control (4390843, Life Technologies). Transient expression of UCHL1 was achieved by transfection with the cDNA encoding human UCHL1 in a pReceiver-02 vector (EX-T2880-M02, GeneCopoeia).

Stable transfectants

ARK1 cells transduced with lentiviral particles containing CMV-firefly luciferase (PLV-10064, Cellomics Technology) were selected for with G418. Successful transduction was confirmed by *in vitro* luciferase detection assay. To generate ARK1 cells with doxycycline-inducible control shRNA (ARK1-luc-dox-shNT) or UCHL1 knockdown (ARK1-luc-dox-shUCHL1), luciferase-labelled cells were transduced with TRIPZ inducible lentiviral non-silencing control (RHS4743, Dharmacon) or TRIPZ inducible lentiviral shRNA against UCHL1 (RHS4696-200764988, Dharmacon), and selected for with puromycin. Induction of UCHL1 knockdown by 2µg/ml doxycycline treatment of ARK1-luc-dox-shUCHL1 was confirmed *in vitro* by western blot.

Antibodies

Anti-cyclin B1 from Santa Cruz (sc-245) was used for immunohistochemistry, western blot, immunoprecipitation, immunofluorescence and the proximity ligation assay. Anti-UCHL1 from Sigma-Aldrich (HPA005993) was used for immunohistochemistry, immunofluorescence and proximity ligation assay; anti-UCHL1 from Cell Signaling (11896) was used for western blot; anti-UCHL1 from R&D Systems (MAB6007) was used for immunoprecipitation. Additional antibodies used for western blot include anti-cyclin D1 (sc-753, Santa Cruz), anti-cyclin E (sc-481, Santa Cruz), anti-p53 (48818, Cell Signaling), anti-ubiquitin (3936, Cell Signaling), anti-β-actin (4967, Cell Signaling), anti-β-catenin (9562, Cell Signaling), anti-GSK3α/β (5676, Cell Signaling), anti-p21 (sc-

31

397, Santa Cruz), and anti-p27 (sc-529, Santa Cruz). MMP-13 (sc-30073, Santa Cruz) was used for immunofluorescence and the proximity ligation assay.

Experimental procedures

Immunohistochemical analysis

Immunohistochemical staining was performed on paraffin embedded tissue. Slides were deparaffinized and rehydrated before antigen retrieval in citrate buffer (S2307, Poly Scientific), in a decloaking chamber (Biocare Medical) at 125℃ for 4 minutes and 90℃ for 1 minute. Slides were then stained with primary and secondary antibody using the Lab Vision Autostainer 360 (Thermo Fisher Scientific). Using a light microscope, digital photomicrographs of representative areas were taken for each slide at x20 magnification; the staining intensity for each slide was then quantified at least 3 times using the Image-Pro Plus software (version 17, MediaCybernetics) by drawing around the stained tumor tissue and obtaining an intensity score from 0 (pure black) to 255 (pure white) with background correction. An average value was calculated for each slide and transformed linearly onto a scale of 0 to 1 for further survival analysis. Slides were also stained with anti-cyclin B1 antibody, and the percentage of tumor cells positive for cyclin B1 was determined by visual observation under a light microscope.

TP53 DNA sequencing

Using DNA extracted from ARK1 and ARK2 cells, exon 5-8 of the *TP53* gene were amplified by PCR. The primers used were as follows: exon 5-6, forward 5'-TGTTCACTTGTGCCCTGACT-3', reverse 5'-GAGGGCCACTGACAACCA-3'; exon 7, forward 5'-AGGTCTCCCCAAGGCGCACTG-3', reverse 5'-TGTGCAGGGTGGCAAGTGGC-3'; exon 8,

forward 5'-TGGGAGTAGATGGAGCCTGG-3', reverse 5'-AGGAAAGAGGCAAGGAAAGG-3'.

Amplified DNA fragments were analyzed by Sanger sequencing.

Quantitative RT-PCR

Total RNA was extracted from adherent cells using the PureLink RNA mini kit (Life Technologies) per the manufacturer's instructions. Total RNA (1 μg per sample) was subjected to reverse transcription for the synthesis of single-stranded cDNA using the high-capacity cDNA reverse transcription kit (Applied Biosystems). Real-time PCR detection was performed using the TaqMan universal master mix (no uracil-N-glycosylase; Applied Biosystems), PPIA-, UCHL1- and cyclin B1-specific TaqMan gene expression assays (Hs04194521_s1, Hs00985157_m1 and Hs01030099_m1, Applied Biosystems) and the CFX96 Touch real-time PCR detection system (Bio-Rad Laboratories). PPIA expression levels were used as a reference to quantify UCHL1 and CCNB1 RNA expression levels via the relative standard curve method.

Western blot analysis

Adherent cell cultures were washed twice with PBS and lysed with RIPA buffer (150 mM NaCl, 1.0% IGEPAL® CA-630, 0.5% sodium deoxycholate, 0.1% SDS, 50 mM Tris, pH 8.0) (Sigma-Aldrich) supplemented with protease inhibitor cocktail (Sigma-Aldrich). Protein concentration was determined by the BCA assay (Pierce). Protein lysates were separated on SDS-polyacrylamide gel and electrophoretically transferred to PVDF membrane (Bio-Rad Laboratories). Membranes were incubated with primary antibodies overnight at 4 ℃, then incubated with the HRP-conjugated secondary antibodies (GE Healthcare Life Sciences) for 1 hour at room temperature. Signals were developed using the HyGlo quick spray chemiluminescent kit (Denville Scientific) and visualized on

autoradiography film (Denville Scientific). Relative protein levels were quantified with ImageJ (version 1.50i, National Institutes of Health) by normalizing to β-actin.

Apoptosis assay

Apoptosis was measured in ARK1 cells by using the Dead Cell Apoptosis Kit (V13241, Invitrogen) per the manufacturer's instructions. Cells were stained with Alexa Fluor 488 annexin V and propidium iodide, then read a Gallios flow cytometer (Beckman Coulter). Cells with both propidium idodide and annexin V were considered apoptotic.

Migration assay

Three days after siRNA transfection, ARK1 and ARK2 cells were serum starved for 24 hours; equal numbers were then plated into migration chambers with 8 µm pore size, (3422, Corning) in serum-free medium. Medium supplemented with 20% fetal-bovine serum was placed below the chamber. Cells were allowed to migrate for 24 hours before fixation with ice-cold methanol and staining with crystal violet solution.

Cell sensitivity to chemotherapeutic agents

Cisplatin (Pfizer) and paclitaxel (Hospira) were obtained from the M.D. Anderson Cancer Center pharmacy in solution. Following siRNA-mediated knockdown of UCHL1, ARK1 and ARK2 cells were treated with a range of doses of paclitaxel or cisplatin for three days before analysis by MTT assay. Dose-response curves were generated for each drug.

MTT assay

Cell proliferation was measured by the MTT assay. Cell cultures were incubated for 2 hours at 37℃ in 0.5 mg/ml thiazolyl blue tetrazolium bromide (MTT) in medium, after which the mixture was aspirated and replaced with DMSO. Absorbance was measured at 590 nm using a FLUOstar Omega plate reader (BMG Labtech). Experiments were performed in triplicate.

In vivo UCHL1 knockdown study

Six-week old, female nude mice received an injection of luciferase-expressing, doxycycline-inducible ARK1-luc-dox-shNT cells or ARK1-luc-dox-shUCHL1 cells. 6×10^6 Cells were injected intraperitoneally in a 200 µl mixture of 2:1 PBS:matrigel. One day after injection, mice were switched from the standard diet to an irradiated diet containing 625 mg/kg doxycycline (TD.01306, Harlan) to induce shRNA expression. To compare survival outcomes between the two groups, mice were sacrificed when moribund and tumors were collected for immunohistochemical analysis.

Establishment of ARK1 subclones from ascitic fluid

Ascites from five mice in the control group were collected to isolate ARK1-luc-dox-NT cells with improved ability to establish tumor *in vivo*. For each sample, 1 ml of ascites was plated onto a culture plate with DMEM and 10% fetal bovine serum. Medium was replaced the next day to remove non-adherent cells. After 2 passages, adherent cells were confirmed to be ARK1-luc-dox-NT cells by doxycycline treatment and confirmation of induced RFP activity. Separately, Asc-ARK1-luc-dox-NT cells were cultured in medium without doxycycline and passaged twice before long-term freezing. One of the subclones were used for the following *in vivo* experiment.

In vivo LDN-57444 treatment

For the LDN-57444 treatment study, six-week old, female nude mice were injected with 6 x 10^6 Asc-
ARK1-lux-dox-NT cells cultured without doxycycline. Cells were injected intraperitoneally in a 200
µl mixture of 2:1 PBS:matrigel. After allowing tumors to establish for 2 weeks, the mice were
assigned randomly to the two groups and treated thrice weekly with 0.5 mg/kg LDN-57444 (Tocris
Bioscience, Bristol, UK) or control PBS with solvent (0.5% DMSO and 2.5% ethanol). LDN-57444
treatment continued until the mice became moribund, at which point they were sacrificed.

In vivo bioluminescence imaging

Imaging of tumors was performed using the IVIS Lumina XR imaging system (Caliper Life Sciences)
and signal quantification was done using Living Image Software (Caliper Life Sciences). Mice were
injected intraperitoneally with 120 mg/kg of luciferin, followed by induction of anesthesia with 2-3%
isoflurane gas. Bioluminescent images were acquired 10 minutes after injection.

Cycloheximide chase assay

ARK1 and ARK2 cells were treated with 20 µg/ml and 10 µg/ml CHX respectively before cell lysis
at the indicated time points for analysis by western blot. Cyclin B1 protein expression levels were
determined relative to zero hours of cycloheximide treatment.

Immunoprecipitation and co-immunoprecipitation

For co-immunoprecipitation studies, cells were harvested in Pierce IP lysis buffer (Thermo Fisher
Scientific). 1-2mg of protein lysate were precleared with 20ul Protein A/G beads for 60 minutes at 4˚
C, then incubated with 4 ug antibody overnight at 4˚ C. 40 ul Protein A/G were added the next day to

pull down bound protein-antibody complexes, and proteins were eluted from the beads with denaturing SDS buffer. For western blot analyses, TrueBlot HRP-conjugated anti-rabbit and anti-mouse antibodies (18-8816-33 and 18-8817-33, Rockland) were used to minimize detection of light- and heavy-chain antibody fragments. For detection of cyclin B1 ubiquitination, cells were pretreated with 25 μg/ml MG132 for 4 hours before harvesting in RIPA buffer with protease inhibitor and PR-619 (25 μM). Ubiquitin staining was quantified with ImageJ (version 1.50i, National Institutes of Health) and normalized to cyclin B1 staining following immunoprecipitation (IP: cyclin B1 – WB: cyclin B1).

Immunofluorescence and Duolink proximity ligation assay

Cells were plated on coated glass slides overnight before fixation with methanol. Slides were blocked with 1% bovine serum albumin (BSA), then incubated with primary antibodies in 1% BSA. For immunofluorescence staining of UCHL1 and cyclin B1, secondary antibodies used were Alexa Fluor 488 anti-rabbit (A-11032) and Alexa Fluor 596 anti-mouse (A-11034) from Thermo Fisher. For detection of protein interaction between UCHL1 and cyclin B1, incubation with primary antibody was followed by use of the Duolink *In Situ* kit (#DUO92101, Sigma-Aldrich) per the manufacturer's instructions. Cells were visualized on the Olympus FV1000 laser confocal microscope.

Double thymidine cell synchronization

ARK1 cells were synchronized in early S phase by 16 hours of thymidine treatment (2 mM) in normal culture medium, followed by 10 hours release in culture medium, and a second thymidine block of 14 hours. Cells were then collected for analysis 10 hours after the second release to enrich for mitotic cells.

Cell cycle analysis by flow cytometry

Adherent cells were trypsinized, washed once with PBS, and fixed overnight at 4°C with 70% ethanol. Cells were then incubated with 0.1 mg/ml RNase A solution and 50 μg/ml propidium iodide at 37°C for 30 minutes. Stained cells were subsequently analyzed using a Gallios flow cytometer (Beckman Coulter) to determine the percentage of cells in the G1, S and G2/M phases.

Statistical analyses

Survival analysis was performed with SPSS software version 19 (IBM Corporation). Median follow up times were calculated by the reverse Kaplan-Meier method [258]. The Kaplan-Meier log-rank test was used for univariate analysis, while cox regression was used for multivariate analysis. Statistical analysis was performed with SPSS and GraphPad PRISM version 6. Comparisons between groups were performed using the Mann-Whitney *U*-test or the Kruskal-Wallis *H*-test for multiple groups. Following Kruskal-Wallis analysis, post-hoc testing for nonparametric pairwise multiple comparisons was performed with the Dunn's test to determine differences between each pair of groups. The adjusted p-values for multiple comparisons was calculated by $p*n*(n\text{-}1)/2$, where *n* is the number of independent groups. Correlation between variables was tested using the Spearman's test for nonparametric data.

CHAPTER 3:

UCHL1 IS UPREGULATED IN UPSC

AND IS ASSOCIATED WITH POORER SURVIVAL OUTCOMES

Specific Aim 1. To identify important genes of interest in UPSC.

    a. Identify differentially expressed genes between normal endometrial tissue and the different subtypes of endometrial cancer.

    b. Confirm upregulation of UCHL1 in an independent sample cohort.

Principal component analysis reveals distinct clusters based on RNA expression profiles

It is known that UPSC is clinically distinct from EEC and also genetically different, with a high percentage of *TP53* mutation and *HER2/neu* overexpression. However, the global genetic profile of UPSC is less clear. To begin to understand the molecular pathogenesis of UPSC, we explored its relationship to normal endometrial tissue and other endometrial carcinomas by principal component analysis.

At the time of download, the TCGA endometrial dataset for RNAseq version 2 contained 21 normal, 87 EEC grade 1 (EEC1), 100 EEC grade 2 (EEC2), 161 EEC grade 3 (EEC3), 15 mixed EEC/UPSC and 91 UPSC samples. Using the level 3 normalized RSEM data, 500 genes with the highest variance were selected for analysis. Figure 4A displays the clustering of samples according to the first two principal components, while Figure 4B includes the first three components. Though only accounting for 26.1% and 32.9% of explained variance respectively, the first two and three components were able to separate normal samples from tumor samples, and also illustrated the clustering together of EEC grade 1 and 2. There was a large variation within the normal tissue samples, with some overlap between the normal cluster and the EEC clusters. Interestingly, grade 3 EEC tumors overlapped with low grade EEC and also UPSC and mixed EEC/UPSC tumors. UPSC samples were clustered away from both normal tissue and EEC1/2.

These findings suggest that pure and mixed UPSC are the most genetically different from normal tissue, suggesting that they have the highest degree of dysregulation at the RNA level. UPSC

is known to have a high number of somatic copy number alterations compared to EEC [259], which could explain this high number of aberrations. It also suggests that there are certain similarities between high grade EEC and UPSC.
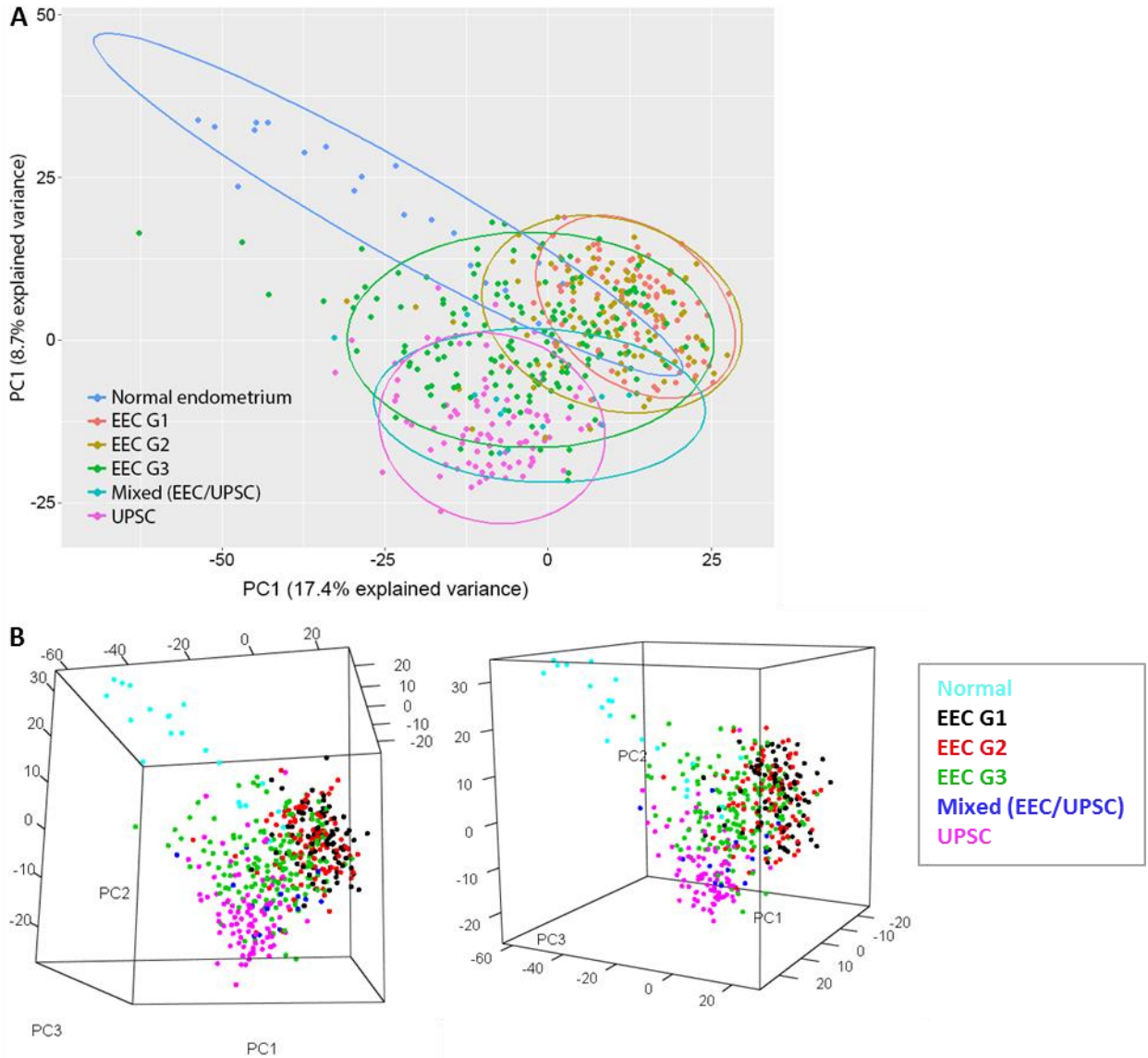
Figure 4. Principal component analysis of RNA expression profiles across endometrial tissue samples.

(A) Scatter plot of first two principal components. 95% confidences ellipses assume a multivariate t-distribution.

(B) 3D plot of the first three principal components.

SAM analysis for the identification of differentially expressed genes between tumor subtypes

Next we sought to further explore differences between different histological subtypes of endometrial carcinoma by identifying differentially expressed (DE) genes between normal and tumor samples, and also between different tumor subtypes. SAM analysis for sequencing data [260] was used to perform two-class, unpaired comparisons between the RNA sequencing profiles of tumors (EEC1, EEC2, EEC3 and UPSC) and normal samples; comparisons between different tumor subtypes were also performed. Level 3 raw read counts from the TCGA RNAseq Version 2 data set were used. Comparisons between grade 1 and 2 EEC yielded no genes with significantly higher expression in grade 2 versus grade 1 EEC, suggesting that these two groups were relatively similar in gene expression; therefore, these two groups were merged together for tumor-tumor comparison analysis.

Genes with $q < 0.05$ and fold change ≥ 2 were considered differentially expressed. A total of 9506 genes were DE in one or more normal-tumor analyses; of these, 4575 genes (48%) were significant in all comparisons. As expected, normal-EEC1 and normal-EEC2 comparisons showed the greatest overlap of significant genes, while normal-UPSC comparison had the least overlap with other normal-tumor comparisons (Figure 5A and B).

When comparing different tumor subtypes, EEC1/2-UPSC comparisons yielded a larger number of DE genes than EEC3-UPSC, suggesting a larger genetic difference between EEC1/2 and UPSC (Figure 5C). EEC1/2-EEC3 comparison yielded the least DE genes, again illustrating that the global expression profile of UPSC is the most distinct from low and high grade EEC. A large number of genes were DE in both the EEC1/2-UPSC and EEC3-UPSC comparisons, which may represent genetic changes that are an indicator of increased aggressiveness as opposed to being specific to a histological type.

In accordance with the principal component analysis results, the SAM analysis output illustrates that EEC1 and EEC2 are genetically most similar, and EEC3 is more similar to UPSC than

EEC1/2 is to UPSC. The intermediate clinical prognosis of EEC3 between low grade EEC and UPSC

is therefore reflected in dysregulation at the RNA level.

A Normal-EEC G2
(7138)

Normal-EEC G3
(6733)

132
(1.4%)

269
(2.8%)

788
(8.3%)

129
(1.4%)

463
(4.9%)

395
(4.2%)

922
(9.7%)

271
(2.9%)

995
(10.5%)

4575
(48.1%)

29
(0.3%)

52
(0.5%)

75
(0.8%)

269
(2.8%)

142
(1.5%)

Normal-EEC G1
(7195)
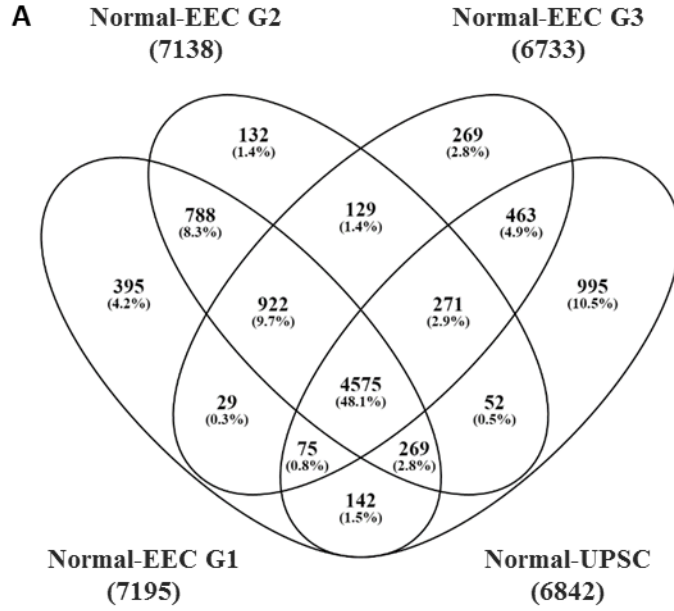
Normal-UPSC
(6842)

B

	Normal-EEC G1	Normal-EEC G2	Normal-EEC G3	Normal-UPSC
Normal-EEC G1	-	68.9%	58.9%	53.2%
Normal-EEC G2	68.9%	-	62.1%	54.3%
Normal-EEC G3	58.9%	62.1%	-	56.7%
Normal-UPSC	53.2%	54.3%	56.7%	-

C EEC G3-UPSC
(2029)

EEC G1/2-UPSC
(3340)

301
(7.5%)

1283
(32.1%)

996
(24.9%)

303
(7.6%)

142
(3.6%)

758
(19%)

215
(5.4%)

EEC G1/2-EEC G3
(1418)

44
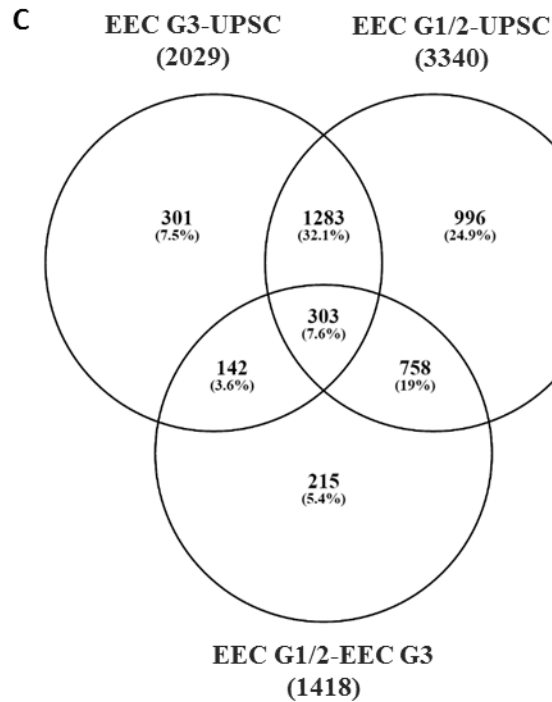
Figure 5. Venn diagrams of differentially expressed genes in SAM analyses.

Genes with q < 0.05 and fold change ≥ 2 were designated as differentially expressed.

(A) Venn diagram showing the overlap of significant genes between different normal-tumor comparisons.

(B) Percentage of genes overlapping between different normal-tumor comparisons.

(C) Venn diagram showing overlap between different tumor-tumor comparisons.

UCHL1 is upregulated in UPSC and is significantly correlated with shorter overall survival time in the TCGA data set

As we observed an overlap between grade 3 EEC and UPSC based on expression profiles, certain drivers of UPSC aggressiveness may also be dysregulated in EEC3; therefore, such genes may not be identified through EEC3-UPSC comparison results. Instead, we chose to focus on the comparison between UPSC and low-grade EEC (workflow in Figure 6).

TCGA: RNA sequencing data

Number of genes:

20531

Removal of low-expressing genes
≤ 10 reads across all samples
≤ 0.5 mean value across all samples

19093

Identification of genes differentially expressed between UPSC and low-grade EEC

SAM analysis
Differentially expressed genes:
$q < 0.05$
fold change ≥ 2

3340

Identification of genes significantly associated with overall survival

Kaplan-Meier log-rank testing
Genes associated with
overall survival
($p < 0.05$)

145

Selection of genes with
- higher expression in UPSC than both low-grade EEC and normal
- association with poorer overall survival

UPSC vs EEC-G1/2:
Hazard ratio > 1
SAM $q < 0.05$
fold change > 2

UPSC vs normal:
SAM $q < 0.05$
fold change > 2

19

Figure 6. Discovery of genes that contribute to UPSC tumor progression.

To identify genes that contribute to the increased aggressiveness of UPSC, we extracted the 3340 genes differentially expressed between EEC G1/2-UPSC to see which were correlated with overall survival in the TCGA data set. For each gene, samples were grouped above and below the median expression level. A two-sample log-rank test of overall survival was then conducted, using survival data from the 91 pure UPSC samples, to find the genes significantly correlated with overall survival in the UPSC data set.

By overlapping survival information with the SAM analysis between EEC grade 1/2 and UPSC, 145 genes were found to be differentially expressed between UPSC and low-grade EEC, and which individually showed a significant association with overall patient survival as determined by the log-rank test ($p < 0.05$) (Table 1 and Figure 7A). Of particular interest were the 19 genes that were

significantly higher in UPSC compared to both normal tissue and low-grade EEC, and for which high expression was associated with poorer overall survival (Table 2). Of these, we chose to study *UCHL1* further, due to it being the most highly expressed in the UPSC group. *UCHL1* exhibited over a 40-fold increase in RNA expression from low-grade EEC to UPSC, with similar expression levels in normal and low-grade EEC (Figure 7B). Both pure UPSC and mixed histology (UPSC/EEC) tumors displayed significantly higher *UCHL1* expression than normal endometrial tissue and EEC. An intermediate level of *UCHL1* expression was observed in grade 3 EEC, which was also significantly higher than in low-grade EEC (Figure 7C). *UCHL1* expression was not significantly different across stages of UPSC, suggesting that its upregulation is an early event (Figure 7D). Furthermore, the copy-number high serous-like cluster, one of four novel groups recently identified using integrated genomic data [259], also had a significantly higher *UCHL1* expression than the other three clusters (Figure 7E). Finally, high *UCHL1* expression correlated with poorer overall survival duration by both Kaplan-Meier analysis (Figure 7F) and multivariate Cox regression analysis (Table 3).

Gene	Entrez ID	Median RSEM value			SAM: UPSC vs normal			SAM: UPSC vs EEC (G1/2)			Log-rank test	
		Normal	EEC (G1/2)	UPSC	q	d	Fold change	q	d	Fold change	p	HR
TFF3	7033	288	8170	63	0.000	-461.4	-4.9	0.000	-7681.6	-135.2	0.011	3.10
UCHL1	7345	166	60	2780	0.000	776.3	15.3	0.000	7130.9	40.9	0.023	2.64
SCGB2A1	4246	508	12796	463	0.089	138.0	-1.2	0.000	-7051.1	-28.3	0.044	0.39
C10orf81	79949	67	1597	79	0.166	67.6	1.1	0.000	-6772.8	-22.0	0.021	2.93
GALNT10	55568	541	1348	415	0.001	-398.3	-1.3	0.000	-6755.1	-3.4	0.047	2.47
SCAMP4	113178	1624	3677	1732	0.232	-19.1	1.1	0.000	-6747.8	-2.2	0.049	0.43
PRKCI	5584	966	772	1785	0.000	578.1	1.8	0.000	6688.2	2.2	0.034	0.37
ARHGAP26	23092	869	1672	489	0.000	-503.3	-1.9	0.000	-6684.9	-3.6	0.018	2.89
ENPP3	5169	30	182	8	0.000	-595.1	-4.0	0.000	-6607.7	-23.0	0.028	2.96
SERPINA3	12	251	1909	88	0.000	-421.4	-2.7	0.000	-6472.2	-21.9	0.021	2.77
RNASE4	6038	2139	425	92	0.000	-943.0	-23.0	0.000	-6201.8	-4.8	0.029	2.65
TSPAN8	7103	92	220	20	0.000	-627.1	-5.0	0.000	-6184.5	-11.4	0.005	3.67
BMPR1B	658	411	1123	303	0.038	-204.2	-1.4	0.000	-6123.6	-4.0	0.041	2.44
TMEM62	80021	296	726	335	0.077	151.4	1.1	0.000	-6092.1	-2.3	0.017	0.34
FMO5	2330	77	67	17	0.000	-794.6	-4.7	0.000	-6046.9	-4.4	0.040	2.77
S100A1	6271	263	150	1206	0.000	619.1	4.1	0.000	6046.1	7.3	0.027	0.37
B4GALNT3	283358	213	947	336	0.001	401.0	1.6	0.000	-5990.9	-2.9	0.032	2.88
CSF3	1440	10	43	1	0.000	-458.1	-9.0	0.000	-5989.8	-38.1	0.009	3.53
SLC6A11	6538	9	0	16	0.023	241.1	1.7	0.000	5985.5	1.8E+09	0.022	2.62
SLC12A2	6558	740	871	407	0.000	-607.2	-1.9	0.000	-5768.3	-2.3	0.015	2.94
STEAP1	26872	108	229	58	0.001	-373.8	-1.9	0.000	-5696.1	-4.1	0.036	2.49
C4orf39	152756	35	6	29	0.115	-113.4	-1.2	0.000	5592.4	4.8	0.040	0.38
CCDC99	54908	154	218	506	0.000	860.7	2.9	0.000	5553.2	2.1	0.014	2.86
BEX2	84707	538	179	556	0.218	25.9	-1.0	0.000	5481.9	2.9	0.024	2.67
CD47	961	2037	1938	4377	0.000	496.6	2.0	0.000	5463.9	2.1	0.029	2.79
STEAP2	261729	755	363	108	0.000	-857.1	-7.0	0.000	-5376.7	-3.6	0.021	2.75
MOSC2	54996	169	187	99	0.000	-534.3	-1.8	0.000	-5336.0	-2.1	0.023	2.90
CCDC42B	387885	11	230	38	0.086	141.0	3.2	0.000	-5279.7	-6.6	0.019	0.35
MUC13	56667	23	284	19	0.198	-45.5	-1.3	0.000	-5212.0	-15.3	0.011	3.74
PODXL	5420	6115	5563	2386	0.000	-613.5	-2.8	0.000	-5195.2	-2.5	0.020	3.09
SCGB1D2	10647	101	877	106	0.085	143.0	-1.0	0.000	-5075.6	-8.8	0.021	0.34
SLC27A2	11001	16	145	51	0.061	171.1	3.0	0.000	-5074.7	-3.1	0.030	2.86
WASF1	8936	346	354	928	0.000	615.4	2.5	0.000	5003.2	2.4	0.045	2.43
LPAR1	1902	412	318	131	0.000	-746.6	-3.2	0.000	-4975.4	-2.5	0.016	3.25
TUBA4B	80086	37	278	63	0.239	8.7	1.6	0.000	-4858.2	-4.7	0.002	0.25
MCC	4163	1102	439	165	0.000	-859.6	-7.4	0.000	-4771.6	-2.8	0.030	2.64
SYCE1L	100130958	33	66	19	0.010	-280.8	-1.7	0.000	-4768.7	-3.6	0.050	2.38
GPX2	2877	10	88	5	0.192	-51.0	-1.9	0.000	-4759.5	-17.1	0.021	3.38
LRCH2	57631	348	16	65	0.000	-608.8	-5.8	0.000	4705.6	3.7	0.037	2.81

ERG	2078	962	227	106	0.000	-570.8	-9.9	0.000	-4701.1	-2.3	0.044	2.43
PPP1R1B	84152	540	1619	404	0.202	-42.4	-1.5	0.000	-4661.8	-4.4	0.014	3.15
PARM1	25849	1908	502	158	0.000	-732.6	-12.8	0.000	-4655.4	-3.4	0.014	3.03
PIP5K1B	8395	136	137	50	0.000	-503.5	-2.8	0.000	-4591.2	-2.8	0.009	3.53
CEACAM5	1048	2	97	5	0.012	278.4	2.9	0.000	-4541.7	-20.6	0.007	3.95
GALNT5	11227	2	23	6	0.014	269.5	2.5	0.000	-4540.5	-4.1	0.043	2.51
COL9A1	1297	3	15	239	0.000	698.0	75.1	0.000	4530.3	14.5	0.039	2.50
HSPC072	29075	2	0	2	0.208	34.3	-1.1	0.000	4529.2	2.3E+08	0.011	2.95
KCNJ12	3768	129	30	173	0.227	18.6	1.3	0.000	4501.2	5.1	0.040	2.49
ITGA10	8515	72	44	18	0.000	-597.1	-4.6	0.000	-4443.3	-2.7	0.022	2.74
HIST2H2AC	8338	16	470	129	0.000	549.8	7.8	0.000	-4440.2	-3.8	0.024	0.37
IGSF5	150084	6	10	3	0.000	-419.4	-2.3	0.000	-4422.0	-3.9	0.048	2.41
NAIP	4671	98	593	302	0.246	-0.5	3.1	0.000	-4386.0	-2.1	0.045	0.42
MAN1C1	57134	806	153	71	0.000	-889.8	-11.5	0.000	-4385.3	-2.2	0.049	2.45
PRAP1	118471	2	8	53	0.000	705.1	27.1	0.000	4381.0	6.2	0.016	0.33
FAM55B	120406	1	2	0	0.000	-468.7	-1.7E+08	0.000	-4333.5	-2.8E+08	0.001	4.14
NKAIN1	79570	4	8	33	0.000	731.6	8.3	0.000	4266.3	3.9	0.008	3.28
CALN1	83698	5	30	3	0.088	-139.5	-1.5	0.000	-4240.0	-9.9	0.024	2.82
PIP	5304	0	2	0	0.002	-351.4	-6.8E+07	0.000	-4191.0	-2.7E+08	0.039	2.97
NCRNA00093	100188954	2	6	2	0.016	-254.5	-1.6	0.000	-4175.5	-4.2	0.044	2.37
IL18R1	8809	69	86	42	0.001	-388.8	-1.8	0.000	-4131.1	-2.3	0.005	3.64
GAL	51083	0	6	27	0.000	738.5	3.8E+09	0.000	4131.0	4.4	0.030	2.75
FOXE1	2304	0	0	4	0.000	683.9	5.3E+08	0.000	4129.4	4.1E+08	0.030	2.75
CXCL3	2921	16	94	24	0.069	161.1	1.5	0.000	-4117.4	-4.0	0.049	2.41
KCNT2	343450	35	2	13	0.003	-331.5	-2.5	0.000	4059.4	5.4	0.048	2.34
GUCY1A3	2982	1175	499	249	0.000	-485.4	-5.1	0.000	-3950.5	-2.2	0.034	2.42
LOC255167	255167	53	1	4	0.000	-805.8	-12.3	0.000	3940.6	5.0	0.002	3.96
CPXM2	119587	772	141	470	0.055	-177.7	-1.8	0.000	3847.2	3.1	0.011	3.74
SLCO4C1	353189	3	5	17	0.000	589.2	4.8	0.000	3818.0	3.3	0.038	2.53
PNMA2	10687	106	8	30	0.001	-405.9	-3.5	0.000	3811.2	3.8	0.004	3.95
SLC16A1	6566	1059	403	1070	0.222	22.1	-1.1	0.000	3803.0	2.4	0.043	2.44
C21orf88	114041	20	15	3	0.000	-538.6	-7.5	0.000	-3794.6	-5.5	0.011	3.06
SYT11	23208	1607	325	822	0.005	-316.0	-2.0	0.000	3789.4	2.3	0.019	2.83
CXCL2	2920	108	112	34	0.000	-411.2	-3.1	0.000	-3774.4	-3.4	0.031	2.77
ADAMTS18	170692	12	26	8	0.015	-260.9	-1.7	0.000	-3707.4	-3.9	0.008	3.32
RIMBP2	23504	261	90	12	0.000	-746.8	-22.9	0.000	-3672.9	-8.0	0.006	3.39
HMX2	3167	0	2	0	0.007	306.4	1.0	0.000	-3664.0	-2.8E+08	0.004	3.55
DPEP1	1800	8	67	19	0.001	392.4	2.2	0.000	-3655.6	-4.0	0.006	3.34
CNTNAP3	79937	95	50	18	0.000	-653.6	-5.6	0.000	-3615.0	-2.9	0.023	2.86
MAOB	4129	5926	545	194	0.000	-954.5	-31.4	0.000	-3613.6	-2.8	0.011	3.02
ADRA1D	146	52	2	5	0.000	-773.3	-10.1	0.000	3601.4	2.9	0.013	3.10
PPAPDC1A	196051	5	10	37	0.000	785.3	8.2	0.000	3584.5	3.4	0.047	2.36
PEG10	23089	1202	362	1404	0.078	150.8	1.1	0.000	3542.2	3.8	0.033	2.56

ASXL3	80816	53	2	12	0.000	-715.1	-4.9	0.000	3478.8	6.0	0.018	3.17
FLG	2312	62	7	30	0.006	-308.0	-2.2	0.000	3391.7	4.3	0.020	2.74
KCNN2	3781	38	24	11	0.000	-491.9	-3.4	0.000	-3345.1	-2.2	0.037	2.81
IL8	3576	30	185	76	0.028	228.1	2.6	0.000	-3323.1	-2.4	0.032	2.54
ARHGAP36	158763	1	0	2	0.053	183.2	2.2	0.000	3315.2	2.7E+08	0.012	3.09
GPR156	165829	15	5	14	0.113	-115.8	-1.1	0.000	3299.6	2.7	0.008	3.17
FBXW10	10517	2	9	3	0.176	59.1	1.4	0.000	-3255.2	-2.9	0.038	0.41
FAM167A	83648	23	54	150	0.000	529.0	6.1	0.000	3225.0	2.6	0.004	3.51
ZSCAN23	222696	39	4	15	0.000	-490.2	-2.7	0.000	3071.3	4.0	0.001	4.11
TBX18	9096	25	142	14	0.122	-107.2	-1.8	0.000	-3061.0	-10.5	0.042	2.44
CXCL5	6374	9	128	32	0.001	385.7	3.7	0.000	-3048.1	-4.2	0.018	2.95
CLCA2	9635	1	3	1	0.024	236.1	1.9	0.000	-3046.7	-2.9	0.012	3.38
C11orf41	25758	6	15	54	0.000	632.4	7.4	0.000	3038.9	3.3	0.021	2.70
F3	2152	676	835	351	0.005	-312.2	-1.9	0.000	-3020.1	-2.6	0.013	3.28
NR5A1	2516	0	0	1	0.006	310.3	1.2E+08	0.000	2977.9	9.6E+07	0.009	3.26
MAP7D2	256714	23	15	39	0.049	189.7	1.5	0.000	2914.3	2.3	0.043	2.44
MAGEA5	4104	0	0	1	0.000	433.1	6.8E+07	0.000	2896.7	5.3E+07	0.012	0.32
GUCA1A	2978	0	1	2	0.002	362.9	3.8	0.000	2798.3	2.2	0.020	0.34
MAGEA9B	728269	0	0	7	0.000	577.3	9.7E+08	0.000	2798.2	7.5E+08	0.044	0.34
LOC400940	400940	0	0	1	0.023	239.2	8.0E+07	0.000	2758.1	6.1E+07	0.008	3.27
SHANK1	50944	54	19	7	0.000	-529.7	-7.7	0.000	-2739.4	-2.6	0.006	3.24
JPH3	57338	19	5	11	0.162	-73.9	-1.8	0.000	2673.2	2.1	0.028	2.74
ABCA8	10351	1048	42	18	0.000	-922.4	-56.7	0.000	-2589.0	-2.3	0.028	2.78
RAD51AP2	729475	2	1	0	0.000	-416.2	-2.9E+08	0.000	-2579.3	-1.1E+08	0.005	3.46
RIMS2	9699	26	24	7	0.000	-508.3	-3.9	0.000	-2578.4	-3.6	0.043	2.39
DDC	1644	1	1	4	0.000	448.1	3.7	0.000	2563.7	3.2	0.018	2.99
SERPINB3	6317	0	5	1	0.099	127.4	1.5E+08	0.000	-2540.0	-5.4	0.012	3.26
CAPN13	92291	19	548	228	0.000	704.4	11.8	0.000	-2478.3	-2.6	0.039	2.59
CD1B	910	2	3	0	0.086	-141.7	-7.1	0.000	-2457.8	-10.3	0.012	2.97
PDE1A	5136	251	53	28	0.000	-802.4	-9.2	0.000	-2441.1	-2.0	0.030	2.62
TRIM58	25893	40	13	78	0.208	34.2	2.0	0.000	2439.5	6.1	0.028	2.80
PLXNA4	91584	119	76	283	0.050	187.8	2.2	0.000	2431.8	3.5	0.020	3.12
RNU11	26824	0	2	0	0.006	312.7	5.1E+07	0.000	-2425.9	-5.6	0.021	0.35
MMP1	4312	1	39	86	0.000	871.6	73.5	0.000	2355.5	2.1	0.001	4.11
CYP2B7P1	1556	19	11	5	0.000	-496.3	-4.0	0.000	-2335.4	-2.3	0.005	3.71
GFRA1	2674	742	28	66	0.000	-657.1	-11.4	0.000	2313.3	2.3	0.031	2.52
KCNIP1	30820	19	8	17	0.196	-47.7	-1.2	0.000	2304.9	2.1	0.043	2.33
LOC339535	339535	205	17	50	0.000	-498.4	-4.1	0.000	2269.8	2.7	0.038	2.78
IGF2	3481	8711	2777	6766	0.175	-63.9	-1.3	0.000	2211.6	2.3	0.042	2.49
C9orf125	84302	477	21	88	0.000	-784.5	-5.6	0.000	2187.1	4.0	0.005	3.41
PRMT8	56341	2	4	2	0.077	-151.2	-1.4	0.000	-2174.0	-2.7	0.013	3.08
COL2A1	1280	3	60	18	0.002	368.4	6.1	0.000	-2145.3	-3.5	0.014	3.29
KLRC1	3821	8	7	3	0.001	-380.1	-2.6	0.000	-2134.7	-2.4	0.046	0.41

Gene												
HOXA6	3203	35	7	17	0.024	-232.9	-2.0	0.000	2106.8	2.5	0.018	3.19
ROS1	6098	0	3	1	0.068	162.5	1.2E+08	0.000	-2099.7	-3.8	0.039	2.47
OR2W3	343171	10	2	6	0.095	-132.2	-1.8	0.000	2059.1	2.7	0.001	4.78
LRRC31	79782	1	26	9	0.000	544.8	8.8	0.000	-2025.4	-3.1	0.007	3.07
PLA2G4E	123745	0	1	0	0.139	90.5	1.0	0.000	-1979.8	-1.1E+08	0.018	2.80
NRN1	51299	422	202	101	0.008	-292.5	-4.2	0.000	-1918.9	-2.0	0.031	2.68
NTSR2	23620	0	0	1	0.212	-34.5	1.2	0.001	1918.6	5.7E+07	0.026	2.74
LHX9	56956	2	1	2	0.095	131.8	1.1	0.003	1775.4	2.1	0.010	3.30
CT45A6	541465	0	0	2	0.001	399.8	2.4E+08	0.003	1720.4	1.8E+08	0.043	0.38
DAD1L	56286	0	0	0	0.009	292.3	5.9E+07	0.003	1720.2	4.5E+07	0.040	2.41
PF4V1	5197	0	3	1	0.000	446.9	2.1E+08	0.001	-1676.9	-2.1	0.023	2.71
MMP10	4319	1	42	115	0.000	609.7	92.2	0.006	1582.8	2.8	0.047	2.44
FAM135B	51059	2	0	1	0.043	-195.7	-1.9	0.014	1398.9	1.0E+08	0.040	2.42
SKINTL	391037	2	2	1	0.121	-108.1	-1.9	0.005	-1380.1	-2.4	0.029	2.67
AMPD1	270	2	1	0	0.001	-376.2	-2.4E+08	0.007	-1324.2	-1.0E+08	0.025	0.33
FOXI2	399823	7	0	1	0.000	-648.7	-16.0	0.019	1311.0	5.3E+07	0.036	2.73
FLG2	388698	0	0	0	0.187	51.0	-1.4	0.019	1310.9	3.7E+07	0.032	2.59
FAM19A1	407738	2	0	1	0.003	-335.5	-3.3	0.024	1240.3	6.8E+07	0.037	2.60
LUZP2	338645	3	2	1	0.002	-347.4	-2.8	0.013	-1182.3	-2.0	0.036	2.50
TBX22	50945	0	0	1	0.001	387.9	1.3E+08	0.041	1072.0	9.8E+07	0.032	2.53

Table 1. Differentially expressed genes between low-grade EEC and UPSC.

Genes are ranked by SAM score (UPSC vs low-grade EEC). SAM analysis was performed with level 3 raw counts from the RNA sequencing dataset. The SAM score (*d*) is the relative difference in gene expression. Hazard ratio is the risk of patients with gene expression above the median divided by the risk of patients with gene expression below the median.

q = q-value; *d* = SAM score; *p* = p-value; HR = hazard ratio.

Gene	Entrez ID	Median RSEM expression			SAM: UPSC vs. normal			SAM: UPSC vs. EEC (G1/2)			Log-rank test	
		Normal	EEC (G1/2)	UPSC	q	d	Fold change	q	d	Fold change	p	HR
UCHL1	7345	166	60	2780	0.000	776.3	15.3	0.000	7130.9	40.9	0.023	2.64
WASF1	8936	346	354	928	0.000	615.4	2.5	0.000	5003.2	2.4	0.045	2.43
CCDC99	54908	154	218	506	0.000	860.7	2.9	0.000	5553.2	2.1	0.014	2.86
PLXNA4	91584	119	76	283	0.050	187.8	2.2	0.000	2431.8	3.5	0.020	3.12
COL9A1	1297	3	15	239	0.000	698.0	75.1	0.000	4530.3	14.5	0.039	2.50
FAM167A	83648	23	54	150	0.000	529.0	6.1	0.000	3225.0	2.6	0.004	3.51
MMP10	4319	1	42	115	0.000	609.7	92.2	0.006	1582.8	2.8	0.047	2.44
MMP1	4312	1	39	86	0.000	871.6	73.5	0.000	2355.5	2.1	0.001	4.11
C11orf41	25758	6	15	54	0.000	632.4	7.4	0.000	3038.9	3.3	0.021	2.70
PPAPDC1A	196051	5	10	37	0.000	785.3	8.2	0.000	3584.5	3.4	0.047	2.36
NKAIN1	79570	4	8	33	0.000	731.6	8.3	0.000	4266.3	3.9	0.008	3.28
GAL	51083	0	6	27	0.000	738.5	3.8E+09	0.000	4131.0	4.4	0.030	2.75
SLCO4C1	353189	3	5	17	0.000	589.2	4.8	0.000	3818.0	3.3	0.038	2.53
FOXE1	2304	0	0	4	0.000	683.9	5.3E+08	0.000	4129.4	4.1E+08	0.030	2.75
DDC	1644	1	1	4	0.000	448.1	3.7	0.000	2563.7	3.2	0.018	2.99
NR5A1	2516	0	0	1	0.006	310.3	1.2E+08	0.000	2977.9	9.6E+07	0.009	3.26
TBX22	50945	0	0	1	0.001	387.9	1.3E+08	0.041	1072.0	9.8E+07	0.032	2.53
LOC400940	400940	0	0	1	0.023	239.2	8.0E+07	0.000	2758.1	6.1E+07	0.008	3.27
DAD1L	56286	0	0	0	0.009	292.3	5.9E+07	0.003	1720.2	4.5E+07	0.040	2.41

Table 2. 19 candidate genes with higher expression in UPSC than in normal tissue and low-grade EEC, and associated with poorer overall survival in UPSC patients.

Genes are ordered by median RSEM expression in UPSC patients. SAM analysis was performed with level 3 raw counts from the RNA sequencing dataset. The SAM score (*d*) is the relative difference in gene expression. Hazard ratio is the risk of patients with gene expression above the median divided by the risk of patients with gene expression below the median.

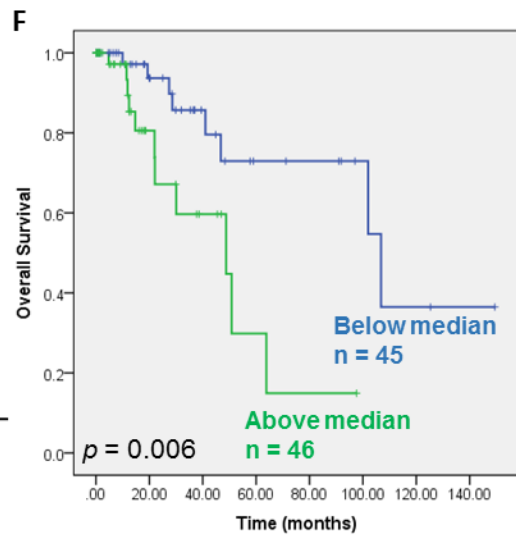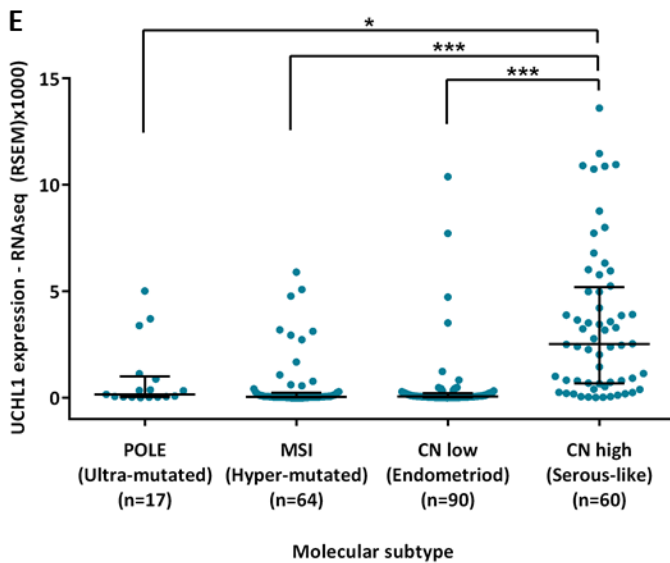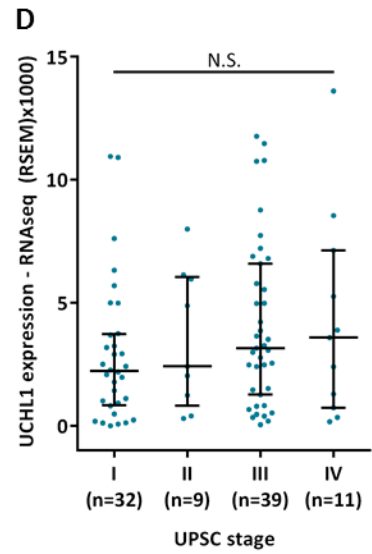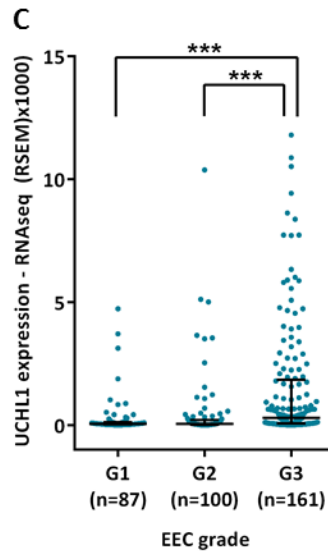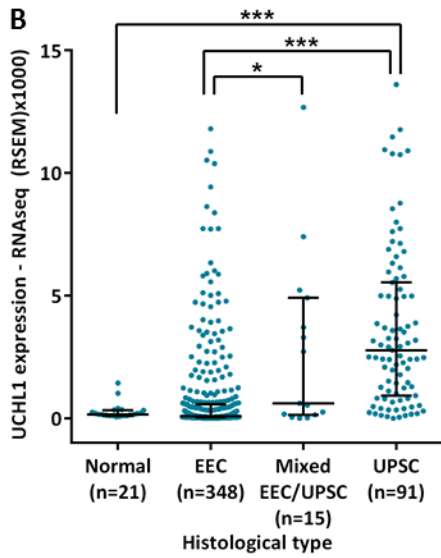*q* = q-value; *d* = SAM score; *p* = p-value; HR = hazard ratio.
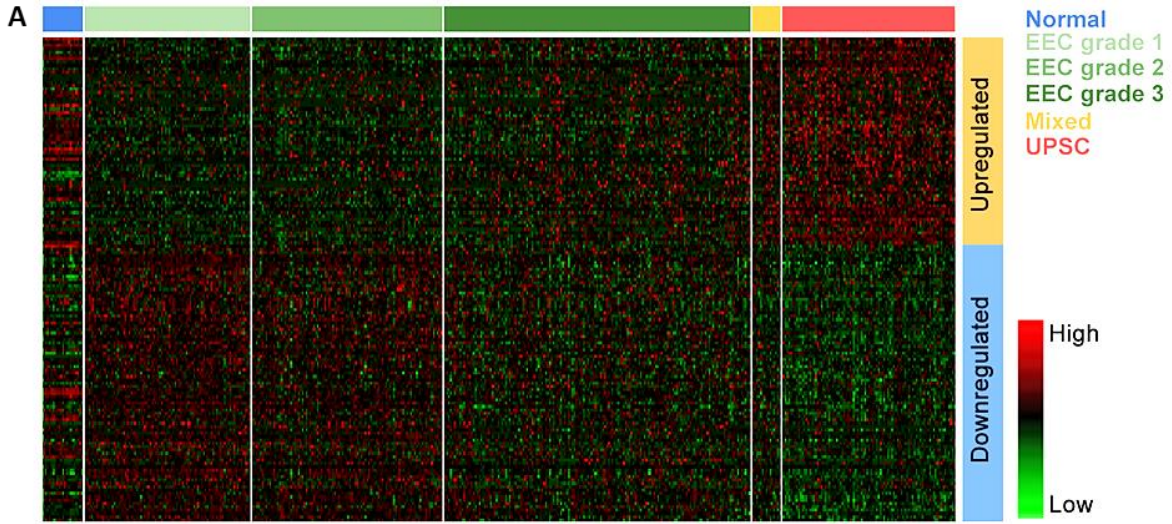
Figure 7. *UCHL1* is upregulated in UPSC and correlates with poorer overall survival in the TCGA data set.

(A) Heat map of the genes differentially expressed between UPSC and low grade EEC, with a significant association with overall survival in UPSC patients.

(B) *UCHL1* RNA expression across histological subtypes of endometrial cancer.

(C) *UCHL1* RNA expression across EEC1 grades.

(D) *UCHL1* RNA expression across UPSC stages.

(E) *UCHL1* RNA expression across integrated molecular subtypes of endometrial cancer.

(F) Kaplan-Meier analysis of *UCHL1* expression and overall survival.

Graphs represent median with interquartile range. N.S. = not significant; p = p-value.

*p<0.05, **p<0.01, ***p<0.001.

Variable		Pts (n)	Events (n)	HR	95% CI	*p*
Age						
		69	15	1.07	0.99-1.17	0.107
Stage*						
	I	29	4	1.00	Reference	
	II	5	1	0.59	0.05-5.73	0.587
	III	30	8	1.57	0.58-9.34	0.230
	IV	5	2	3.07	1.61-211.97	0.019[a]
Residual tumor*						
	R0	55	10	1.00	Reference	
	R1-R2	24	5	0.88	0.23-3.44	0.855
UCHL1 expression*						
	Below median	36	6	1.00	Reference	
	Above median	33	9	3.24	1.01-10.44	0.049[a]

Table 3. Cox regression analysis of overall survival of UPSC patients.

Cases with missing information were excluded from analysis.

R0 = no residual tumor; R1 = microscopic residual tumor; R2 = macroscopic residual tumor; Pts = patients; HR = hazard ratio; CI = confidence intervals; *p* = p-value; * = categorical variable; a = statistically significant.

UCHL1 upregulation and correlation with shorter overall survival time is validated in immunohistochemical staining of paraffin-embedded tumor samples

To validate the increased expression of *UCHL1* in UPSC that we observed with the TCGA data set, we performed immunohistochemical staining of UCHL1 in an independent cohort of UPSC, ECC, and normal endometrial tissue paraffin-embedded samples. Normal samples were from a mixture of pre- and postmenopausal individuals. Patient demographics are shown in Table 4. In concordance with the TCGA data set, quantification of staining intensity showed that UCHL1 expression was significantly higher in pure and mixed UPSC than in normal tissue and ECC, and there was no significant difference between mixed and pure UPSC (Figure 8 and 9A).

UCHL1 staining intensity was the lowest in normal endometrial tissue. In all normal endometrial samples and the majority of grade 1 and 2 EEC, there was negative staining or a dotted cytoplasmic staining pattern near the apical surface of the glandular cells. UCHL1 was also strongly positive in the epithelial cells of normal ovarian tissue and in a small fraction of epithelial cells in the normal fallopian tube. In contrast, the majority of UPSC tumors (42/50 pure UPSC samples) exhibited a diffuse staining pattern in the carcinoma cells, with occasional nuclear staining. Age, ethnicity, histological purity, and tumor stage were not significantly correlated with UCHL1 expression in the UPSC subset (Figure 9B and Table 5).

| Parameter	Endometrioid (n=34) n (%)	Serous (n=74) n (%)	Total (n=108) n (%)
Age, years			
Mean	64.2	68.5	67.2
SD	8.5	8.0	8.3
Median	63.0	69.0	67.0
Minimum	53.0	43.0	43.0
Maximum	83.0	85.0	85.0
Ethnicity			
Caucasian	25 (74)	45 (61)	70 (65)
African American	2 (6)	22 (30)	24 (22)
Hispanic	7 (21)	5 (7)	12 (11)
Asian	0	2 (3)	2 (2)
Histology purity			
Pure	34 (100)	49 (66)	83 (77)
Mixed	0	25 (34)	25 (23)
Grade			
1	10 (29)	0	10 (9)
2	15 (44)	0	15 (14)
3	9 (27)	74 (100)	83 (77)
Stage			
I	19 (56)	31 (42)	50 (46)
II	4 (12)	3 (4)	7 (7)
III	6 (18)	24 (32)	30 (28)
IV	5 (15)	16 (22)	21 (19)
UCHL1 staining intensity			
Low (< Mean - 0.5 SD)	31 (91)	20 (27)	51 (47)
Average (Mean ± 0.5 SD)	2 (6)	21 (28)	23 (21)
High (> Mean + 0.5 SD)	1 (3)	33 (45)	34 (32)
BMI (kg/m^2)			
Eutrophic (18.50 - 24.99)	0	14 (19)	14 (13)
Overweight (25 - 29.99)	6 (18)	9 (12)	15 (14)
Obese (≥ 30)	27 (79)	40 (54)	67 (62)
Unknown	1 (3)	11 (15)	12 (11)

Table 4. Demographic characteristics of patients in the immunohistochemical analysis of UCHL1.

Mean and S.D. UCHL1 staining intensity was taken from all tumor samples. n = number of patients.
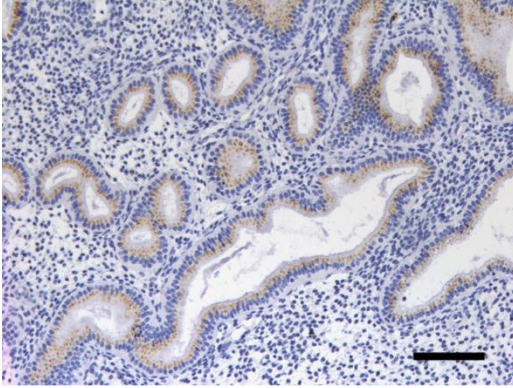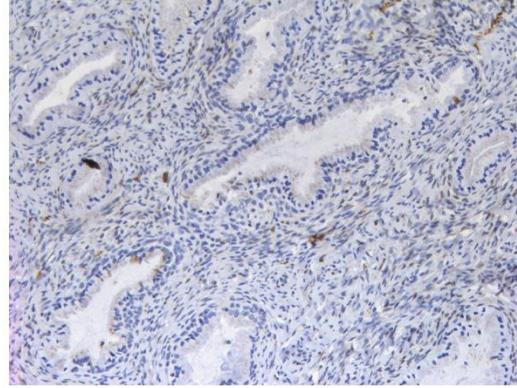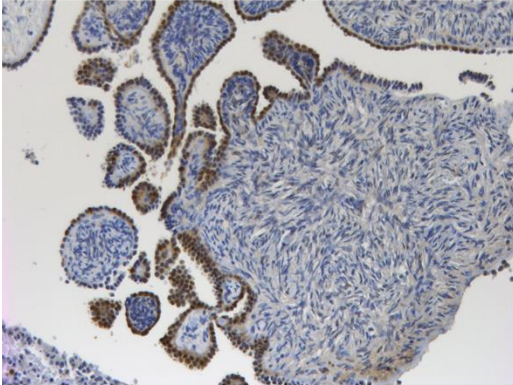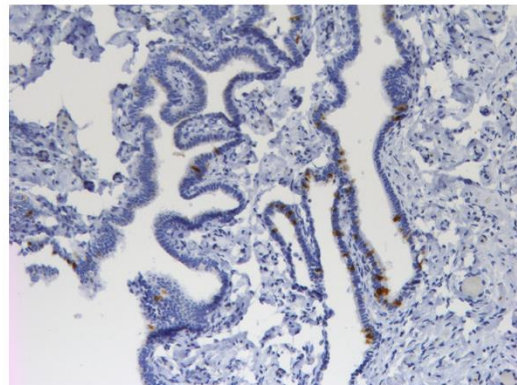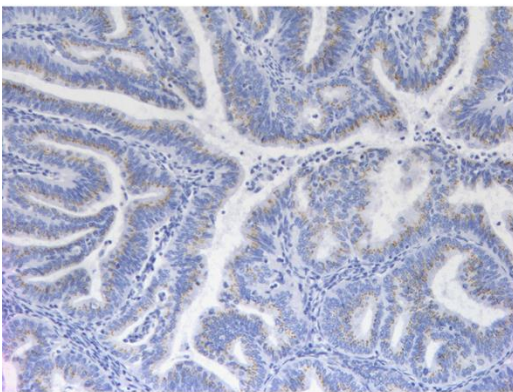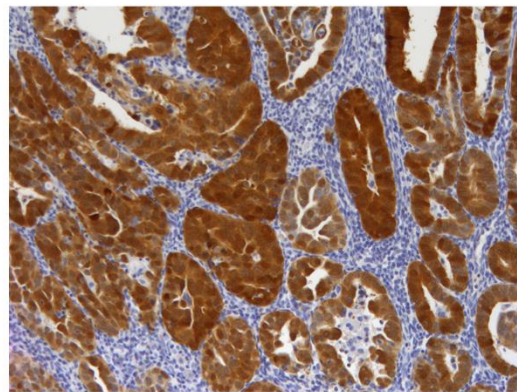
Figure 8. Representative slides for UCHL1 staining in various gynecological tissues.

Scale bar, 100 µm
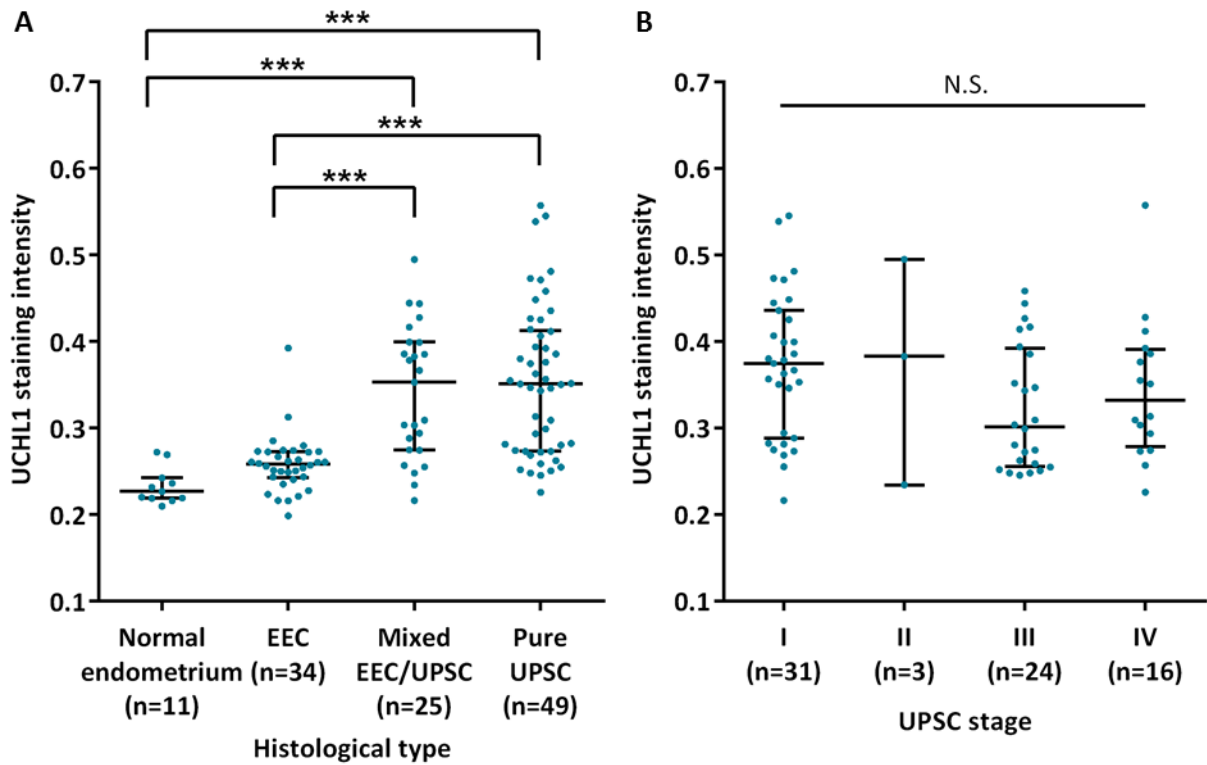
Figure 9. UCHL1 upregulation in UPSC is validated in immunohistochemical staining of an independent cohort of paraffin-embedded tumor samples.

(A) Quantified UCHL1 staining intensity across tissue types. 6 normal samples were from premenopausal women (3 proliferative, 3 secretory), and 5 from postmenopausal women.

(B) UCHL1 staining intensity across stages of UPSC (pure/mixed).

Graphs represent median with interquartile range. N.S. = not significant.

*p<0.05, **p<0.01, ***p<0.001.

Variable	p-value
Age	0.278
Ethnicity	0.142
Purity	0.771
Stage	0.145

Table 5. Association of clinical factors with UCHL1 staining intensity in UPSC paraffin samples.

The Kruskal-Wallis test was used to test for difference in UCHL1 staining intensity across groups. For age, patients were grouped by 10 year intervals. Graphs represent median with interquartile range.

There was no association between UCHL1 expression and survival when analyzing early stage patients alone or all patients together. However, in the 24 late stage patients with no evidence of disease after completion of treatment, high UCHL1 expression was significantly associated with poorer disease-free survival (p=0.031) and overall survival (p=0.028) by univariate analysis (Figure 10A and B). The association between high UCHL1 expression and overall survival remained significant with multivariate analysis, while a similar trend was seen for disease-free survival (Table 6). Overall, this suggests that UCHL1 affects the clinical outcome of late-stage UPSC patients rather than early-stage patients.
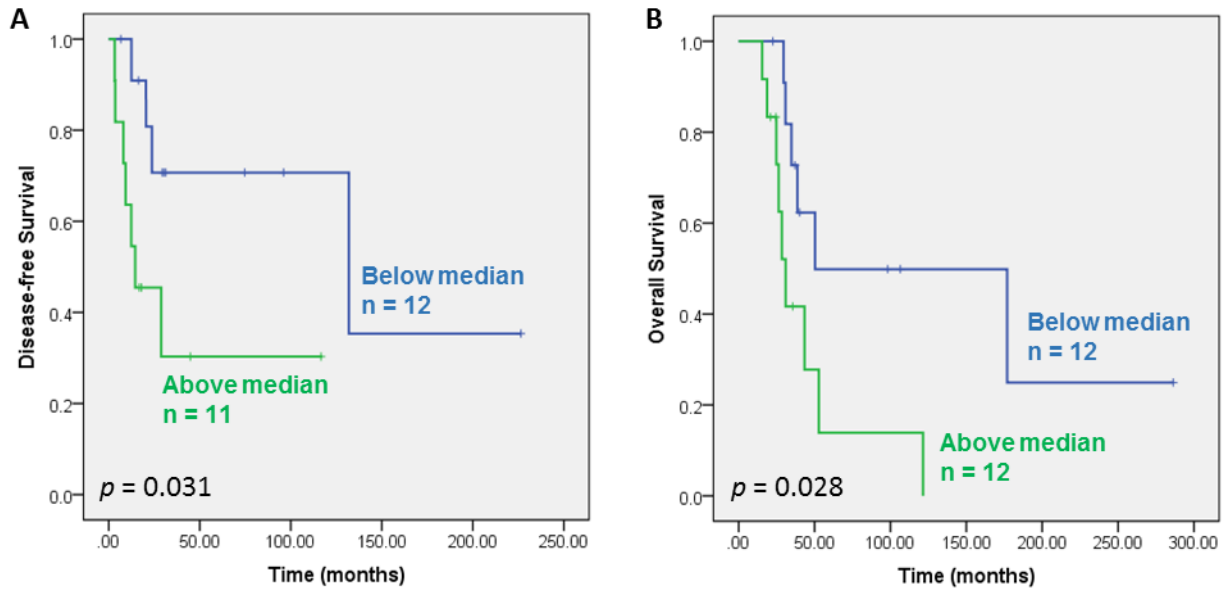
Figure 10. High UCHL1 staining intensity exhibits a trend towards poorer disease-free and overall survival in late-stage UPSC patients.

Kaplan-Meier analysis of (A) disease-free and (B) overall survival of UPSC patients grouped above and below the median UCHL1 staining intensity. Analysis is of late-stage UPSC patients with no evidence of disease after treatment. Cases with missing survival data have been excluded. *p* = p-value.

Variable	Disease-free survival					Overall survival				
	Pts (n)	Events (n)	HR	95% CI	*p*	Pts (n)	Events (n)	HR	95% CI	*p*
Age										
	23	11	0.98	0.90-1.07	0.636	24	15	1.01	0.93-1.10	0.754
Histology*										
Pure UPSC	18	9	1.00	Reference		19	12	1.00	Reference	
Mixed: EEC/UPSC	6	2	1.05	0.20-5.56	0.958	5	3	0.60	0.15-2.51	0.487
Stage*										
III	15	6	1.00	Reference		15	8	1.00	Reference	
IV	9	5	3.23	0.78-13.39	0.105	9	7	3.70	1.05-12.98	0.041[a]
UCHL1 expression*										
Below median	12	4	1.00	Reference		12	6	1.00	Reference	
Above median	11	7	3.89	0.92-16.51	0.065	12	9	3.99	1.18-13.51	0.026[a]

Table 6. Cox regression analysis of late-stage UPSC patients with no evidence of disease after treatment.

Cases with missing survival information were excluded from analysis.

Pts = patients; HR = hazard ratio; CI = confidence intervals; *p* = p-value; * = categorical variable; a = statistically significant.

Conclusion

In this chapter, we demonstrated that UPSC is genetically distinct from low-grade EEC but shares some similarities with grade 3 EEC. By performing SAM analysis to compare the RNA expression profiles of UPSC vs. low-grade EEC and UPSC vs. normal endometrial tissue, we found *UCHL1* expression to be significantly higher in UPSC than both low-grade EEC and normal endometrium; high expression was also associated with poorer overall survival. This was validated by immunohistochemical staining of an independent cohort of patient samples, where high UCHL1 staining intensity was associated with poorer disease-free and overall survival in late-stage patients by univariate analysis, and with poorer overall survival by multivariate analysis. Taken together, this suggests that UCHL1 has an oncogenic role in UPSC.

CHAPTER 4:

UCHL1 PROMOTES TUMOR CELL PROLIFERATION IN UPSC

Specific Aim 2. To delineate the functional role of UCHL1 in UPSC tumor progression.

UCHL1 is a deubiquitinating enzyme in the family of ubiquitin carboxyl-terminal hydrolases and is primarily located in the cytoplasm, with possible transient localization to the nucleus [112]. Both oncogenic and tumor suppressive functions have been described for UCHL1 in a variety of cancer types. Transgenic mice overexpressing UCHL1 under a ubiquitous promoter developed spontaneous lipomas, lymphomas and lung adenomas [132]. Further studies using immortalized human B-cell lines showed that UCHL1 promoted cell proliferation and survival. UCHL1 has also been implicated in cell invasion and motility in lung, colorectal and prostate cancer cells [140, 141], as well as epithelial-to-mesenchymal transition in prostate cancer [142].

On the other hand, silencing of UCHL1 has been reported in breast carcinoma cell lines compared to normal breast tissue and mammary epithelial cells [143], nasopharyngeal carcinoma cells [124] and in human prostate cancer samples [127]. Reintroduction of UCHL1 suppressed colony formation and proliferation through G0/G1 cell cycle arrest and apoptosis in breast carcinoma cell lines [143]; induced apoptosis in nasopharyngeal cell lines [124]; and reduced proliferation and anchorage-independent growth in prostate cancer cells [127].

The functional role of UCHL1 in endometrial cancer remains unknown. Upregulation of UCHL1 in UPSC compared to normal tissue and an association with worse prognosis indicate an oncogenic function; we therefore sought to determine how its expression contributed to UPSC aggressiveness.

siRNA-mediated silencing of UCHL1 reduces proliferation of UPSC cell lines *in vitro*

To determine the role of UCHL1 in UPSC progression *in vitro*, UCHL1 expression was first measured in a panel of type I and II endometrial cell lines. UCHL1 RNA and protein expression was

detected in all type II cell lines except ACI-158, as well as in poorly differentiated MFE-280 and the moderately differentiated MFE-296 cell line of unknown histological origin (Figure 11A and B). All type II cell lines were *TP53*-mutants (Figure 12), similar to the observation of *TP53* mutation in the majority of UPSC tumors. On the other hand, cell lines derived from type I endometrial tumors did not show any detectable UCHL1.
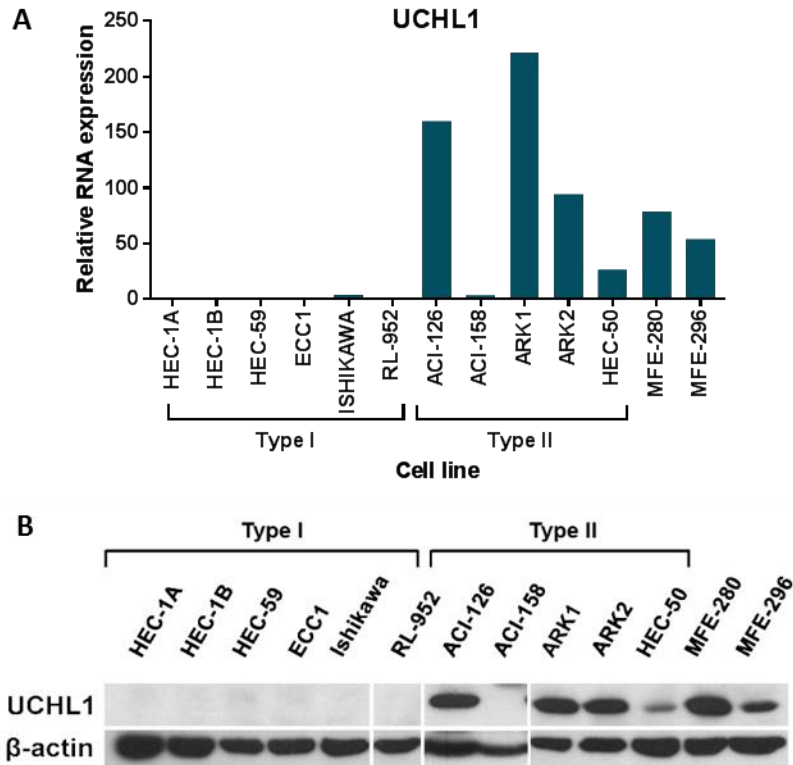
Figure 11. UCHL1 is expressed in type II endometrial cancer cell lines.

(A) Quantification of *UCHL1* RNA expression in endometrial cancer cell lines by qRT-PCR.

(B) Western blot analysis of UCHL1 protein expression in endometrial cancer cell lines.
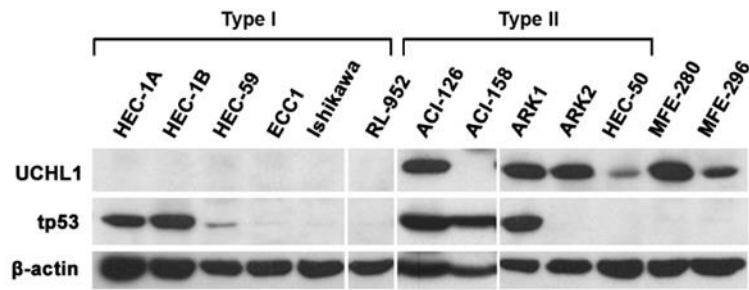
Cell line	P53 status	p53 mutation
ACI-126	GOF	P72R, R248Q
ACI-158	GOF	R248W
ARK1	GOF	R248L
ARK2	null	Q165*
HEC50	null	Intron 6 splice mutant
MFE-280	null	c.919+1G>C
MFE-296	null	Y220C, R306*

Figure 12. All type II endometrial cancer cell lines are *TP53*-mutant.

Using UPSC cell lines ARK1 and ARK2, the effect of UCHL1 silencing on apoptosis, migration and proliferation was determined. Significant knockdown of UCHL1 was achieved at 72 hours after siRNA transduction (Figure 13).
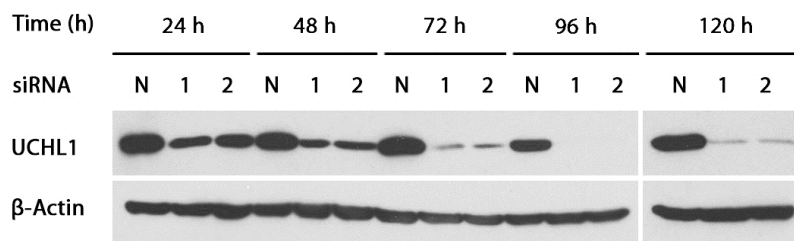
Figure 13. Silencing of UCHL1 in ARK1 cells following transfection with UCHL1 siRNA.

N = control siRNA; 1 = UCHL1 siRNA #1; 2 = UCHL1 siRNA #3

We did not observe any significant change in apoptosis (Figure 14) or migration following UCHL1 silencing (Figure 15). In addition, sensitivity to paclitaxel and cisplatin was not increased in UCHL1-silenced cells (Figure 16). However, we did observe by the MTT assay a significant reduction in the growth rate of cells transfected with UCHL1 siRNA compared to those transfected with control siRNA (Figure 17A). On the other hand, siRNA transfection in the UCHL1-negative ACI-158 UPSC cell line did not significantly affect cell proliferation (Figure 17B). These results suggest that UCHL1 expression increases the cell proliferation of UPSC tumor cells *in vitro*.
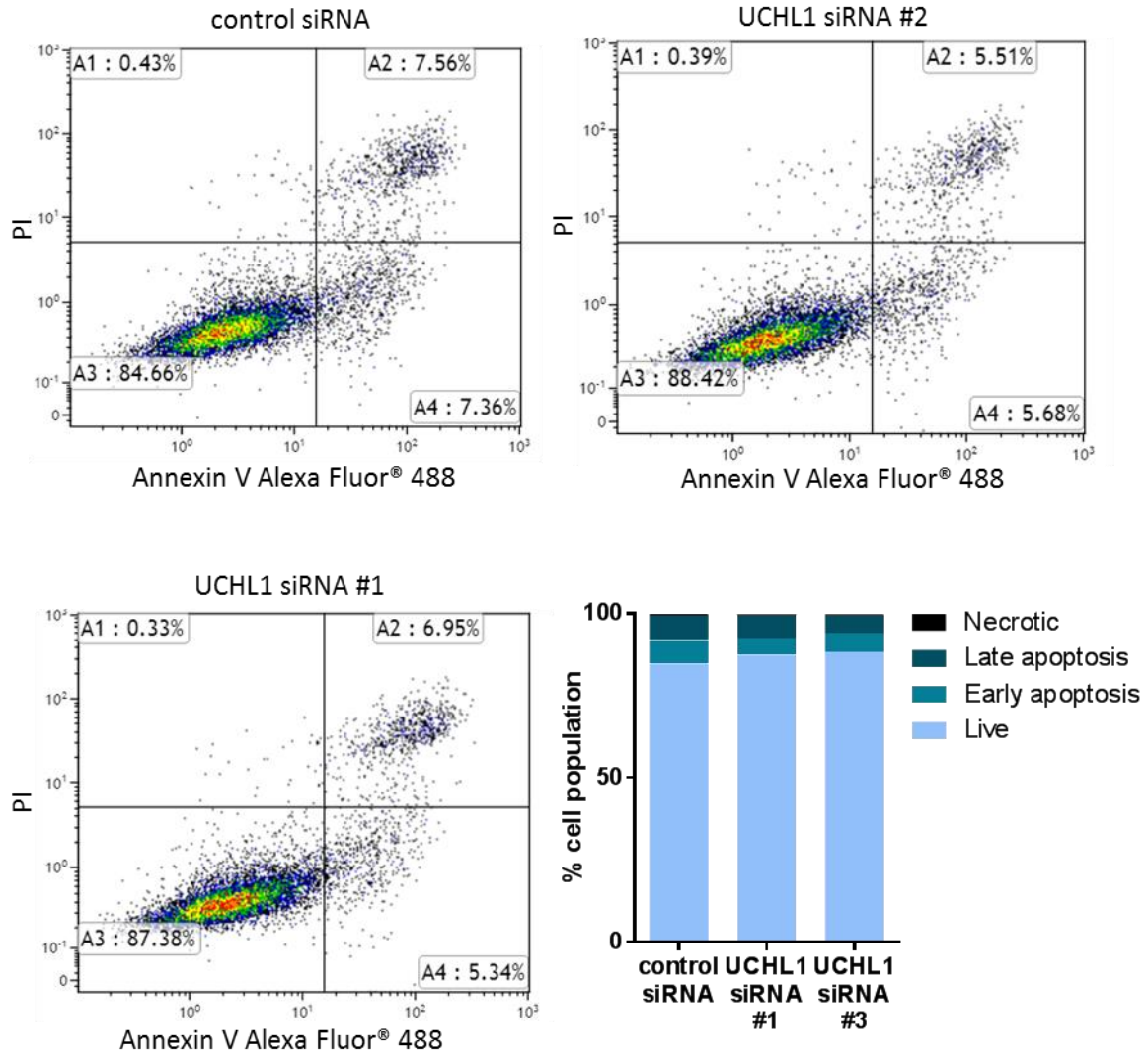
Figure 14. UCHL1 knockdown does not affect apoptosis in ARK cells.

Apoptosis was measured four days after tranfection with control or UCHL1-silencing siRNA by

labelling with annexin V Alexa Fluor 488 and propidium iodide.
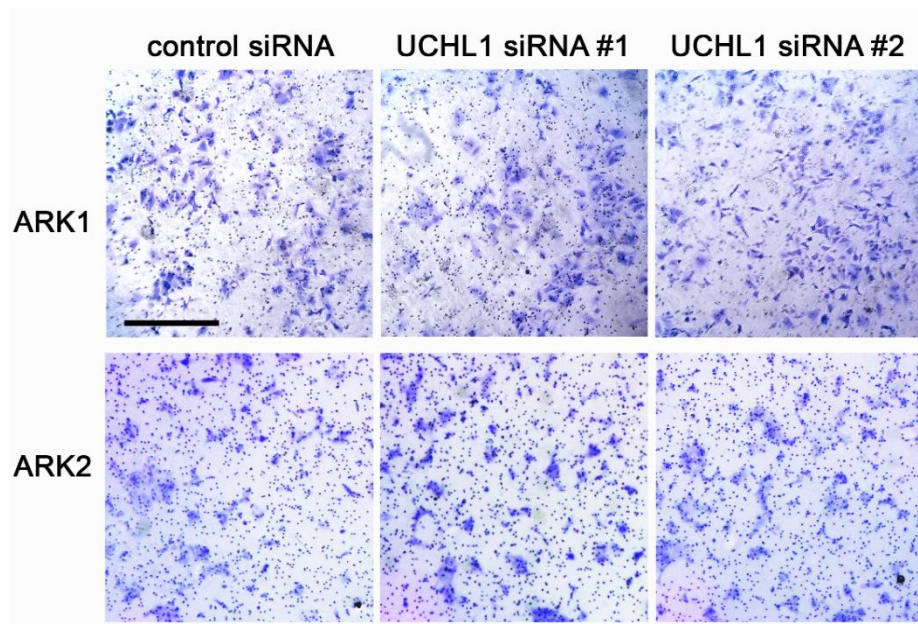
Figure 15. UCHL1 knockdown does not affect migration of ARK1 and ARK2 cells.

Four days after siRNA transfection, equal numbers of ARK1 and ARK2 cells were seeded onto 8 µm

transwell inserts. 24 hours later, migrated cells were visualized by crystal violet staining.

Scale bar, 500 µm.
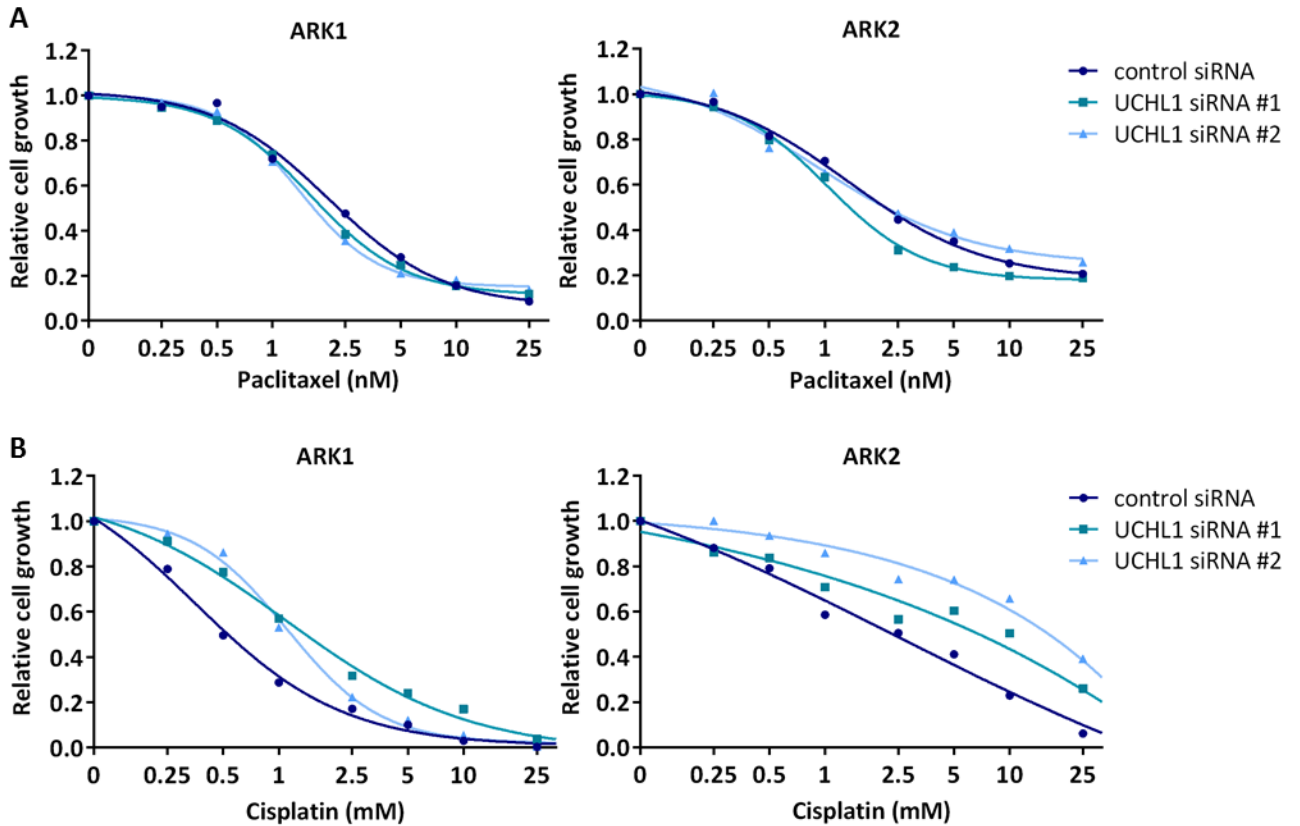
Figure 16. UCHL1 expression does not increase tumor cell resistance to paclitaxel or cisplatin

in vitro.

Following siRNA-mediated knockdown of UCHL1, ARK1 and ARK2 cells were treated with

paclitaxel or cisplatin for three days before cell growth measurement by MTT assay.

(A) Dose-response curve for paclitaxel treatment.

(B) Dose-response curve for cisplatin treatment.
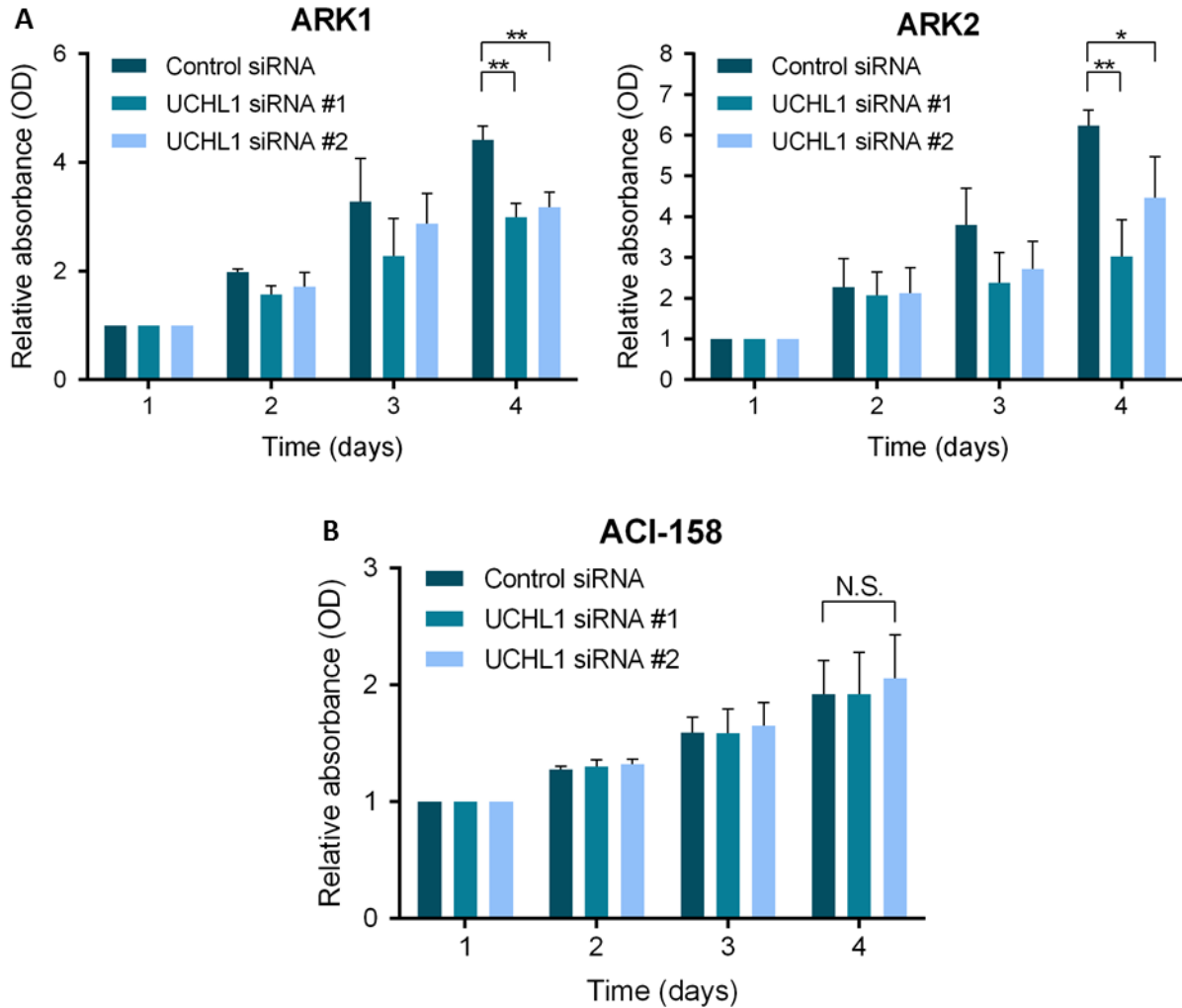
Figure 17. UCHL1 knockdown reduces UPSC cell proliferation *in vitro*.

Effect of UCHL1 knockdown on cell proliferation of (A) the UCHL1-positive ARK1 and ARK2 cells

and (B) UCHL1-negative ACI-158 cells *in vitro*, as measured by the MTT assay.

Graph represents mean ± SD. *p<0.05, **p<0.01, ***p<0.001.

Doxycyline-inducible shRNA-mediated silencing of UCHL1 reduced tumor growth *in vivo*

To determine whether UCHL1 stimulates UPSC cell proliferation *in vivo*, we utilized luciferase-labelled ARK1 cells transduced with doxycycline-inducible control shRNA (ARK1-luc-dox-shNT) or anti-UCHL1 shRNA (ARK1-luc-dox-shUCHL1). Successful doxycycline-induced silencing of UCHL1 was first confirmed *in vitro* (Figure 18).
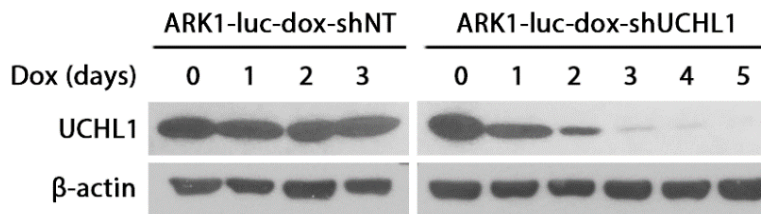
Figure 18. Doxycyline-induced UCHL1 knockdown in ARK1 cells.

Cells were cultured in medium with 2µg/ml doxycycline.

Control cells and knockdown cells were injected intraperitoneally into two groups of nude mice, which were then switched to a doxycycline diet (Figure 19A), followed by measurement of *in vivo* bioluminescence every two weeks. By week ten, the control group had significantly higher luciferase activity (Figures 19B and 19C), suggesting that UCHL1 contributes to tumor growth *in vivo*. We also observed a trend towards improved overall survival in mice injected with ARK1-luc-dox-shUCHL1 (Figure 19D).
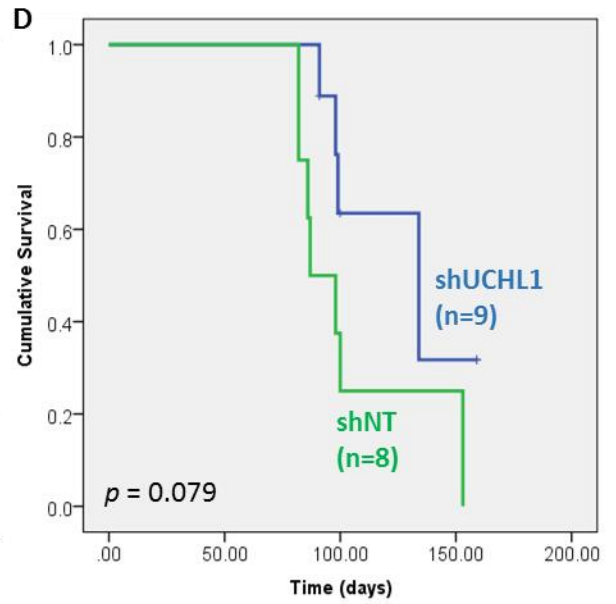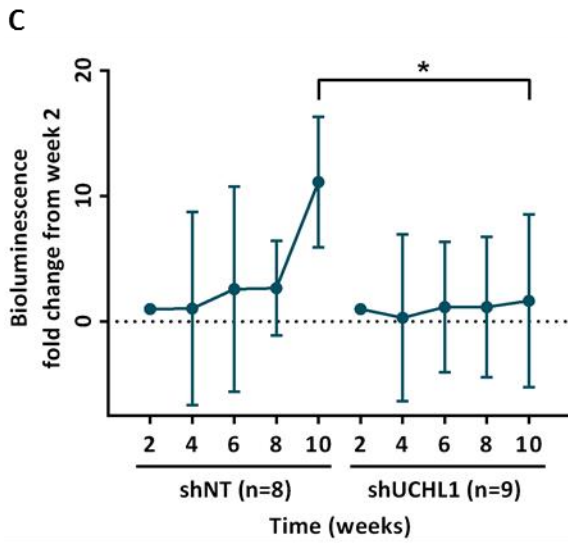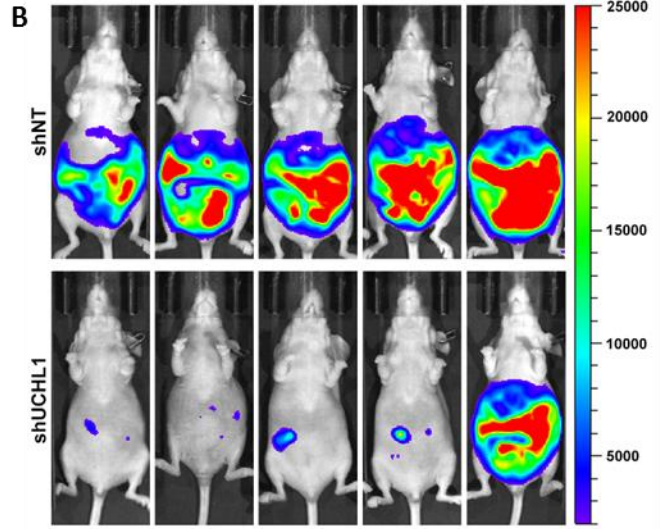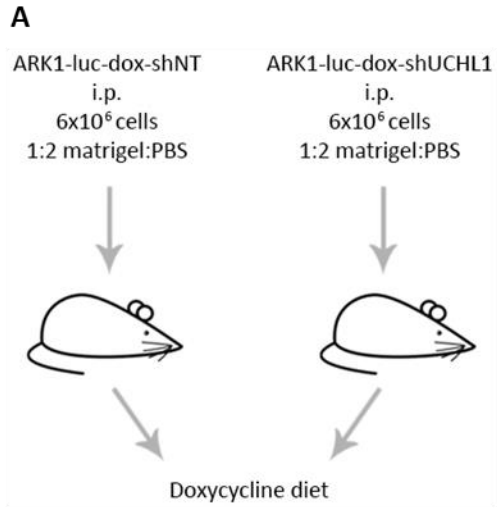
Figure 19. UCHL1 knockdown reduces UPSC cell proliferation *in vivo*.

(A) Luciferase-labelled ARK1 cells transduced with doxycycline-inducible control shRNA or anti-UCHL1 shRNA were injected intraperitoneally into nude mice; mice were then switched to a doxycycline diet (625 mg/kg).

(B) Representative images of *in vivo* bioluminescence imaging at week 10. Mice with bioluminescent intensities nearest to the mean are shown.

(C) Geometric mean of the fold change in *in vivo* bioluminescence intensity relative to week 2. Standard deviation was calculated from log2 fold change and converted back to linear values. The Mann-Whitney test was used to test for significant differences between log2 fold changes. Graph represents mean ± SD.

(D) Kaplan-Meier survival curves of nude mice injected with ARK1 cells transduced with doxycycline-inducible control shRNA or anti-UCHL1 shRNA.

p = p-value. *p<0.05, **p<0.01, ***p<0.001.

LDN-57444 treatment *in vivo* reduces tumor growth and improves overall survival

As UCHL1 promotes tumorigenesis of UPSC, we sought to determine if suppressing UCHL1 activity by UCHL1 inhibitors would reduce tumor growth and improve survival. To do so, we again established UPSC tumors *in vivo* and treated the mice thrice weekly with intraperitoneal injection of the small-molecule UCHL1 inhibitor, LDN-57444 [261] (Figure 20A). There was no significant drop in body weight, suggesting a lack of systemic toxicity (Figure 20B). By week 6, the treatment group had significantly lower bioluminescence than the control group, indicating that LDN-57444 treatment had an anti-proliferative effect on ARK1 cells *in vivo* (Figure 20C-E). Furthermore, the treatment group showed improved overall survival, with a mean survival time of 68.1 days compared to 56.9 days for the control group (Figure 20F). These results suggest that targeting of UCHL1 would aid in the management of UPSC.

A ARK1-luc-dox-NT
i.p.
6×10^6 cells
1:2 matrigel:PBS

PBS control
0.25% DMSO
0.5% ethanol

LDN-57444
0.5 mg/kg

B Mouse weights

C

D

E

F
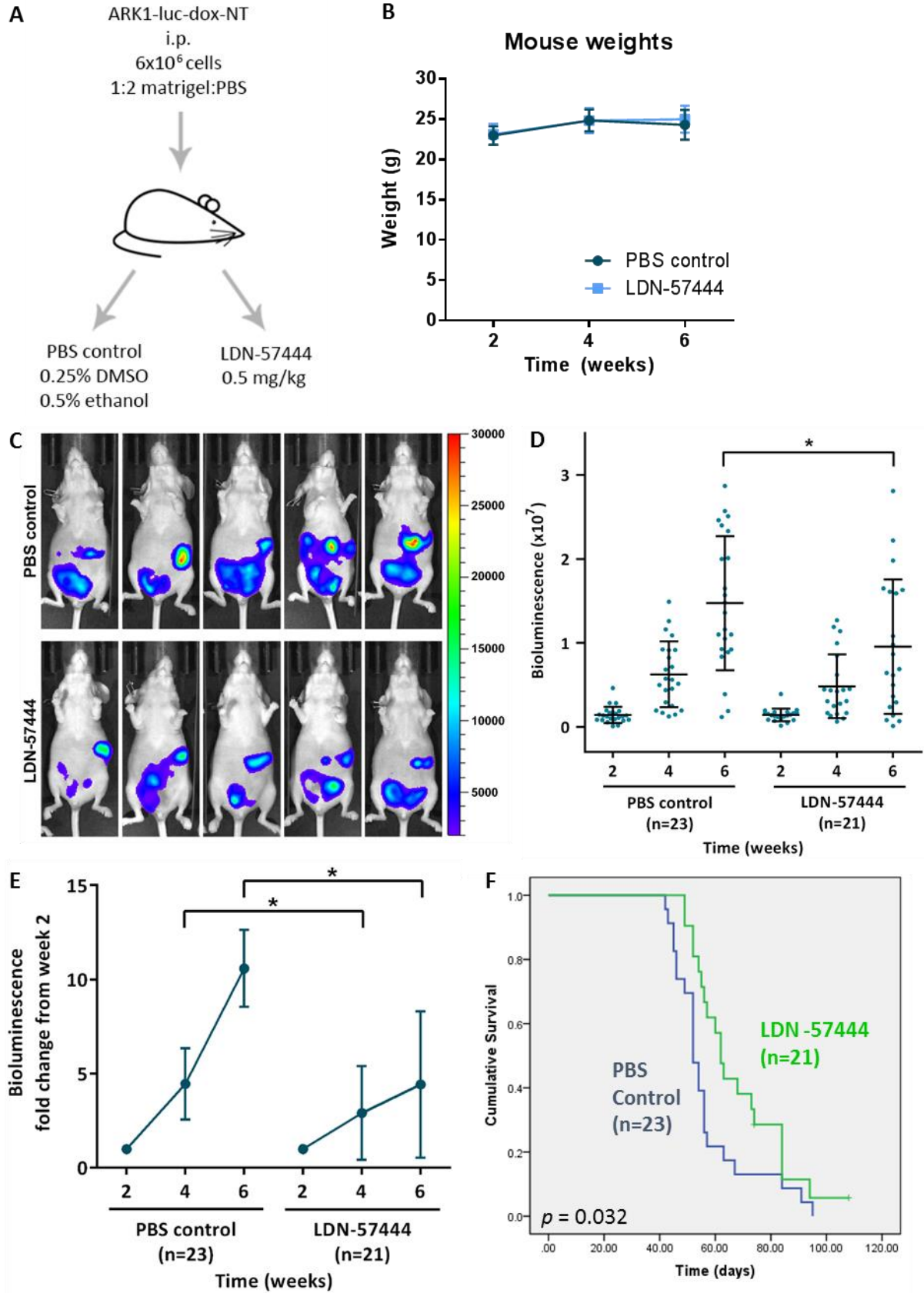
Figure 20. LDN-57444 exhibits anti-proliferative effect *in vivo*.

(A) Luciferase-labelled ARK1 cells were injected intraperitoneally into nude mice; after 2 weeks, mice were treated thrice weekly with PBS control or LDN-57444.

(B) Mouse weights of nude mice following treatment with PBS control (0.5% DMSO, 2.5% ethanol) or 0.5 mg/kg LDN-57444.

(C) Representative images of *in vivo* bioluminescence imaging at week 6. Mice with bioluminescent intensities nearest to the mean are shown.

(D) *In vivo* bioluminescence of tumors at week 2, 4 and 6.

(E) Geometric mean of the fold change in *in vivo* bioluminescence intensity relative to week 2. Standard deviation was calculated from log2 fold change and converted back to linear values. The Mann-Whitney test was used to test for significant differences between log2 fold changes.

(F) Kaplan-Meier survival curves of the LDN-57444 treatment group and control group.

Graphs represent mean ± SD. *p* = p-value. *$p<0.05$, **$p<0.01$, ***$p<0.001$.

Conclusion

In this chapter, we demonstrated that UCHL1 is expressed in type II and poorly differentiated endometrial cell lines. UCHL1 knockdown did not affect apoptosis or migration, or increase sensitivity to paclitaxel or cisplatin. However, UCHL1 silencing reduced cell proliferation *in vitro* and tumor growth *in vivo*. In addition, inhibition of UCHL1 *in vivo* by the UCHL1-specific small-molecule inhibitor LDN-57444 reduced tumor growth and improved overall survival in nude mice.

CHAPTER 5:

UCHL1 PROMOTES CYCLIN B1 PROTEIN STABILITY

AND CELL CYCLE PROGRESSION

Specific Aim 3. To determine the mechanisms through which UCHL1 modulates UPSC tumor progression.

UCHL1 has been reported to interact with a variety of targets in different cancer types. As a deubiquitinating enzyme with reported dual ubiquitin hydrolase/ligase function [106], UCHL1 has been shown to interact with and affect the stability of various proteins. UCHl1 interacts with JAB1 in lung cancer cells, resulting in nuclear translocation and promotion of p27 degradation [112]. In nasopharyngeal cancer cells, UCHL1 forms a complex with p53, p14^{ARF} and MDM2, promoting degradation of MDM2 and stabilization of p53/p14^{ARF} [124]. In colorectal cancer, UCHL1 carries out its oncogenic function by stabilizing β-catenin through its deubiquitinating activity [150]. UCHl1 also interacts with and enhances the kinase activity of the cyclin-dependent kinases 1, 4 and 5 to increase cell proliferation, independent of its deubiquitinating function [147].

In spite of this, the mechanism through which UCHL1 affects tumor progression of UPSC remains unknown. We therefore sought to identify its downstream targets.

Correlation of *UCHL1* RNA expression with proteins in the RPPA data set

To determine potential downstream targets of UCHL1 that mediate the effect of UCHL1 in UPSC progression, we identified genes whose protein expression levels correlated with *UCHL1* RNA expression in the TCGA data. As UCHL1 is a deubiquitinating enzyme, of particular interest were the genes whose expression was associated with UCHL1 expression at the protein level but not at the RNA level, as they were more likely to be direct targets (Figure 21).

Correlation:
RPPA protein expression
(166 proteins)
vs
UCHL1 RNA expression levels

p > 0.05
(159 proteins)

p < 0.05
(17 proteins)

No correlation:
RNA vs UCHL1 RNA
(10 proteins)

Positive correlation
(6 proteins)
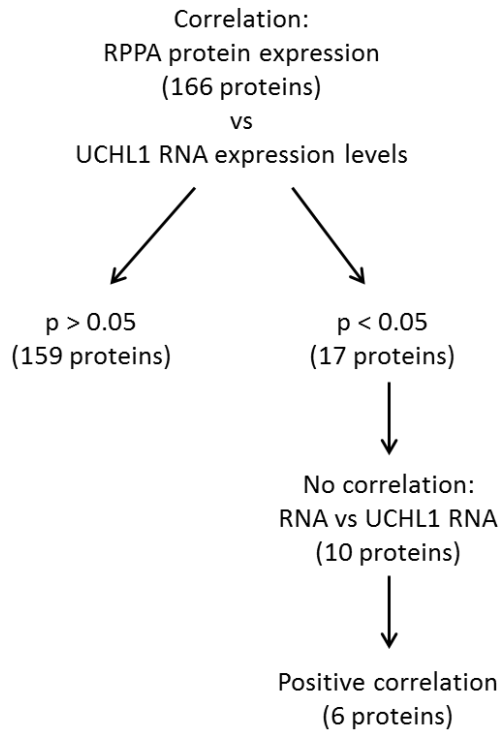
Figure 21. Discovery of potential protein targets of UCHL1.

Using the 22 pure UPSC samples with both RPPA and RNA sequencing data available,

Spearman's test of correlation was performed for each protein probe to measure its strength of

correlation with *UCHL1* RNA expression. Of 166 probes, 17 proteins were significantly correlated at

the protein level (Table 7). Of these, 10 were not correlated at the RNA level with *UCHL1*

expression. 6 of the 10 proteins (cyclin B1, p21, GSK3α, GSK3β, MSH2, RAD50) were positively

correlated with *UCHL1* expression at the protein level, suggesting that their protein stability may be

increased by the deubiquitinating activity of UCHL1.

Entrez ID	Gene	Protein	UCHL1 vs RPPA		UCHL1 vs RNAseq	
			Spearman's coefficient	*p*	Spearman's coefficient	*p*
840	CASP7	Caspase 7	-0.54	0.010[a]	-0.19	.393
841	CASP8	Caspase 8	-0.44	0.039[a]	-0.34	.120
891	CCNB1	Cyclin B1	0.43	0.044[a]	0.31	.164
1026	CDKN1A	p21	0.43	0.045[a]	-0.12	.601
2931	GSK3A	GSK3α	0.55	0.008[a]	-0.07	.759
2932	GSK3B	GSK3β	0.55	0.008[a]	0.09	.687
3485	IGFBP2	IGFBP2	0.45	0.036[a]	0.50	.018[a]
8821	INPP4B	INPP4B	-0.50	0.017[a]	-0.63	.002[a]
3725	JUN	c-Jun	0.51	0.015[a]	0.60	.003[a]
3932	LCK	LCK	-0.47	0.028[a]	-0.55	.009[a]
4233	MET	c-Met	-0.58	0.005[a]	-0.49	.020[a]
4436	MSH2	MSH2	0.59	0.004[a]	0.14	.533
2956	MSH6	MSH6	0.56	0.006[a]	0.45	.035[a]
57111	RAB25	RAB25	-0.60	0.003[a]	0.06	.805
10111	RAD50	RAD50	0.45	0.035[a]	-0.18	.417
7408	VASP	VASP	-0.46	0.030[a]	-0.63	.002[a]
7515	XRCC1	XRCC1	-0.42	0.049[a]	0.15	.503

Table 7. Proteins significantly correlated with *UCHL1* RNA expression in the TCGA dataset.

Genes from the RPPA dataset were analyzed by Spearman's correlation to identify proteins

significantly correlated with *UCHL1* RNA expression in 22 pure UPSC samples. RNA expression

data was extracted for significant genes and correlation analysis was again performed against *UCHL1*

RNA expression.

p = p-value; a = statistically significant.

UCHL1 upregulates cyclin B1 protein expression

While MSH2 and RAD50 are involved in DNA mismatch repair [262] and double-strand break repair [263, 264] respectively, cyclin B1, p21, GSK3α and GSK3β are directly involved in pathways that dictate cell proliferation [153, 154, 265, 266]. These four proteins were therefore of particular interest, as our primary observation was an effect of UCHL1 on UPSC proliferation. UCHL1 has also been reported to affect the protein stability of cell cycle-related proteins p27 [112], p53 [124] and β-catenin [150]. Although these were not significantly correlated with UCHL1 in the TCGA RPPA dataset, we also sought to determine if UCHL1 increased p53 and β-catenin proteins levels or reduced p27 protein levels *in vitro* as previously described.

Following siRNA-mediated silencing of UCHL1, we could not observe a consistent decrease in p21, GSK3α or GSK3β protein level (Figure 22). We also did not see a change in p53 or β-catenin protein by western blot after UCHL1 silencing; the change in p27 levels was not consistent across the two cell lines. In contrast, siRNA-mediated silencing of UCHL1 led a reduction in cyclin B1 levels in ARK1, ARK2 and HEC-50 cells compared with cells transfected with control siRNA (Figure 23A). Cyclin D1 and cyclin E levels were largely unchanged. In addition, the RNA level of cyclin B1 after transfection was not significantly lower than cells transfected with control siRNA (Figure 23B), suggesting that the reduction in cyclin B1 protein level was due to changes in protein stability and not due to reduced RNA transcription. Conversely, transient expression of UCHL1 in UCHL1-negative ACI-158 cells led to increased protein levels of cyclin B1 (Figure 23C). Cyclin B1 was therefore of particular interest, due to its role as a positive regulator of cell cycle progression that could potentially mediate the effects of UCHL1 on increased cell proliferation.
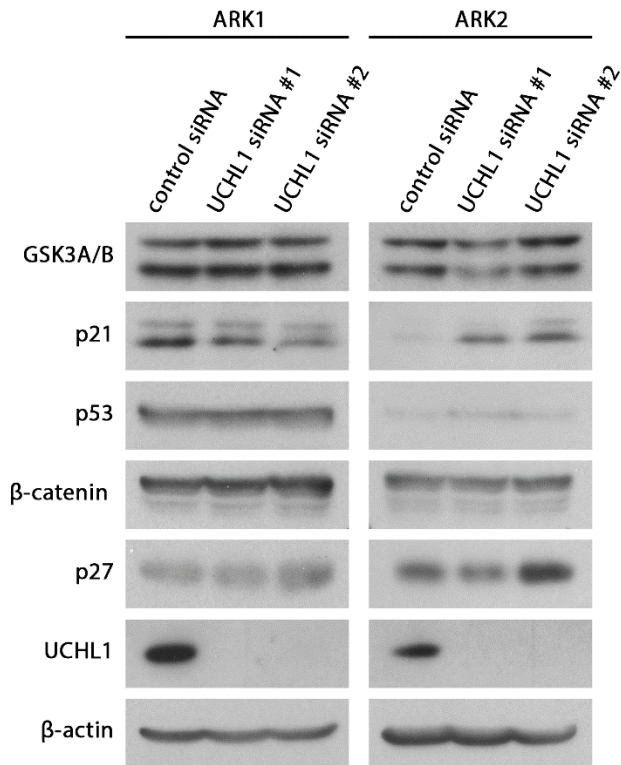
Figure 22. The effect of UCHL1 silencing on the protein levels of genes involved in cell cycle and proliferation.

Western blot was performed four days after transfection with control or anti-UCHL1 siRNA in ARK1 and ARK2 cells.
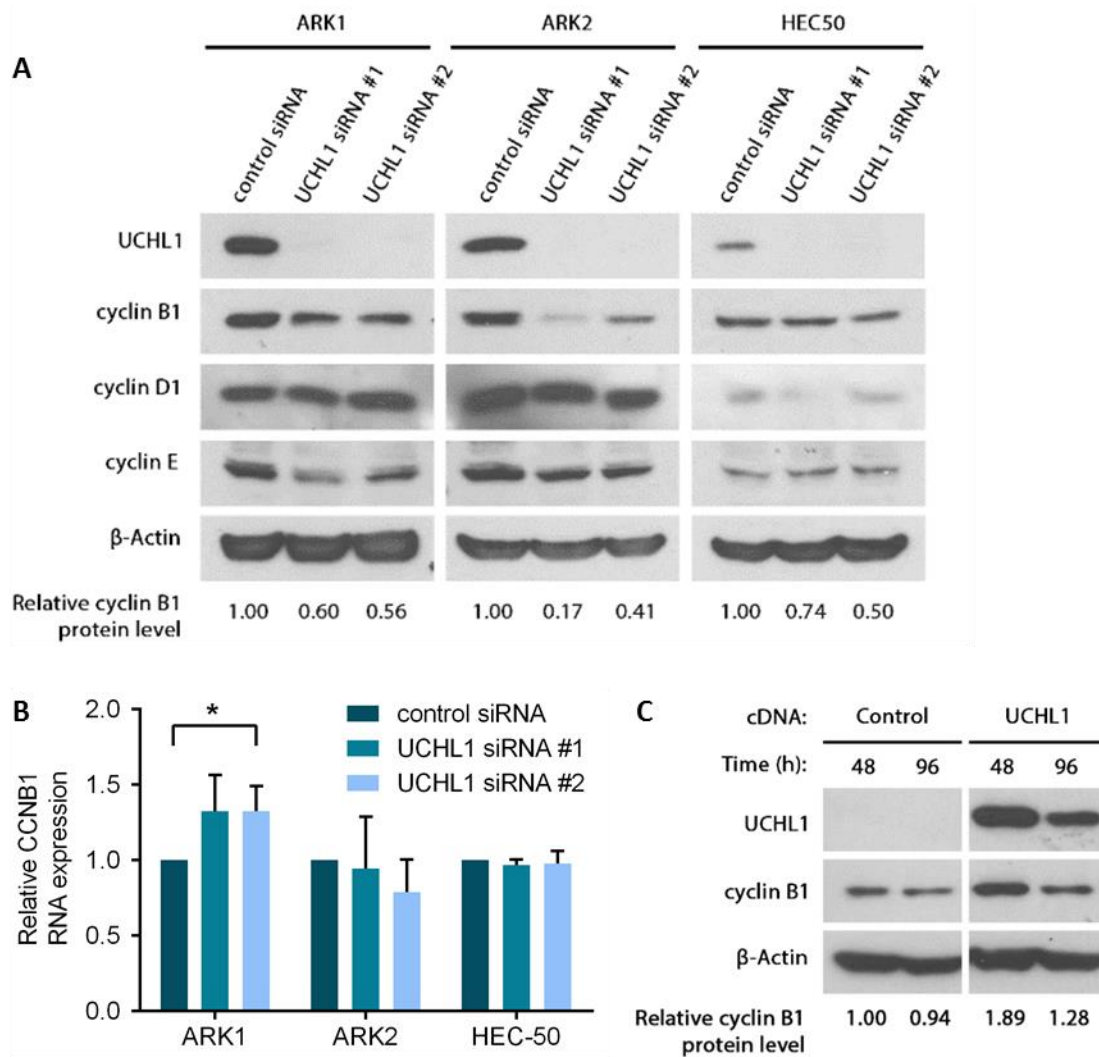
Figure 23. UCHL1 upregulates cyclin B1 protein expression *in vitro*.

(A) Expression of cyclin proteins four days after transfection with control or anti-UCHL1 siRNA in ARK1, ARK2 and HEC-50 cells.

(B) qRT-PCR quantification of cyclin B1 four days after siRNA-mediated UCHL1 silencing. Graph represents mean ± SD. *p<0.05, **p<0.01, ***p<0.001.

(C) Cyclin B1 expression following transient UCHL1 overexpression in ACI-158 cells.

Cyclin B1 is a positive regulator of cell cycle progression that could potentially mediate the effects of UCHL1 on increased cell proliferation. In comparison, protein expression of the other cyclins in the TCGA RPPA data set, cyclin D1 and E1, were not correlated with UCHL1 expression patients with UPSC (Table 8). Similar to UCHL1, cyclin B1 protein expression was significantly higher in UPSC and grade 3 EEC than in low-grade EEC in the TCGA data set (Figure 24).

Histology	Pts (n)	Cyclin B1		Cyclin D1		Cyclin E1	
		Spearman's coefficient	p	Spearman's coefficient	p	Spearman's coefficient	p
All EC	196	0.334	<0.001[a]	-0.037	0.603	0.333	<0.001 [a]
EEC	171	0.255	<0.001[a]	-0.065	0.401	0.291	<0.001 [a]
Pure UPSC	22	0.433	0.044 [a]	0.163	0.468	-0.137	0.543

Table 8. Protein expression of cyclin proteins against *UCHL1* RNA expression.

Cyclin B, D and E protein expression in the TCGA RPPA dataset were correlated with *UCHL1* RNA expression.

Pts = patients; p = p-value; a = statistically significant.
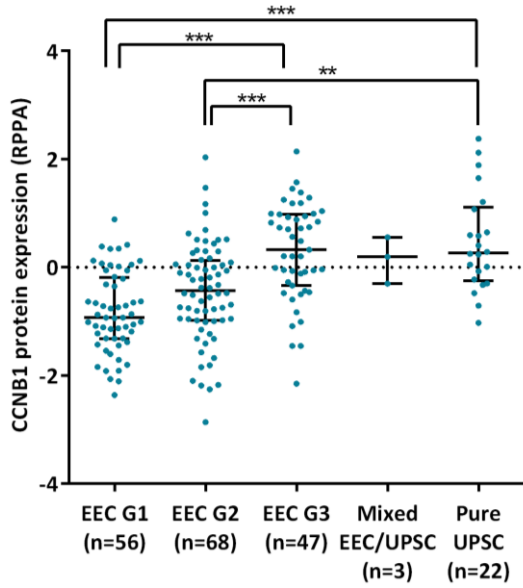
Figure 24. Cyclin B1 protein expression across histological subtypes of endometrial cancer.

Graph represents median with interquartile range. *p<0.05, **p<0.01, ***p<0.001.

To validate the correlation of UCHL1 with cyclin B1 protein levels that we observed in the TCGA

data set, we performed immunohistochemical staining of cyclin B1 in the UPSC samples that were

previously stained for UCHL1. The results showed a significant positive correlation between

percentage of tumor cells positive for cyclin B1 and UCHL1 staining intensity (p=0.009) (Figure 25A

& B).
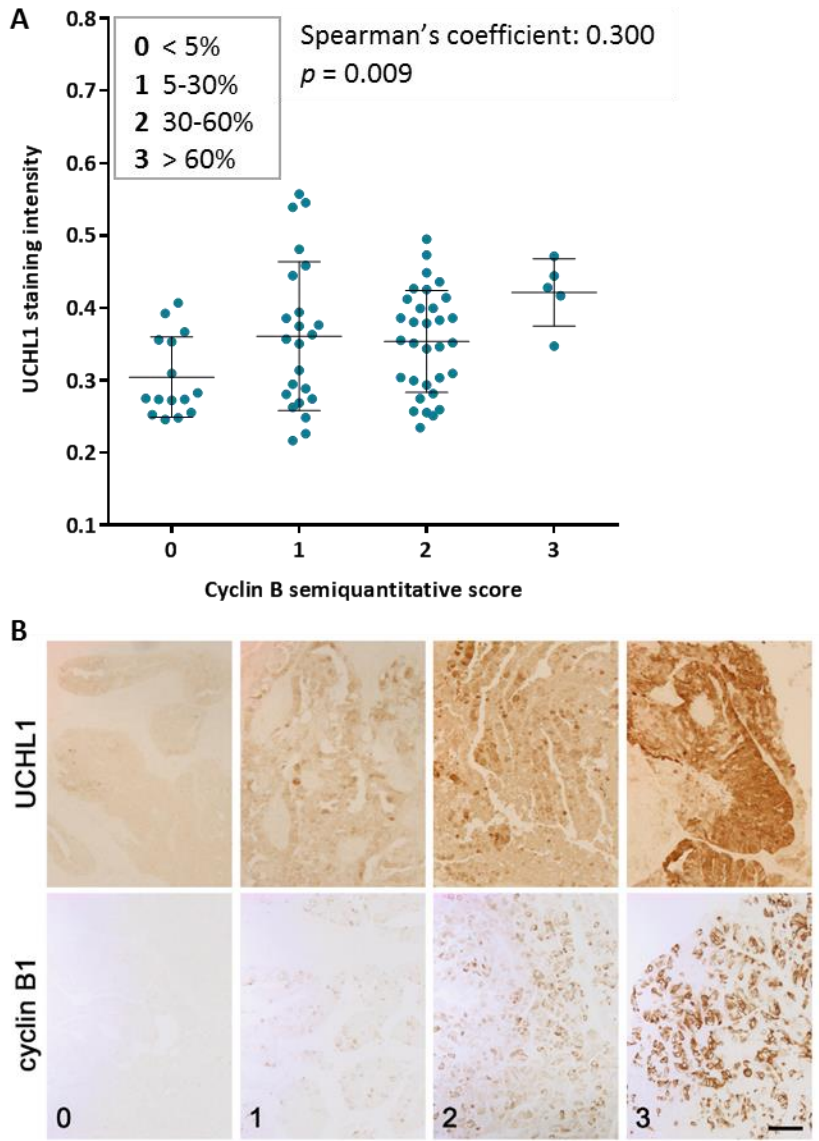
Figure 25. Cyclin B1 positivity correlates with UCHL1 staining intensity.

(A) Correlation between cyclin B1 positivity and UCHL1 staining intensity in the UPSC cohort.

(B) Representative slides of samples stained for both cyclin B1 and UCHL1 with increasing

semiquantitative score. Scale bar, 100 µm.

Graph represents mean ± SD.

To confirm that UCHL1 upregulates cyclin B1 protein expression *in vivo*, immunohistochemical staining of cyclin B1 was performed in the doxycycline-induced control and UCHL1-silenced tumors from our previous mouse study. The results showed that cyclin B1 positivity was reduced in the tumors established from ARK1 cells transduced with doxycycline-inducible UCHL1 shRNA compared to control shRNA (Figure 26A and B), suggesting that UCHL1 upregulates cyclin B1 protein expression *in vivo*.
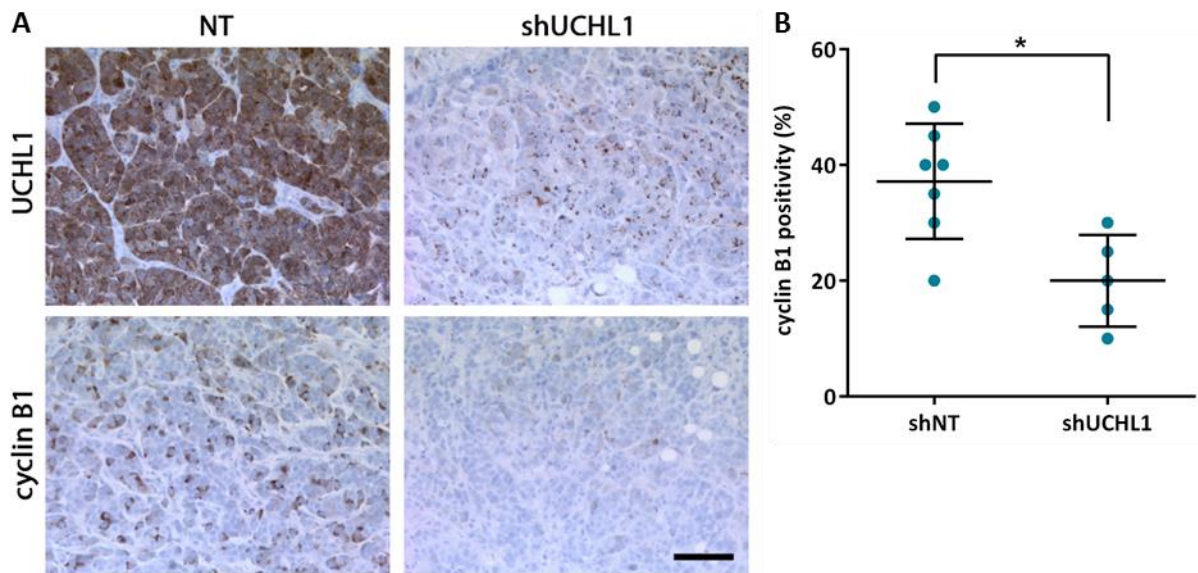
Figure 26. UCHL1 upregulates cyclin B1 protein expression *in vivo*.

(A) Cyclin B1 and UCHL1 staining in tumors that developed following intraperitoneal injection of nude mice with ARK1 cells transduced with doxycycline-inducible control shRNA or anti-UCHL1 shRNA. Scale bar, 100 µm.

(B) Percentage positivity of cyclin B1 in tumor cells at time of sacrifice.

Graph represents mean ± SD. *p<0.05, **p<0.01, ***p<0.001.

UCHL1 interacts with cyclin B1

To delineate the molecular mechanism by which UCHL1 regulates cyclin B1 expression, we first determined whether UCHL1 interacts with cyclin B1 in a protein complex, which is essential for UCHL1 to exert its effect on cyclin B1. To determine if UCHL1 interacted with cyclin B1, co-immunoprecipitation was performed with pull-down of UCHL1 and cyclin B1, which indicated protein-protein interaction between UCHL1 and cyclin B1 (Figure 27).
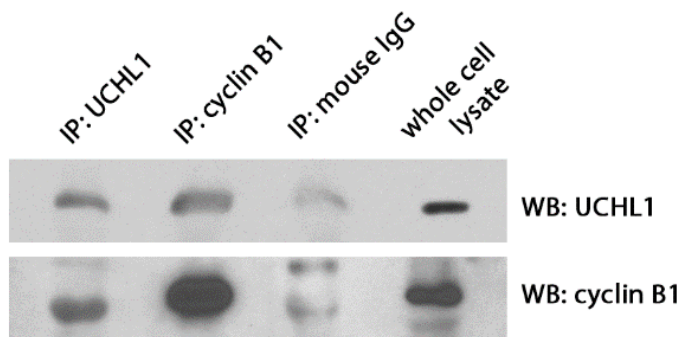
Figure 27. Protein interaction between UCHL1 and cyclin B1 is confirmed by co-immunoprecipitation.

Co-immunoprecipitation was performed using antibodies against UCHL1 and cyclin B1, with normal mouse IgG as a control.

Furthermore, through immunofluorescence imaging UCHL1 and cyclin B1 were shown to colocalize (Figure 28). This was additionally supported by the proximity ligation assay, which revealed red fluorescent spots in ARK1 and ARK2 cells but not UCHL1-negative HEC-1A cells upon co-incubation with anti-UCHL1 and anti-cyclin B1 antibody, indicating an interaction between the two proteins. Additionally, the number of red fluorescent spots observed was considerably lower when ARK1 cells were assayed without primary antibody, with anti-UCHL1 antibody only, or with anti-MMP-13 and anti-cyclin B1 together, as we did not anticipate MMP-13 and cyclin B1 to interact with each other. Similar results were seen with ARK2 probed with anti-UCHL1 antibody only.

89
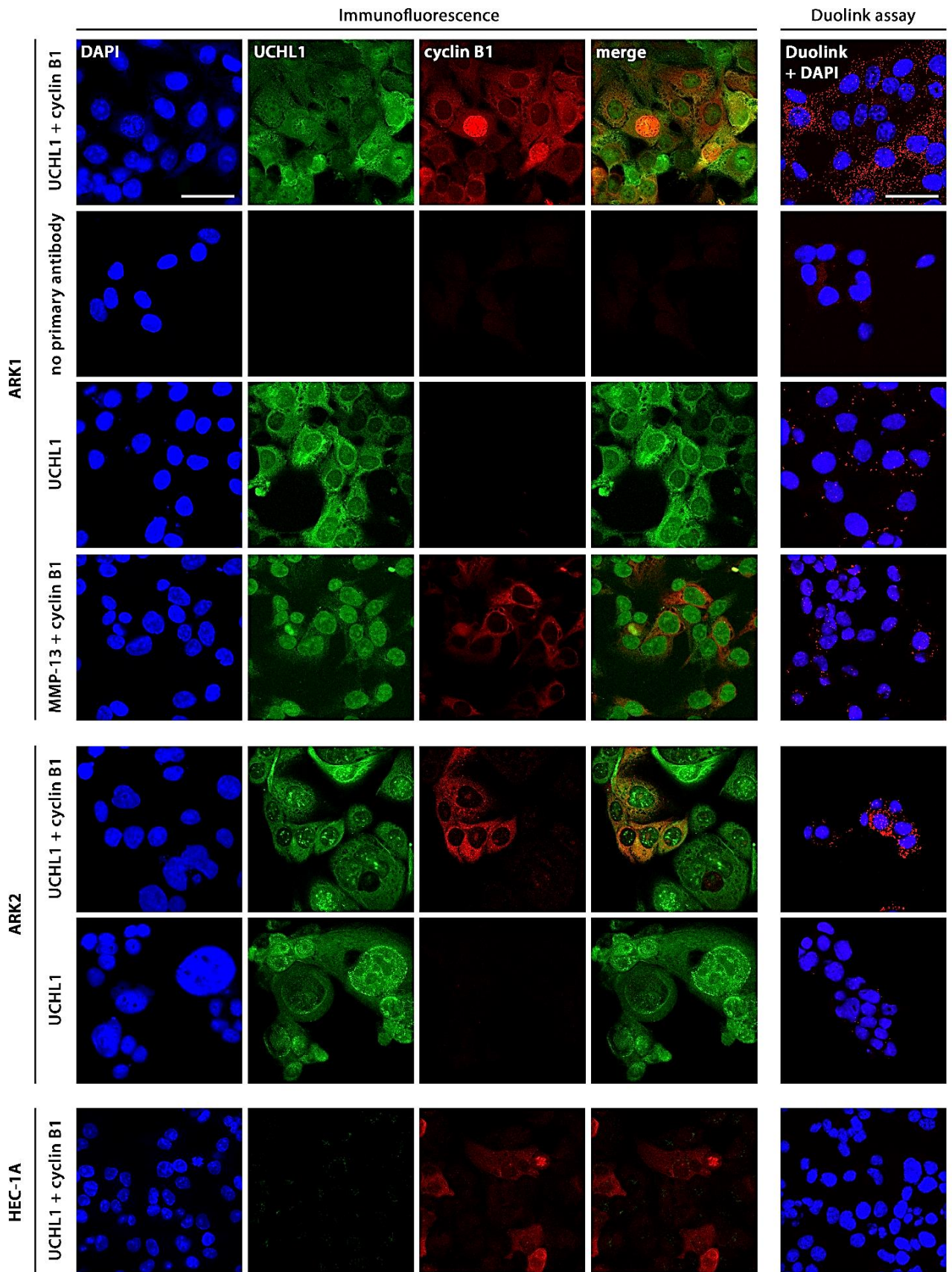
Figure 28. UCHL1 and cyclin B1 colocalize and interact *in vitro*.

Immunofluorescence staining and the Duolink proximity ligation assay was performed on ARK1 and ARK2 cells. As a control, ARK1 cells were also stained without primary antibody, with anti-UCHL1 antibody only, and with anti-MMP-13 and anti-cyclin B1. ARK2 cells were also stained with anti-UCHL1 antibody only; staining of UCHL1-negative HEC-1A cells was also performed. Scale bar, 50 µM.

As previously discussed, in the immunohistochemical analysis of our UPSC patient cohort, we observed strong cytoplasmic staining and occasional nuclear staining of UCHL1. Similarly, immunofluorescence showed that UCHL1 was expressed in both the cytoplasm and nucleus of ARK1 and ARK2 cells (Figure 28). On the other hand, the variation in cyclin B1 expression and localization was more pronounced, with expression observed in the cytoplasm of some cells and in the nucleus in others. Immunofluorescence of ARK1 cells undergoing mitosis indicated that cyclin B1 entered the nuclear space during late interphase (Figure 29); colocalization of UCHL1 and cyclin B1 then persisted through mitosis until degradation of cyclin B1 at the metaphase-anaphase transition. Therefore, the majority of fluorescent spots were in the cytoplasm; however, when cyclin B1 entered the nucleus, interaction between the two proteins was also observed.
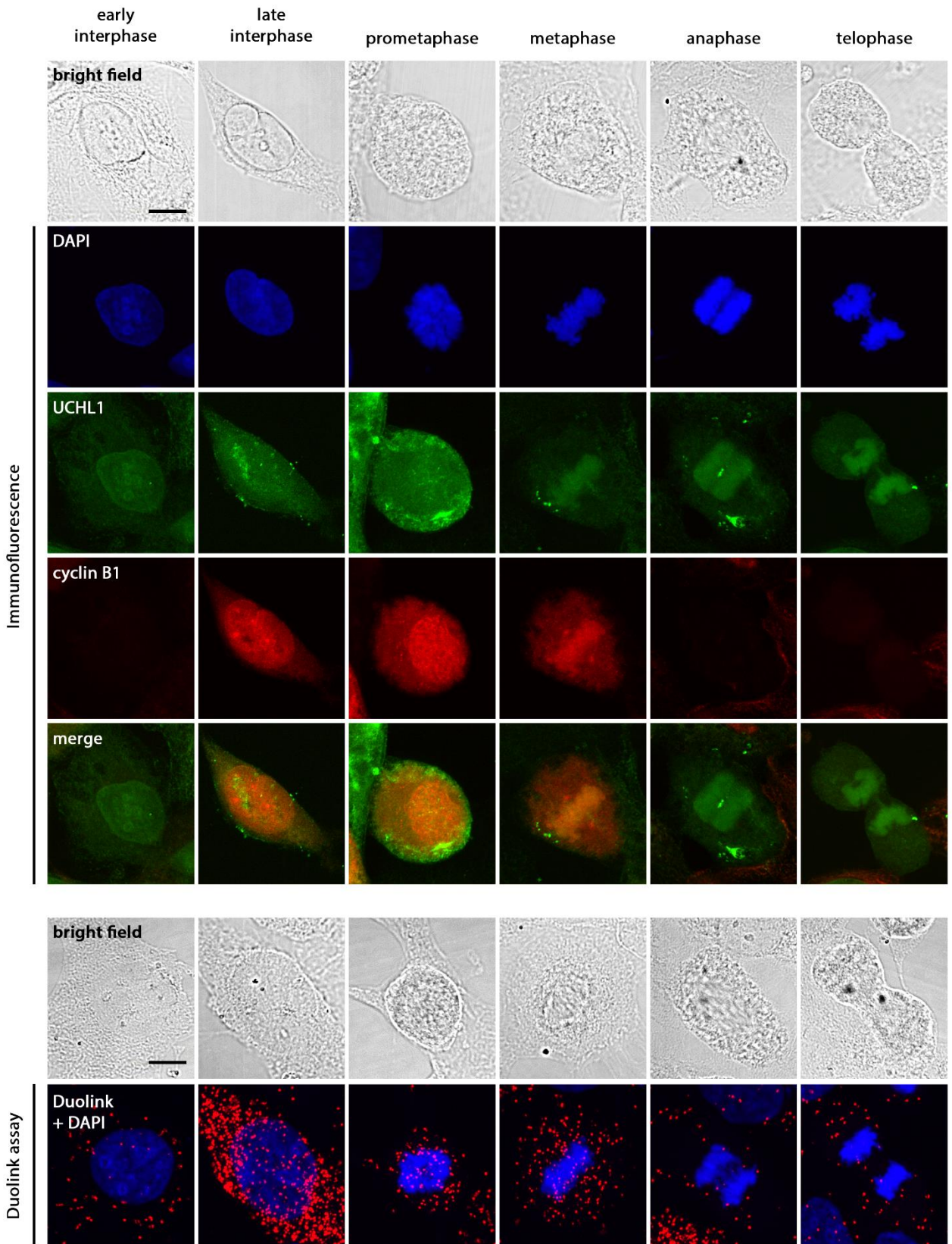
Figure 29. UCHL1 and cyclin B1 interact during interphase and mitosis.

ARK1 cells were synchronized by double thymidine block, then collected 10 hours after release to enrich for mitotic cells. Scale bar, 10 µM.

UCHL1 silencing by siRNA transduction abrogated the fluorescent signal. (Figure 30). Overall, these results suggest that UCHL1 and cyclin B1 are in close proximity and interact with each other in all phases of the cell cycle where cyclin B1 is present.
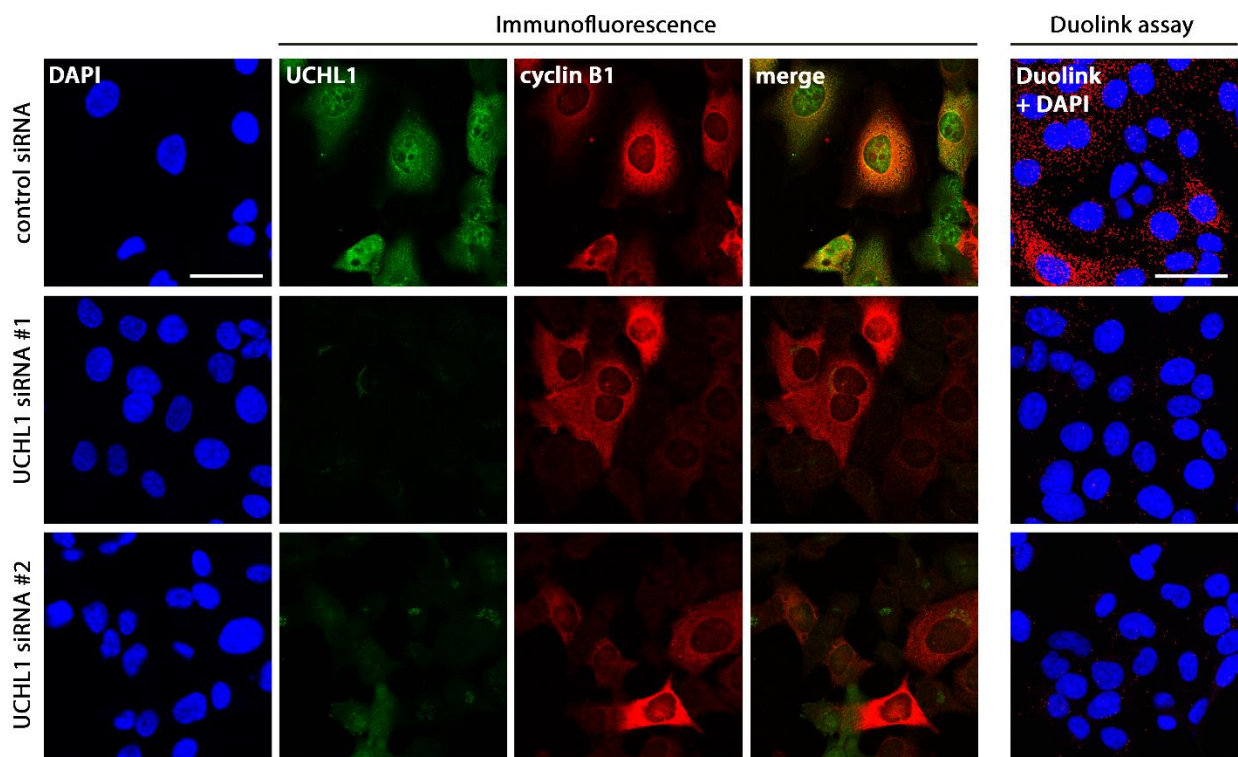
Figure 30. UCHL1 silencing by siRNA transduction abrogates the fluorescent signal representing UCHL1-cyclin B1 interaction.

Immunofluorescence staining and the Duolink proximity ligation assay was performed on ARK1 cells 4 days after transfection with control siRNA or anti-UCHL1 siRNA. Following the Duolink assay, red fluorescent spots indicate presence of protein-protein interaction. Scale bar, 50 µM.

UCHL1 increases protein stability of cyclin B1

Since UCHL1 has been shown to affect the protein stability of target proteins in other cancer types by altering their ubiquitination [124, 150, 152], we next sought to establish whether UCHL1 directly affected the protein stability of cyclin B1. Cycloheximide chase assay showed a reduction in cyclin B1 protein half-life in ARK1 and ARK2 cells transfected with anti-UCHL1 siRNA compared to control siRNA (Figure 31), suggesting that UCHL1 increases the stability of cyclin B1 protein and impedes its degradation.
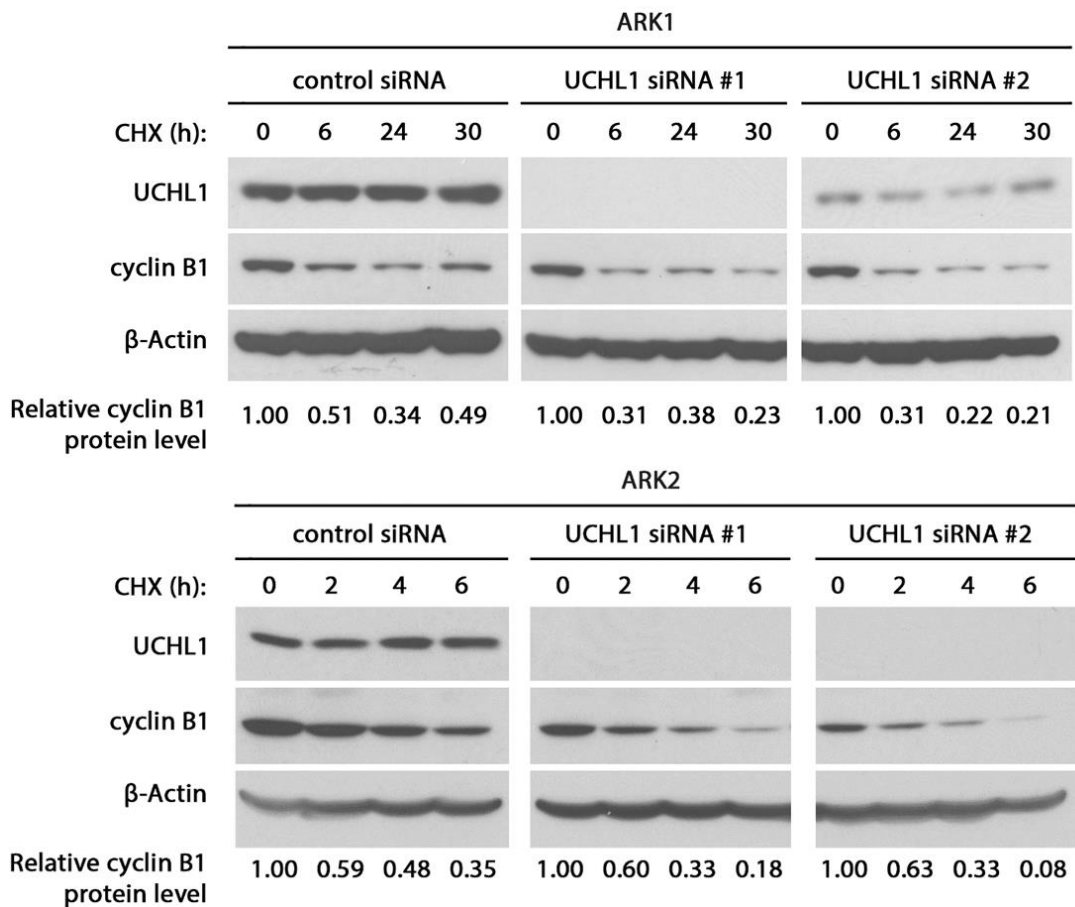
Figure 31. UCHL1 silencing reduces cyclin B1 protein half-life.

Cycloheximide (CHX) chase assay of cyclin B1 was performed in ARK1 and ARK2 cells 4 days after transfection with UCHL1 siRNA. Protein lysate was collected at the indicated time points after the addition of CHX.

To further determine whether ubiquitination plays a role in mediating the effect of UCHL1 on cyclin B1 stabilization, we evaluated the ubiquitination of cyclin B1 in UCHL1 silenced ARK1 cells. As cyclin B1 may be targeted for degradation by the anaphase-promoting complex via K48-ubiquitination, K11-ubiquitination or multiple monoubiquitination [181, 182], we chose to detect total ubiquitin levels after immunoprecipitation of cyclin B1. The results showed an increase in ubiquitination of cyclin B1 in UCHL1-silenced cells as revealed by Western blot analysis (Figure 32). Together, these results suggest that UCHL1 stabilizes protein levels of cyclin B1 by reducing its ubiquitination and subsequently impairing its degradation.
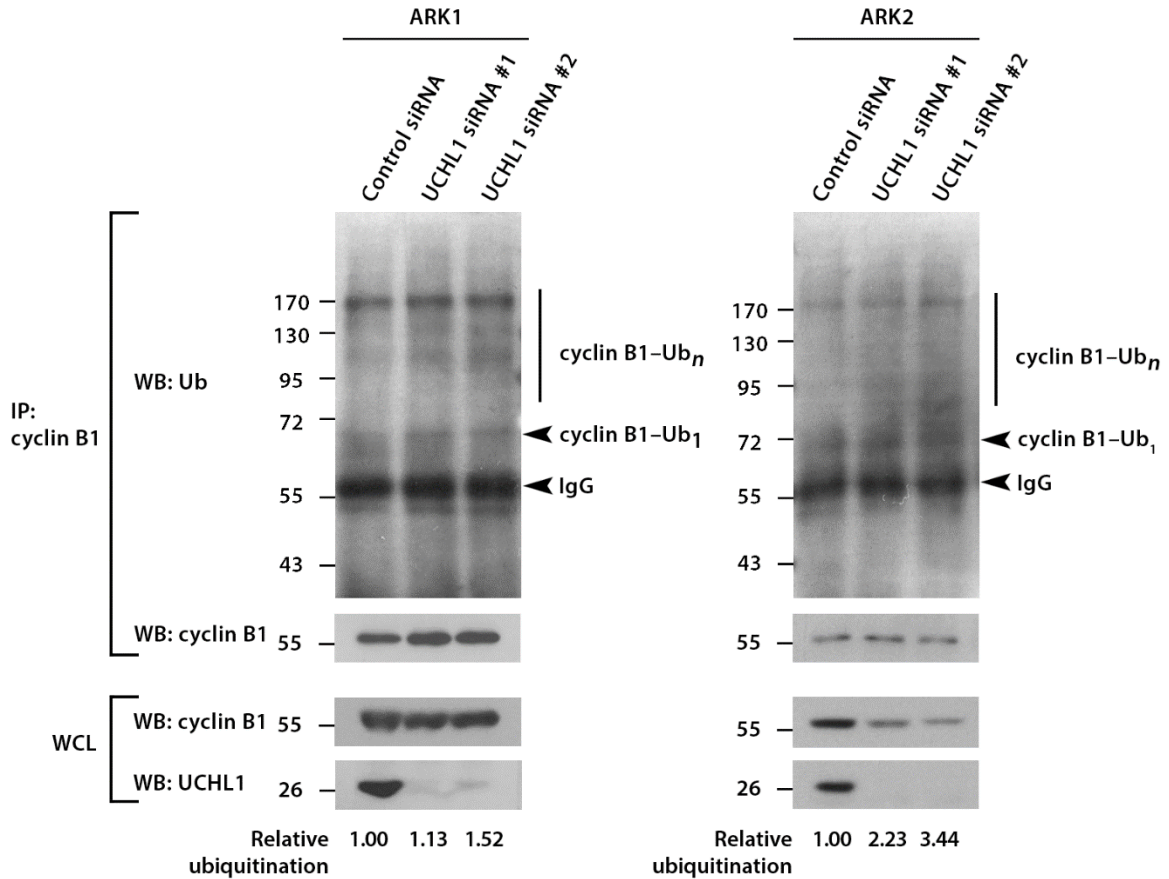
Figure 32. UCHL1 modulates cyclin B1 protein stability by deubiquitination.

Ubuiquitination of cyclin B1 in ARK1 and ARK2 cells was evaluated 4 days after siRNA

transfection. Cells were pretreated 25 μg/ml MG132 for 4 hours before protein extraction. Ubiquitin

staining was quantified with ImageJ and normalized to cyclin B1 staining following

immunoprecipitation (IP: CCNB1, WB: CCNB1). Degree of ubiquitination is shown relative to cells

transfected with control siRNA.

IP = immunoprecipitation; WCL = whole cell lysate; WB = western blot; Ub_1 = monoubiquitin;

Ub_n = multiple ubiquitin conjugates; IgG = heavy antibody chain.

UCHL1 promotes cell cycle progression

Since UCHL1 can up-regulate cyclin B1 protein expression and cyclin B1 is essential for cells to enter mitosis, we sought to determine the effect of UCHL1 on cell cycle progression in UPSC cells. ARK1 cells transfected with UCHL1 siRNA or control siRNA were synchronized in early G1 by serum starvation for 24 hours. After reintroduction of serum, cells were collected at 0h, 6h and 24h and subjected to cell cycle analysis by flow cytometry. Knockdown cells progressed slower through the cell cycle compared to control cells (Figure 33A). In particular, the percentage of control cells in G2/M increased 17.4% from 0h to 24h, whereas cells transduced with shRNA 1 and 2 increased 3.9% and 12.2% respectively, suggesting that UCHL1 affects cell cycle progression through its effect on cyclin B1 protein levels. Inhibition of UCHL1 by LDN-57444 following synchronization at G1 by serum starvation also indicated a drop in cyclin B1 levels by 23 hours after release from synchronization (Figure 33B). Taken together, our results demonstrate that high levels of UCHL1 in UPSC stabilizes cyclin B1 by reducing its ubiquitination and preventing its degradation, which subsequently promotes mitotic entry.
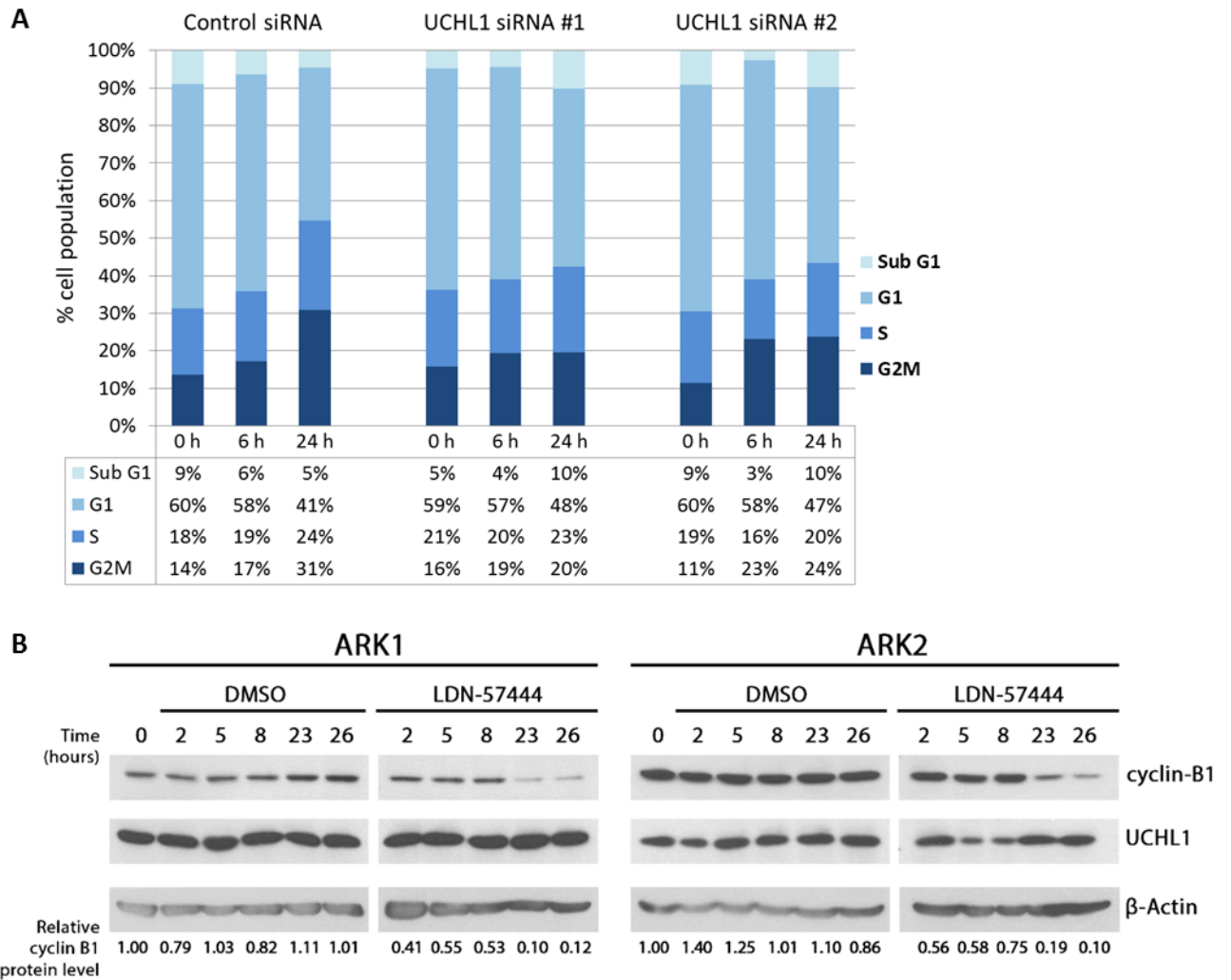
Figure 33. UCHL1 promotes cell cycle progression through stabilization of cyclin B1.

(A) ARK1 cells transfected with control or anti-UCHL1 siRNA were serum starved for 24-hours before release into medium with 10% FBS; cells were collected for flow cytometry analysis at the indicated time points.

(B) ARK1 and ARK2 cells were serum-starved for 24-hours before release into medium with 10% FBS and 50 µM LDN-57444. Protein lysate was collected at indicated time points to measure cyclin B1 levels.

Conclusion

In this chapter, we demonstrated that cyclin B1 protein levels correlated positively with *UCHL1* RNA expression in the TCGA data set. This was validated in our independent cohort of patient samples, where the percentage of tumor cells positive for cyclin B1 correlated with UCHL1 staining intensity. In ARK1 and ARK2 cells, knockdown of UCHL1 decreased cyclin B1 protein levels, while transient expression in ACI-158 increased cyclin B1 protein levels. Percentage cyclin B1 positivity was also reduced *in vivo* in UCHL1-silenced tumors. Protein interaction between UCHL1 and cyclin B1 was confirmed by co-immunoprecipitation, immunofluorescence, and proximity ligation assay. The UCHL1-cyclin B1 complex was detected both in the cytoplasm and in the nucleus in early mitosis. UCHL1 was shown to promote protein stability and prolong the protein half-life of cyclin B1 by deubiquitination, consequently promoting mitotic entry and cell cycle progression.

CHAPTER 6:

DISCUSSION

Due to the rarity of UPSC, information is lacking regarding optimal treatment and prognosis. In addition, no targeted therapies are currently approved for UPSC, and there are limited candidate targets. Therefore, the aim of this dissertation was to identify novel therapeutic targets using the substantial number of cases found in The Cancer Genome Atlas (TCGA) database, containing 91 pure UPSC samples with RNA sequencing data at time of download. We first utilized a purpose-driven approach to identify genes contributing to tumor progression of UPSC. After we determined UCHL1 to have a potentially oncogenic role in UPSC, we began our hypothesis-driven approach to study its role in UPSC tumorigenesis.

The genomic landscape of UPSC

It is known that the pathogenesis and genetic profile of UPSC is distinct from that of endometrioid carcinomas. A previous study by Risinger et al. performed multidimensional scaling using the RNA expression profiles of tumor samples as measured by cDNA microarray [267], which confirmed that EEC, UPSC and CC tumors formed distinct clusters. However, this was a small study of 7 age-matched normal endometrial samples and 19 EEC, 13 UPSC, and 3 CC tumors. In addition, there was no distinction made between low-grade and grade 3 EEC, which are categorized into the type I and type II groups respectively, due to the differences in clinical aggressiveness [268]. We therefore sought to further examine the relationship between tumor subtypes using the larger TCGA dataset.

Through principal component analysis of a larger group of samples in the TCGA dataset, we observed the clustering of grade 1 and 2 EEC together, reflecting their close similarities. We also observed a large variation within the normal tissue samples, with significant overlap with the EEC clusters. This could be due to two possibilities. Firstly, being the tumor subtype with the best prognosis and the least genetic aberrations, they are expected to be genetically closest to normal

samples. Secondly, as these were paired samples obtained from uterine tissue adjacent to tumor and verified by histology to be normal, this suggests that some normal tissue may already undergo genetic changes prior to the development of hyperplasia or malignant histology. Therefore, adjacent tissue may not be the best comparison for tumors.

On the other hand, mixed and pure UPSC samples were furthest away from normal samples, reflecting their increased tumor aggressiveness and high frequency of copy-number alterations. The grade 3 EEC cluster overlapped with both low grade EEC and UPSC, supporting the notion that there are certain similarities between grade 3 EEC and UPSC at the RNA level. Zannoni et al. concluded that grade 3 EEC was an intermediate group between low-grade EEC and other type II tumors, in terms of clinical features such as local invasion, lymph node positivity and extra-uterine spread, and histological features such as p53 mutation frequency, and ER, PR and Ki67 positivity [269]. In addition, the clustering of endometrial tumors by The Cancer Genome Atlas Network [72], based on mRNA expression profiles, also revealed that 56% of the grade 3 EEC samples clustered with the majority of UPSC tumors in the mitotic group.

The survival outcomes of grade 3 EEC and UPSC have also been compared to each other. The largest study comparing survival outcomes of 2316 grade 3 EEC and 1473 UPSC patients indicated significantly poorer survival in UPSC at each stage [68], suggesting that grade 3 endometrioid carcinoma is of intermediate risk between grade 1 and 2 endometrioid carcinomas and non-endometrioid carcinomas.

Identification of UPSC-promoting genes

With grade 3 EEC exhibiting molecular similarities with UPSC and an intermediate aggressiveness between low-grade and UPSC, we chose to compare the RNA expression profile of UPSC with low-grade EEC to discover differentially expressed genes. By filtering for genes with significantly higher expression in UPSC compared to both normal endometrium and low-grade EEC,

and which correlated with poorer overall survival, we derived a list of 19 genes with possible

oncogenic function. Although we filtered the genes prior to analysis to remove genes with a mean raw

count below 0.5 or 10 or less reads across all samples, 6 of the 19 genes had a median expression

below 10 for all three groups (normal, low-grade EEC, UPSC) and an extremely high fold change as

calculate by the SAM analysis. These genes were effectively ignored, as low-expressing genes have a

low signal-to-noise ratio and are therefore commonly unreliably deemed significant in analysis of

microarray and RNA sequencing data [270]. Excluding these 6 genes and *UCHL1*, which will be

discussed later, the list of candidate genes and known roles in cancer will be discussed.

WASF1

Wiskott-Aldrich syndrome protein family member 1 (WASF1) interacts with the actin-related

protein (Arp) 2/3 complex to form an actin nucleation site, initiating actin polymerization [271].

While WASF1 is non-essential for lamellipodia formation, it is instead involved in dorsal ruffle

formation [272], which in turn modulates cell motility and internalization of extracellular material

and membrane proteins [273]. Normal expression of WASF1 is mainly restricted to the brain [274],

but its overexpression has been associated with aggressive disease in ovarian carcinoma [275] due to

its effect on tumor cell migration and invasion, adhesion, colony formation and proliferation [276].

WASF1 overexpression has also been reported in prostate cancer, where it was involved in cell

invasion and proliferation [277].

CCDC99

Coiled-coil domain-containing protein 99 (CCDC99) was initially discovered to be an

essential recruiter of dynein to kinetochores in early mitosis before kinetochore-microtubule

attachment [278]. CCDC99 is therefore is involved in overcoming the spindle-assembly checkpoint,

as dynein is required for the removal of spindle-assembly checkpoint proteins from the kinetochore as

they become correctly aligned, thus allowing cells to overcome the checkpoint and proceed to anaphase. Loss of CCDC99 leads to chromosome misalignment and metaphase arrest [278, 279].

CCDC99 overexpression has been observed in lung cancer cell lines, where silencing of CCDC99 enhanced the cytotoxic activity of paclitaxel by increasing the length of mitotic arrest [279]. Paclitaxel targets the microtubules to prevent deactivation of the spindle-assembly checkpoint; the subsequent induction of prolonged arrest leads to apoptosis [280-282]. However, cancer cells can escape by mitotic slippage due to compensatory mechanisms such as premature degradation of cyclin B1 [283]. Targeting CCDC99 may therefore be a viable method to increase the cytotoxic effects of paclitaxel before mitotic slippage occurs. Recent reports indicate that farnesylation of CCDC99 by farnesyltransferase is required for its localization to the kinetochore, and treatment with farnesyltransferase inhibitors FTI-277 and L-744-832 *in vitro* led to a phenotype similar to cells with CCDC99 silencing [284, 285], providing a possible method of CCDC99 inhibition. The farnesyltransferase inhibitor Lonafarnib is currently being evaluated in a phase II trial for patients infected with the hepatitis delta virus [286].

PLXNA4

Plexin-A4 (PLXNA4) is a transmembrane receptor for the class-3 and -6 semaphorins SEMA3A, SEMA6A and SEMA6B, which were originally discovered as axon guidance factors in the central nervous system [287-289]. In HUVEC endothelial cells, PLXNA4 was found to mediate the effects of semaphorins on the actin cytoskeleton and cell morphology [290]. PLXNA4 also affects cancer cell function independent of its role in cytoskeletal organization, as it is able to complex with FGFR1, FGFR2 and VEGFR2 to enhance bFGF and VEGF signaling. Accordingly, PLXNA4 inhibition in U87MG glioblastoma cells and A549 lung cancer cells resulted in reduced cell proliferation *in vitro* and impaired tumor forming ability *in vivo* [290]. In addition, amplification of *PLXNA4* has been observed in melanoma and lung tumors [291], suggesting an oncogenic function in cancer.

COL9A1

Collagen type IX alpha 1 chain (COL9A1) is an extracellular protein and a component of collagen that is preferentially expressed in chondrocytes [292, 293]. Hypomethylation of *COL9A1* has been observed in breast cancer [294], and its expression is associated with stem-like prostate cancer cells [295], suggesting an oncogenic role in cancer. In addition, COL9A1 expression was reported in a high-grade, serous-like cluster of ovarian, fallopian tube and peritoneal advanced serous cancers [296]. In normal endometrial stromal cells, COL9A1 expression was reported to increase upon estrogen stimulation [297].

FAM167A (aka C8orf13)

Little is known about family with sequence similarity 167, member A (FAM167A); its conserved domain, DUF3259, is also of unknown function. Polymorphisms in the *FAM167A-BLK* gene locus have been associated with several autoimmune diseases [298-300].

MMP1 and MMP10

Matrix metalloproteinase-1 and -10 (MMP1 and MMP10) are involved in the degradation of the extracellular matrix [301]. MMP1 expression has been observed in other cancer types and promotes tumor invasiveness [302]; overexpression has also been observed in endometrial cancer, but the histological subtypes of the tumor samples studied were unclear [303]. Nevertheless, MMP1 was stimulated by EGFR and HER2 signaling in ARK2 cells, and treatment of ARK1 and ARK2 cells with the EGFR/HER2 inhibitor lapatinib downregulated MMP1 RNA and protein expression.

MMP10 expression is limited to epithelial cells in normal tissue [304] and targets collagen, elastin and laminin [305]. MMP10 expression is a poor prognostic marker for ovarian cancer; in addition, it is highly expressed in ovarian cancer stem-like cells and contributes to resistance to

platinum-based chemotherapy [306]. Expression of MMP10 was also associated with increased

invasiveness of cervical cancer, and also promoted angiogenesis and suppressed apoptosis [307].

C11orf41

C11orf41 is a protein with unknown function, and is almost exclusively expressed in the

brain [308]. A novel *PAX5-C11orf41* fusion transcript was found in one case of pediatric B-cell

precursor acute lymphoblastic leukemia [309], while a *RUNX1-C11orf41* fusion transcript was

identified in a case of acute myeloid leukemia [310].

PPAPDC1A

Phosphatidic acid phosphatase type 2 domain containing protein 1A (PPAPDC1A) is from

the phosphatidic phosphatase family of proteins, which are involved in lipid metabolism and signal

transduction [311]. While PPAPDC1A is preferentially expressed in endothelial cells and testis [312],

its overexpression has been reported in ductal breast cancer [313]; however, its role in cancer

development has not been studied.

NKAIN1

Na,K-ATPase interacting 1 (NKAIN1) is a member of the NKAIN family of membrane

proteins, first identified as interacting partners of Na,K-ATPase [314], an enzyme that transports

sodium and potassium ions across the membrane to maintain an electrochemical gradient. This

regulation of ionic and osmotic homeostasis is required for normal cell function and cell survival

[315].

The NKAIN proteins are neuron-specific, while Na,K-ATPase is ubiquitously expressed

[316, 317]. However, the NKAIN proteins may promote proper functioning of Na,K-ATPase in the

brain: two patients with a truncated form of NKAIN2 have been reported to have severe neurological

impairment [318, 319]. Overexpression of NKAIN2 has also been observed in more aggressive neuroblastoma cell lines and high-risk tumor samples [320].

Apart from its role as an ion pump, Na,K-ATPase has also been shown to be involved in protein scaffolding and signal transduction [321-323], affecting tumor cell proliferation, apoptosis, adhesion and motility [324, 325]. Altered activity of Na,K-ATPase itself has been observed in various tumor types and cancer cell lines, leading to interest in the anti-cancer properties of Na,K-ATPase inhibitors [324, 326]. The most well-known class of Na,K-ATPase inhibitors are cardiac glycosides, plant- and mammal-derived steroids that have long been used for the treatment of cardiac disease [327, 328]. Taken together, this suggest that NKAIN1 may promote tumor aggressiveness of UPSC through its effects on Na,K-ATPase function, and the use of Na,K-ATPase inhibitors may be of clinical benefit.

GAL

Galanin (GAL) is a neuropeptide expressed in the brain and peripheral nervous system [329-331] that modulates a broad range of physiological effects, such as nociception, memory, learning, feeding, and hormone secretion [332, 333]. Its various physiological effects are mediated by the G protein-coupled receptors GalR1, GalR2 and GalR3 [332], which have distinct downstream functions.

Both pro- and anti-tumor effects have been described: galanin upregulation in tumor and serum has been reported in patients with colorectal cancer, where it is also a poor prognostic marker [334]; in addition, expression is associated with increased invasiveness of colorectal cancer cells [335]. On the other hand, expression of galanin, GALR1 and GALR2 have been linked to an anti-proliferative, pro-apoptotic effect in neuroblastoma and oral carcinoma cell lines [336, 337]. Another study found that while GALR1 was anti-proliferative, a net pro-proliferative effect was observed when keratinocytes expressing all three receptors were stimulated with galanin, suggesting that the receptors may have opposing effects [338].

In endometrial cancer, GALR1 was identified as one of the most significantly hypermethylated genes compared to normal endometrial tissue [339]. However, only 3 out of the 64 tumor samples were of serous histology.

SLCO4C1

The organic anion transporter family (OATP) is a group of plasma membrane transporters for a wide range of organic compounds [340]. Solute carrier organic anion transporter family member 4C1 (SLCO4C1) was first characterized as a transporter of digoxin, a commonly prescribed drug for heart failure [341]. SLCO4C1 is predominantly expressed in the kidney, and is involved in the elimination of digoxin from the circulatory system. Other substrates include the drugs ouabain and sitagliptin, thyroid hormones, cAMP, methotrexate and uremic toxins [341-343]. SLCO4C1 expression has also been detected in the brain and mammary gland, as well as in ovarian, breast and lung cancer cell lines [344]. In addition, two SNPs associated with response to platinum-based chemotherapy were also strongly associated with the expression of SLCO4C1 and SLC22A5, suggesting that they may be involved in the transport of carboplatin in tumor cells [345, 346].

While we were able to discover potentially oncogenic genes using the TCGA data set, one limitation was the lack of follow up data provided. At the time of download in May 2013, two follow up files had been released; however, the median follow up times and number of deaths occurred were both substantially less than in our own patient cohort (Table 9). The third and last follow up file that has been released was in late 2013. An update to the follow up data would greatly increase the statistical power of survival analyses and allow researchers to fully utilize the data.

	TCGA (pure UPSC) n=91	IHC (mixed/pure) n=74
Median follow up (years)	1.51	8.88
95% CI	0.81-2.22	2.77-14.98
Recurrences	11/24 (46%)	21/60 (35%)
Deaths	19/91 (21%)	43/74 (58%)

Table 9. Median follow up times and number of events in patient cohorts.

Median follow up times were calculated by reverse Kaplan-Meier analysis [258].

UCHL1 upregulation in UPSC

Based on our analysis with the TCGA data, we chose to study *UCHL1* further for the purposes of this dissertation, as *UCHL1* had the highest median RSEM expression and one of the highest fold change differences between UPSC and low-grade EEC among the 13 genes with non-negligible expression. There was a marked upregulation of *UCHL1* compared to all grades of EEC and normal endometrial tissue. In addition, grade 3 EEC had an intermediate level of expression between low-grade EEC and UPSC.

We also compared *UCHL1* expression between the molecular clusters, as recently identified by The Cancer Genome Atlas Research Network using integrated genomic data [72]. The copy-number high (serous-like) cluster of endometrial cancer samples had significantly higher *UCHL1* expression compared to the other three clusters. This is to be expected, as the vast majority of UPSC cases were in this cluster, which also included a quarter of all grade 3 EEC cases. Therefore, although these molecular clusters may be useful in identifying high- and low-risk EEC patients, the clinical utility for UPSC is limited. Further examination of UPSC patients alone to stratify patients into high- and low- risk groups may have clinical benefit.

To validate our finding that *UCHL1* was upregulated and associated with poorer clinical outcome, we performed immunohistochemical staining of our own cohort of UPSC samples, which confirmed that UCHL1 protein expression was significantly higher in UPSC than in EEC and pre- and post-menopausal normal endometrium. In normal endometrial tissues and the majority of EEC, there was either no staining or cytoplasmic staining of UCHL1 near the apical surface of the glandular cells. While the study by Kajimoto et al. reported lack of UCHL1 in most tissues, expression in the uterus was not evaluated [116]. Although the expression level observed is low, the role of UPSC in normal endometrium remains unknown.

Although *UCHL1* was associated with poorer overall survival in the TCGA data set, we did not find an association between UCHL1 expression and survival when analyzing early stage patients alone or all patients together. However, in the 24 late stage UPSC patients (pure or mixed) with no evidence of disease after completion of treatment, high UCHL1 expression was significantly associated with poorer disease-free survival by univariate analysis, and overall survival by both univariate analysis and multivariate analysis, suggesting that UCHL1 affects the clinical outcome of late-stage UPSC patients rather than early-stage patients.

UCHL1 overexpression [128-132] and loss [120-127] has been reported in numerous cancer types. Subsequently, there are conflicting reports that UCHL1 is a tumor suppressor [347] or oncogene [136-139]. There are several possible reasons for the discrepancy between studies, even within the same cancer type [106]. Firstly, reports of UCHL1 acting as a tumor suppressor has mostly been inferred from *in vitro* studies and observed downregulation in patient samples, rather than by survival analysis of patient data. One of the few studies that analyzed survival data found that UCHL1 promoter methylation was associated with poorer clinical survival in sporadic breast cancer patients, but only by univariate analysis and not multivariate analysis [347].

Secondly, studies in different cancer types have reported several distinct downstream signaling pathways, suggesting that UCHL1 has multiple possible target proteins and is context-specific. For example, since UCHL1 has been reported to stabilize both wild-type p53 and various

110

p53 mutants [124, 127, 143], the mutation status of *TP53* may determine whether the net effects of UCHL1 are tumor-suppressive or oncogenic. *TP53* is mutated in the majority of UPSC; our five type II cell lines were all *TP53*-mutant.

The specific tumor subtype studied may also determine the effect of UCHL1. For example, Xiang et al. reported a loss of UCHL1 protein in a panel of breast cancer cell lines compared to normal breast cells [143]. However, four out of nine cell lines retained UCHL1 expression at varying levels: of these, BT-549 and MB-468 are triple negative, SK-BR3 is ER/PR negative, HER2 positive, and YCC-B3 is of unknown receptor status [348, 349]. In addition, they observed promoter methylation of UCHL1 in primary tumors; however, over half the cases had unknown hormone receptor status, and the rest were split evenly between receptor-positive and receptor-negative. In contrast, Lien et al. reported association of UCHL1 expression with the more aggressive triple negative and basal-type breast cancers [350], suggesting that negative hormone receptor status is associated with UCHL1 upregulation. UCHL1 has been associated with poorer survival in breast cancer by both univariate analysis and multivariate analysis [139, 350]. Taken together, these studies point to possibility that UCHL1 upregulation is an alternative to hormone signaling in the promotion of tumorigenesis, and hence does not have a tumor-promoting effect in those that are hormone-sensitive. Interestingly, UPSC shares molecular characteristics with triple negative and basal breast cancers, such as frequent p53 mutation, negative hormone receptor status and HER2 amplification/overexpression. It remains to be seen if the effect of UCHL1 on endometrial cancer progression is dependent on hormone status.

Lastly, the discrepancy between different studies may also be due to the stage of tumor studied [106]. Reports of a tumor-suppressive function in prostate cancer used LNCaP cells taken from the lymph node metastasis of an androgen-dependent tumor. In contrast, UCHL1 expression was detected in the more aggressive, androgen-independent PC-3 and DU145 cell lines, which are taken from bone metastasis and brain metastasis respectively [129, 142]. Again, it is possible that hormone dependency determines the effect of UCHL1, but this will need to be studied further.

Overall, it appears that UCHL1 is downregulated by hypermethylation in a subset of cancers, as it may provide a tumor suppressive effect based on other signaling pathways involved. Conversely, it is apparent that there is often a tumor-promoting effect, for example in hormone-negative breast, prostate and endometrial cancer. This highlights the need to study the effects of UCHL1 in clearly defined patient subpopulations that are relatively homogenous.

The functional role of UCHL1 in UPSC tumorigenesis

While differential expression of UCHL1 between serous and endometrioid endometrial carcinomas has been previously reported in a microarray [351], and the function of this protein has been studied in other cancers, the role of UCHL1 in endometrial cancer had not been explored in depth. Although we did not observe changes in apoptosis, migration or invasion following UCHL1 silencing *in vitro*, there was a decrease in cell proliferation of ARK1 and ARK2 cells, suggesting that UCHL1 promotes tumor cell proliferation. In contrast, there was no significant difference in cell proliferation when the UCHL1-negative ACI-158 was transfected with anti-UCHL1 siRNA, suggesting that the reduction in growth observed in ARK1 and ARK2 was not due to toxicity of the siRNA.

We also observed a reduction in tumor growth *in vivo* with mice injected with ARK1-luc-dox-shUCHL1 compared to ARK1-luc-dox-NT. Although this difference was significant, we observed a large variation in our study utilizing ARK1 cells transduced with doxycycline-inducible shRNA. One possible reason for this variation is errors in injection of the tumor cells. In one study examining the errors of intraperitoneal injection in mice, the injection of radiological Ethiodol by five experienced researchers was found in other organs instead of the peritoneal cavity in 21 of 150 mice (14%) [352], most commonly in the stomach or small bowel. Other studies have reported a typical failure rate of 10-20% [353], which could not be improved by procedure optimization such as varying the needle size, angle of needle at penetration or injection into the right versus left lower abdominal

112

quadrant [354]. Regardless, the lower right quadrant is preferred due to the stomach and cecum being on the left side.

For our experiments, injections were on the right lower abdominal quadrant. With the second *in vivo* experiment involving LDN-57444 treatment, extra care was taken to tilt the mouse slightly with the head downwards, which may allow the stomach and bowels to move higher up the peritoneal cavity and decrease chances of injection into those sites. This inherent failure rate also led us to increase the number of mice used in the second *in vivo* experiment. We began with 50 mice for intraperitoneal injection of ARK1 cells; two weeks later, we used the *in vivo* bioluminescence intensities to exclude the 5 mice with the lowest bioluminescence. We then split the mice so that the control and treatment group had a similar, mean, median and range of bioluminescent intensity.

Another possible reason for the large variation of tumor growth observed is the heterogeneity of the ARK1 cell line during prolonged culture *in vitro*. We postulated that cancer cells taken from the tumors successfully established *in vivo* may provide more consistent results in future experiments. Therefore, using the mice in the control group (injected with ARK1-luc-dox-NT) that were moribund at relatively early time points, we collected ascitic fluid immediately after sacrifice and plated it *in vitro* to isolate the tumor cells. We were able to confirm successful isolation by treatment with doxycycline, as red fluorescent protein was induced and detected with fluorescence microscopy. Cells from the ascites of one mouse was then used for our second *in vivo* study involving LDN-57444 treatment.

Overall, with our modifications, we observed reduced variability of tumor growth in the second *in vivo* study before we began treatment with LDN-57444 vs. control. With this experiment, we observed a reduction in tumor growth and improved survival when mice with UPSC tumors were treated with LDN-57444, indicating that inhibition of UCHL1 can reduce tumor burden and improve overall survival.

LDN-57444 has previously been used *in vivo* in several studies, but to our knowledge LDN-57444 treatment has not been administered over such a long period of time as in our experiment. For

113

example, Goto et al. injected 0.5 mg/kg LDN-57444 intraperitoneally into nude mice for three consecutive days before the mice were sacrificed a week later [139]. Although we found that LDN-57444 could only be successfully dissolved in PBS with 0.5% DMSO and 2.5% ethanol, a thrice-weekly injection of 0.5 mg/kg for 4 weeks did not lead to a noticeable drop in mouse body weight or other visible adverse effects, suggesting that the treatment was well tolerated.

In spite of this, UCHL1 is abundant in the brain and peripheral nervous tissue; therefore, potential side effects will need to be considered. The development of UCHL1 inhibitors with increased specificity and tumor-specific delivery may increase the efficacy and lower the toxicity of UCHL1-targeting drugs for clinical use.

Effect of UCHL1 on cyclin B1 protein stability

As a deubiquitinating enzyme from the family of ubiquitin carboxyl-terminal hydrolases [112], UCHL1 has been shown to affect the protein stability of various cancer-related proteins. This includes proteins related to cell cycle progression, such as p27 [112], p53 [124] and β-catenin [150]. However, when analyzing the RPPA data set from TCGA, we did not find any correlation between *UCHL1* mRNA expression and protein expression of p27, p53 or β-catenin. We also did not see a change in p53 or β-catenin protein by western blot after UCHL1 silencing; the change in p27 levels was not consistent across the two cell lines ARK1 and ARK2. Instead, we demonstrated for the first time a significant correlation between UCHL1 and cyclin B1 protein expression, which was validated by immunohistochemical staining of our own UPSC cohort.

Our *in vitro* studies demonstrated that UCHL1 silencing by siRNA reduced cyclin B1 protein levels; the percentage of tumor cells positive for cyclin B1 was also lower in mice injected with ARK1-luc-dox-shUCHL1 instead of ARK1-luc-dox-NT. Through immunoprecipitation studies, we found that the decrease in cyclin B1 after UCHL1 silencing was due to an increase in ubiquitination.

114

Our cycloheximide chase assay also showed that cyclin B1 protein half-life is shortened in UCHL1-silenced cells.

UCHL1 has been shown to promote the kinase activity of CDK 1, 4 and 5, independent of its deubiquitinating activity [147]. In addition, one previous study observed that UCHL1 interacted with both cyclin B1 and CDK1 in *Xenopus* oocytes by immunoprecipitation [355]. In our study, we also observed an interaction between cyclin B1 and UCHL1 by co-immunoprecipitation. To confirm this finding, we performed the Duolink proximity ligation assay. Since cyclin B1 is predominantly cytoplasmic during interphase, the red fluorescent spots were seen in the cytoplasm of the majority of cells, indicating an interaction between UCHL1 and cyclin B1. However, when cells entered mitosis, condensation of the chromosomes as seen by DAPI staining was accompanied by nuclear localization of the red fluorescent spots, which persisted until anaphase when levels of cyclin B1 protein decreased. As cyclin B1 begins its interaction with CDK1 as soon as it is expressed, UCHL1 is likely interacting with the cyclin B1-CDK1 complex as a whole. Therefore, UCHL1 appears to interact with cyclin B1-CDK1 throughout the cell cycle, regardless of cellular location, and is able to impair the degradation of cyclin B1 by the APC at the metaphase-anaphase transition. The balance between cyclin B1 ubiquitination by the APC and deubiquitination by UCHL1 could determine the degree and rate of cyclin B1 degradation at the metaphase-anaphase transition, and also affect the basal level of cyclin B1 observed in cells as they exit mitosis and enter interphase (Figure 34).
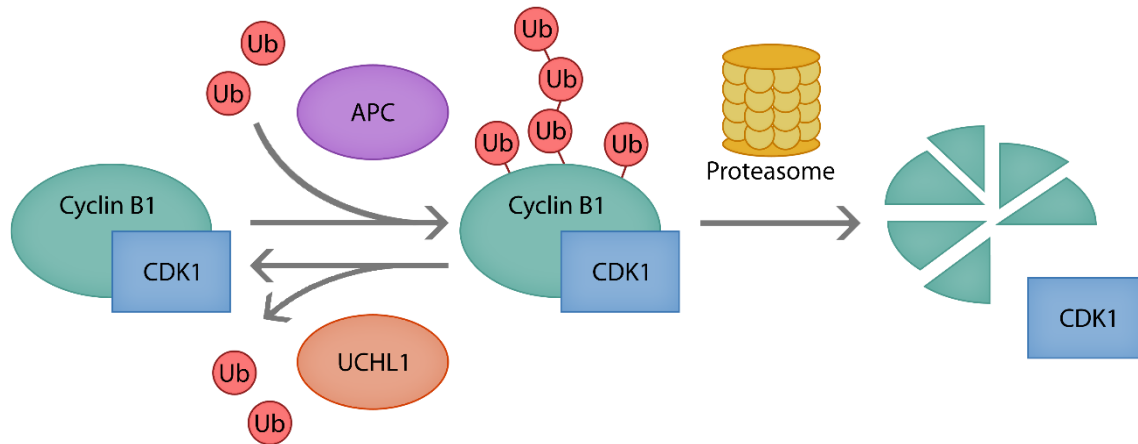
Figure 34. Proposed model for the effect of UCHL1 on cyclin B1 ubiquitination and degradation.

Dysregulation of cyclin B1 in cancer

Cyclin B1, complexed with CDK1, is the primary regulator of mitosis. As uncontrollable cell proliferation is a hallmark of cancer [356], cyclin B1 overexpression has been observed in many cancer cell lines and tumor samples [222-225]. For example, total/cytoplasmic cyclin B1 positivity was associated with grade, mitosis and absence of estrogen/progesterone receptor in breast carcinomas, while nuclear cyclin B1 was associated with poorer disease-free survival and overall survival by multivariate analysis [226]. In an immunohistochemical study of EEC, cyclin B1 was associated with increasing grade, stage, and poorer cancer-specific survival by univariate analysis [229].

Previous studies suggest that uncontrolled mitosis is an early event in UPSC and contributes to tumor development. Stage I UPSC samples had a significantly higher mitotic index than stage I, low-grade EEC [357]. Using the TCGA data set, unsupervised clustering of RNA sequencing profiles revealed that the majority of UPSC tumors were in the mitotic cluster, of which the most enriched pathways were "mitotic roles of polo-like Kinase", "G2/M DNA damage checkpoint regulation", and

"cell cycle control of chromosomal replication" by Ingenuity Pathway Analysis [72]. Cyclin B2 and *CDK1* were two of the four most upregulated genes. In addition, clustering based on integrated analysis of exome sequencing, copy number alterations and microsatellite instability showed that the majority of UPSC cases were in the copy-number high cluster, which had overexpression of cyclin B1, CDK1 and cyclin E1 protein.

While cyclin E1 overexpression in UPSC is frequently due to its amplification, cyclin B1 is not amplified or mutated in the UPSC samples of the TCGA data set, suggesting other mechanisms of upregulation. In addition to mRNA upregulation and/or possible mRNA stabilization, our results indicate that the frequent dysregulation of mitosis in UPSC is promoted by UCHL1 and its stabilizing effect on cyclin B1. As we did not observe a significant difference in UCHL1 expression between stages of UPSC in the RNA sequencing data from TCGA, or by immunohistochemical staining of our own cohort of patient samples, this suggests that UCHL1 is overexpressed in UPSC early on in tumor progression and can promote cyclin B1 protein stability, even when the tumor is confined to the primary site. It is also possible that UCHL1 is an early event in UPSC pathogenesis that promotes tumor development; however, this would require assessing UCHL1 levels in precursors to UPSC, namely lesions of glandular dysplasia or intraepithelial carcinoma.

Effects of cyclin B1 on tumor progression

Defects in cyclin B1 degradation can affect cell cycle regulation and promote tumor progression in several ways. Firstly, cyclin B1 overexpression shortens the cell cycle length [194, 230]. In our study, we observed slower progression of UCHL1-silenced ARK1 cells through the cell cycle, which is in agreement with other studies.

Secondly, suppression of cyclin B1-CDK1 activity is essential for activation of the G2-M checkpoint; therefore, cyclin B1 overexpression can allow cells to overcome the G2-M checkpoint even when conditions have not been met to do so; i.e. DNA damage has not been repaired. This is

further promoted when wild-type p53 function is lost, as transcription of cyclin B1 is negatively regulated by p53 during induction of the G2-M checkpoint in response to cell stress and DNA damage [231, 241]. As the vast majority of UPSC cases are *TP53*-mutant, this suppression does not occur, which may further increase the ability of cells with extensive DNA damage to accumulate cyclin B1 and overcome the G2-M checkpoint.

Thirdly, impaired cyclin B1 degradation at the metaphase-anaphase transition promotes chromosomal instability by re-activating the spindle-assembly checkpoint, which in turn gives rise to aneuploidy [358-360], a common feature of UPSC [43, 44, 361]. While cyclin B1 protein must accumulate in order for cells to overcome the G2-M checkpoint, the opposite holds true for the spindle-assembly checkpoint: rapid loss of cyclin B1 and CDK1 inactivation is required for cells to overcome the checkpoint. In normal cells, this occurs at the metaphase-anaphase transition when the sister chromatids are correctly aligned and attached to microtubules, resulting in activation of APC^{Cdc20} and rapid degradation of cyclin B1 [243, 255]. However, even with a slight retardation of cyclin B1 degradation, cells can induce reactivation of the spindle checkpoint [362, 363]. As a result, the cell fails to divide and undergoes mitotic arrest.

In normal tissue, cells that have undergone aberrant mitosis and have arrested undergo mitotic catastrophe, where they are irreversibly committed to death or senescence [364]. However, a fraction of these cells can gradually undergo mitotic slippage and escape mitotic arrest. This is due to a gradual decrease in cyclin B1 until its levels are lower than the threshold needed to maintain the checkpoint [365], or due to other compensatory mechanisms such as inactivation of CDK1 [366]. Slippage also occurs more easily in tumors if there are defects in spindle-assembly checkpoint proteins [367].

As a result of mitotic slippage, tetraploid cells are able re-enter G1. Here, such cells can again be detected and committed to G1 arrest or cell death. However, like the G2-M checkpoint, activation of the G1 checkpoint in response to DNA damage also relies on functional p53, which is lost in the majority of UPSC. Therefore, tetraploid cells are able to escape mitotic arrest, the G1 checkpoint and

118

G2-M checkpoint. Tetraploid cells can in turn act as an unstable intermediate that eventually generates aneuploid cells [368, 369].

Yin et al. previously reported that the oncogene c-Myc increased the transcription of cyclin B1; the effect was enhanced when p53 was inactive [360]. In addition, constitutive cyclin B1 expression alone was sufficient to induce tetraploidy in a small fraction of myeloid cells after several months of passage, and there was an additive effect when cyclin B1 overexpression was combined with c-Myc overexpression. Similarly, we propose that the upregulation of UCHL1 in UPSC, coupled with loss of p53 function, results in unscheduled cyclin B1 expression and/or impaired cyclin B1 degradation. Subsequently, UPSC tumors undergo increased cell cycle proliferation, and are able to accumulate extensive chromosomal instability and aneuploidy without being directed to cell death or senescence (Figure 35).
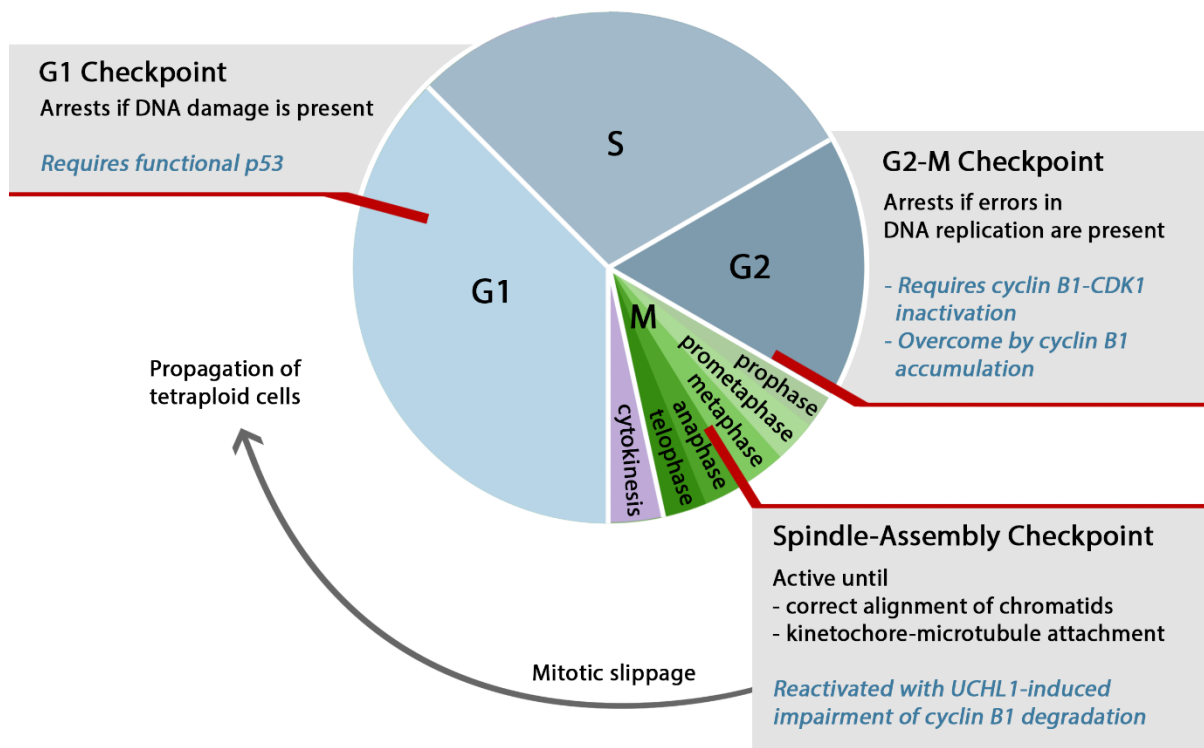
Figure 35. Proposed model of cyclin B1-mediated effects of UCHL1 on cell cycle progression in *TP53*-mutant UPSC.

Future directions

Cyclin B1 degradation kinetics

Although we showed that UCHL1 affects the ubiquitination and degradation of cyclin B1, it remains to be seen whether UCHL1 promotes a slow but complete degradation of cyclin B1 at the end of mitosis, or whether UCHL1 leads to increased basal levels of cyclin B1 carried over into interphase. To determine the levels of cyclin B1 in interphase, one possible experiment would be to perform multi-parameter flow cytometry: control and UCHL1-silenced cells would be labelled with anti-cyclin B1 antibody, followed by a FITC-conjugated secondary antibody. DNA content would also be labelled by staining with propidium iodide. Subsequently, flow cytometry analysis of these samples would allow us to plot cyclin B1 expression against DNA content, which doubles from G1 to mitosis [224].

The degradation of cyclin B in individual cells can also be monitored *in vitro* with expression of the fusion protein cyclin B-SNAP [370, 371]. Endogenous cyclin B is silenced by shRNA, while silent mutations are introduced into the cyclin B-SNAP sequence at the shRNA annealing site to prevent its knockdown [371]. Addition of the SNAP-tag substrate during a labelling reaction allows for fluorescent visualization of the cyclin B protein, whereby the drop in fluorescent intensity over time reflects the rate of protein degradation [372, 373]. The addition of GFP-labelled histone H2 allows for the concurrent monitoring of chromosome alignment during mitosis.

The contribution of UCHL1 to pathogenesis

A mouse model of UCHL1 overexpression would be useful in studying the contribution of UCHL1 to UPSC pathogenesis *in vivo*. A transgenic mouse overexpressing UCHL1 alone has previously been described [132]; although UCHL1 expression in the endometrium was not reported, UCHL1 expression was detected in most major organs. UCHL1-overexpressing mice exhibited an increased rate of spontaneous tumors compared to wild-type mice at 16-18 months (70% vs. 16%),

with the majority of tumors being lymphomas or lung adenomas. In addition, UCHL1 overexpression accelerated the development of lymphoma in Eμ-*myc* mice.

The presence of endometrial tumors was not reported, and it is unknown if any precursor lesions were present. To determine whether UCHL1 overexpression alone is sufficient for the development of UPSC, mice with overexpression of UCHL1 in the uterine epithelium could be generated using the Cre-*loxP* model [374]. Similar to the SOX9 mouse model developed by Gonzalez et al. [375], a mouse model with UCHL1 overexpression in the uterine epithelium may be developed by first generating mice carrying a construct with a ubiquitous CAG promoter; a *loxP*-flanked *RFP*-polyA cassette that terminates transcription at its end; and a *UCHL1* and *EGFP* cassette (*CAG-UCHL1* mice). *Cre* expression leads to DNA recombination at the *loxP* sites, removing the *RFP*-polyA cassette and allowing *UCHL1* and *EGFP* expression. These mice can then be crossed with mice carrying the progesterone receptor promoter (*PGR-Cre*) to generate *PGR-Cre$^+$/CAG-UCHL1$^+$* male mice. Finally, these male mice would be crossed with homozygous *CAG- UCHL1$^+$/CAG-UCHL1$^+$* female mice to obtain *PGR-Cre$^+$/CAG-UCHL1$^+$/CAG-UCHL1$^+$* female mice with UCHL1 overexpression in the endometrium. If UCHL1 is indeed involved in tumorigenesis, UPSC tumors should be observed at a higher frequency than in control mice.

Although the progesterone receptor promoter (*PGR-Cre*) has been used for the investigation of endometrial hyperplasia and cancer [375-377], PGR is expressed in all the major cell types of the uterus in the adult mouse, as well as in the ovary, oviduct, pituitary and mammary gland [378], leading to interest in the use of alternative genes. An alternative promoter that may be used is *Lactoferrin-iCre*, the activity of which is strongly detectable in the uterine epithelium of adult mice but not the ovary and pituitary; in addition, *Lactoferrin-iCre* activity is only weakly detectable in various other tissues [379]. *Sprr2f-Cre* activity is also specific to Müllerian epithelial cells of the uterus, oviduct and cervix, as well as the urothelium of the bladder and uterer [380]. *Sprr2f-Cre*-mediated inactivation of *LKB1* resulted in diffuse malignant transformation of the uterus and highly invasive endometrial cancer in 100% of mice.

If UCHL1 overexpression alone is insufficient to induce tumor development, it may be combined with other genetic alterations, such as a *TP53* deletion or a gain-of-function *TP53* mutation, as both are observed in UPSC. One study utilized *Ksp1.3-Cre* to generate mice with a kidney and genitourinary tract-specific deletion of *TP53* during embryogenesis (*Ksp1.3-Cre/+;Trp53^{fl/fl}* mice). Mice sacrificed at week 24-29 displayed regions of endometrial glandular dysplasia (EmGD), while all mice sacrificed at week 47-58 displayed regions of EmGD and/or EIC. At 65-79 weeks, 16 of the 19 mice were found to have endometrial carcinomas, with frequent co-occurrence of tumors of differing histology in one mouse. While the majority of tumors were of serous histology with or without a clear cell component, several undifferentiated carcinomas and carcinosarcomas were also observed. The combination of *TP53* deletion or mutation and other genetic changes, such as overexpression of HER2, cyclin E1 or p16, may also accelerate UPSC development.

UPSC tends to arise in postmenopausal women with atrophic or resting endometrium, and are typically estrogen and/or progesterone receptor-negative [34]. Although mice do not undergo menopause, reproductive senescence and loss of cyclic activity has been reported to occur in C57BL/6J mice at approximately 11-16 months of age [381], leading to a reduction in estradiol levels [382], albeit not as drastically as in postmenopausal women. It is unknown whether genetic changes that initiate UPSC require a long period of time to develop or are inhibited by a premenopausal environment; nevertheless, it is possible that the induction of menopause in future mouse models may accelerate the development of UPSC. The industrial chemical 4-vinylcyclohexene diepoxide (VCD) has been shown to induce gradual menopause in mice by accelerating degeneration of the primordial and primary ovarian follicles. Administration of VCD in 28 day-old B6C3F1 mice by 20 consecutive days of intraperitoneal injection resulted in ovarian failure at a mean of 52 days after onset of dosing [383]. Plasma levels of follicle-stimulating hormone (FSH) were also significantly increased compared to control mice at a mean of 35 days after onset of dosing, due to loss of 17β-estradiol and progesterone secretion by the ovarian follicles [384, 385].

The contribution of UCHL1 to aneuploidy

It is unknown whether UCHL1 overexpression precedes the development of aneuploidy in UPSC. To our knowledge, only one study has measured the presence of aneuploidy in precursor lesions. In this study of concurrent endometrial intraepithelial carcinoma (EIC) and serous ovarian carcinoma in nine patients, six of the EIC lesions displayed some degree of aneuploidy as determined by *in situ* DNA ploidy analysis [386]. It remains to be seen whether aneuploidy is also present in the less malignant endometrial glandular dysplasia (EmGD). As both precursor lesions have been frequently observed in patients with concurrent UPSC (53% for EmGD [387]; 89% for EIC [38]), the expression of UCHL1 by immunohistochemical analysis of all three lesions from the same patient, along with DNA ploidy analysis by *in situ* image cytometry [388, 389], would allow us to determine whether UCHL1 overexpression is frequently detected before the development of aneuploidy.

To establish whether UCHL1 induces aneuploidy, a potential *in vitro* experiment, similar to the study by Yin et al. [360], would be to generate UCHL1-overexpressing and cyclin B1-overexpressing stable clones of UCHL1-negative endometrial cancer cell lines, and observe changes in DNA ploidy over a prolonged period of cell culture. Tetraploidy may also be induced shortly after generation of stable clones by treatment with the mitotic spindle inhibitor, Nocodazole [360, 390]. To determine whether loss of wild-type p53 is also required for the generation of aneuploidy, stable UCHL1 expression could also be combined with the reintroduction or loss of wild-type *TP53*.

To study the contribution of UCHL1 to aneuploidy development *in vivo*, a mouse model of UPSC, such as mice with endometrium-specific *TP53* deletion or mutation, with and without UCHL1 overexpression, can be used to study the contribution of UCHL1 to aneuploidy development and tumor initiation. If UCHL1 contributes to aneuploidy, we would expect an increase in the degree of aneuploidy in the tumors of mice with UCHL1 overexpression.

Translational significance of study

The rarity of UPSC has been a constant challenge in the development of novel targeted therapies. The collection of a relatively large cohort of UPSC cases from multiple institutions in the TCGA data sets allowed us to discover novel therapeutic targets with sufficient statistical power. We subsequently found *UCHL1* RNA expression to be upregulated in UPSC compared to the more benign low-grade endometrioid endometrial carcinoma and normal endometrial tissue. In addition, we were able to validate our findings by immunohistochemical staining of our own smaller patient cohort, where high UCHL1 expression was associated with disease-free and overall survival in late-stage patients with no evidence of disease after treatment. As over 50% of patients with UPSC are diagnosed at a late stage, this suggests that targeting UCHL1 could be of benefit to a large subset of UPSC patients.

Our studies showed that UCHL1 promoted cell cycle progression both *in vitro* and *in vivo*; treatment of UPSC-bearing mice with the UCHL1-specific inhibitor LDN-57444 also reduced tumor growth and increased overall survival times. Subsequently, we demonstrated that the effect of UCHL1 on tumor growth was due to its ability to impair the ubiquitination and degradation of cyclin B1, an essential protein in mitotic progression.

As mitotic dysregulation was frequently seen in the serous-like cluster as described by the TCGA network [72], our results provides insight into how this possibly occurs. The frequent loss of p53 in UPSC, coupled with UCHL1 overexpression, promotes the stabilization of cyclin B1 and the propagation of tumor cells with extensive chromosomal stability. This suggests that UCHL1 has a role in the increased aggressiveness of UPSC compared to other endometrial cancer subtypes, due to its contribution to cyclin B1 dysregulation.

Targeting the ubiquitin-proteasome system as an anti-cancer strategy has been gaining interest. Inhibitors of the 20S catalytic subunit of the proteasome, bortezomib and carfilzomib, are FDA-approved for the treatment of hematological malignancies [391, 392]. However, toxicity and

drug resistance to bortezomib is observed in patients with multiple myeloma after prolonged treatment [393-395]. In addition, bortezomib and carfilzomib are administered systemically, and the efficacy of bortezomib for the treatment of solid tumors has been disappointing [396]. The second-generation proteasome inhibitor MLN2238 is orally bioavailable and has demonstrated anti-cancer effect in breast cancer [396]. Nevertheless, inhibitors that target specific components of the ubiquitin-proteasome system upstream from the 26S proteasome, such as the deubiquitinating enzymes (DUBs), should improve toxicity profiles [397].

Apart from UCHL1, other DUBs such as UCHL5, USP4, USP6, USP7, USP8, USP14 and USP28 have cancer-promoting functions [398]. While DUBs are promising therapeutic targets, no DUB inhibitors have been FDA-approved so far [399-401]. VLX1570, an inhibitor of USP14 and UCHL5, is currently being evaluated in a phase I/II trial for patients with relapsed/refractory multiple myeloma (NCT02372240 [402]). Drugs approved for other diseases have also shown anti-cancer potential due to their DUB-inhibitory activity. Pimozide, an anti-psychotic drug, has been found to inhibit USP1 [403], while auranofin, a gold-containing compound approved for the treatment of rheumatic arthritis, has emerged as an inhibitor of USP14 and UCHL5 [404]. Although several compounds, including LDN-57444 [261, 405, 406], have been identified as UCHL1 inhibitors, their role is currently restricted as research tools. *MISSION* Therapeutics are in the process of developing specific DUB inhibitors with oral bioavailability, including one or more that specifically targets UCHL1 [401, 407].

In addition to targeting UCHL1 activity, inhibition of cell cycle proteins may also be beneficial in the management of UPSC. For over 20 years, there has been interest in the development of CDK inhibitors as an anti-cancer strategy. The first generation of drugs consisted of "pan-CDK" inhibitors that affected multiple CDK proteins with limited success in clinical trials. For example, the plant-derived flavopiridol was the first CDK inhibitor to be evaluated in clinical trials [408, 409]; treatment has shown clinical benefit for certain hematological malignancies [410-413], but the same efficacy could not be observed in solid tumors [414-416]. Other first-generation inhibitors have

similarly shown limited success in solid tumors, due to lack of bioavailability and toxicity issues from the lack of CDK specificity [415, 417, 418].

Second-generation inhibitors were subsequently developed with the aim of improved specificity, with much of the focus being on CDK4 and CDK6, which together with cyclin D1 promote G1-S transition. Palbociclib is a small-molecule CDK4/6 inhibitor that prevents downstream phosphorylation of functional Rb and blocks G1-S transition [419, 420]. A phase II trial found significantly improved progression-free survival when postmenopausal women with estrogen receptor-positive, HER2-negative metastatic breast cancer were treated with palbociclib plus letrozole versus letrozole alone (20.2 months versus 10.2 months) (PALOMA-1/TRIO-18 [421]); therefore, its use in combination with letrozole has been approved for first-line treatment of this patient population [422].

Development of inhibitors against the other CDK proteins is ongoing. CYC065 is an orally available, second-generation CDK2/9 inhibitor that interferes with cyclin E1-CDK2 activity, resulting in anaphase catastrophe [423]. Cyclin E1 amplification/overexpression has been proposed as a mechanism of resistance to the anti-HER2 antibody trastuzumab in *HER2*-amplified breast cancer; CYC065 treatment of mice with xenografts derived from *CCNE1*-amplified, trastuzumab-resistant breast cancer cells led to a significant reduction in tumor growth [424]. In addition, CYC065 inhibited tumor growth of *CCNE1*-amplified UPSC cell lines *in vitro* and cell line-derived xenografts *in vivo*; combination treatment of CYC065 with the PIK3CA inhibitor taselisib showed a synergistic effect [425]. The use of CYC065 is currently being evaluated in a phase I clinical trial for patients with advanced cancer (NCT02552953 [426]).

8-hydroxypiperidine-methyl-baicalein (BA-j) has recently been designed and synthesized as a flavonoid derivative with improved bioavailability compared to the parent compound baicalein and other flavonoids, either injected or orally administered. BA-j was demonstrated to have selective CDK1 inhibitory activity and only weak activity against CDK2/4/6. BA-j treatment of MCF-7 and

HL-60 cells led to G1 and G2 arrest and a dose-dependent increase in apoptosis [427, 428], indicating potential as an anti-cancer drug.

In summary, we have established that UCHL1 is a novel prognostic marker for UPSC and a viable therapeutic target. Further development of UCHL1 and CDK1 inhibitors would potentially benefit this understudied population of patients with aggressive disease.

BIBLIOGRAPHY

1.   Siegel, R.L., K.D. Miller, and A. Jemal, *Cancer Statistics, 2017.* CA Cancer J Clin, 2017. **67**(1): p. 7-30.

2.   Siegel, R.L., K.D. Miller, and A. Jemal, *Cancer statistics, 2016.* CA Cancer J Clin, 2016. **66**(1): p. 7-30.

3.   Rahib, L., B.D. Smith, R. Aizenberg, A.B. Rosenzweig, J.M. Fleshman, and L.M. Matrisian, *Projecting cancer incidence and deaths to 2030: the unexpected burden of thyroid, liver, and pancreas cancers in the United States.* Cancer Res, 2014. **74**(11): p. 2913-21.

4.   Calle, E.E., C. Rodriguez, K. Walker-Thurmond, and M.J. Thun, *Overweight, obesity, and mortality from cancer in a prospectively studied cohort of U.S. adults.* N Engl J Med, 2003. **348**(17): p. 1625-38.

5.   James, W.P., *WHO recognition of the global obesity epidemic.* Int J Obes (Lond), 2008. **32 Suppl 7**: p. S120-6.

6.   Mitchell, N.S., V.A. Catenacci, H.R. Wyatt, and J.O. Hill, *Obesity: overview of an epidemic.* Psychiatr Clin North Am, 2011. **34**(4): p. 717-32.

7.   Carlson, M.J., K.W. Thiel, S. Yang, and K.K. Leslie, *Catch it before it kills: progesterone, obesity, and the prevention of endometrial cancer.* Discov Med, 2012. **14**(76): p. 215-22.

8.   Wartko, P., M.E. Sherman, H.P. Yang, A.S. Felix, L.A. Brinton, and B. Trabert, *Recent changes in endometrial cancer trends among menopausal-age U.S. women.* Cancer Epidemiol, 2013. **37**(4): p. 374-7.

9.   Bokhman, J.V., *Two pathogenetic types of endometrial carcinoma.* Gynecol Oncol, 1983. **15**(1): p. 10-7.

10.   Roque, D.M. and A.D. Santin, *Updates in therapy for uterine serous carcinoma.* Curr Opin Obstet Gynecol, 2013. **25**(1): p. 29-37.

11. Mendivil, A., K.M. Schuler, and P.A. Gehrig, *Non-endometrioid adenocarcinoma of the uterine corpus: a review of selected histological subtypes.* Cancer Control, 2009. **16**(1): p. 46-52.

12. Fadare, O. and W. Zheng, *Endometrial serous carcinoma (uterine papillary serous carcinoma): precancerous lesions and the theoretical promise of a preventive approach.* Am J Cancer Res, 2012. **2**(3): p. 335-9.

13. Figge, D.C., P.M. Otto, H.K. Tamimi, and B.E. Greer, *Treatment variables in the management of endometrial cancer.* Am J Obstet Gynecol, 1983. **146**(5): p. 495-500.

14. DiSaia, P.J., W.T. Creasman, R.C. Boronow, and J.A. Blessing, *Risk factors and recurrent patterns in Stage I endometrial cancer.* Am J Obstet Gynecol, 1985. **151**(8): p. 1009-15.

15. Hanson, M.B., J.R. van Nagell, Jr., D.E. Powell, E.S. Donaldson, H. Gallion, M. Merhige, and E.J. Pavlik, *The prognostic significance of lymph-vascular space invasion in stage I endometrial cancer.* Cancer, 1985. **55**(8): p. 1753-7.

16. Creasman, W.T., C.P. Morrow, B.N. Bundy, H.D. Homesley, J.E. Graham, and P.B. Heller, *Surgical pathologic spread patterns of endometrial cancer. A Gynecologic Oncology Group Study.* Cancer, 1987. **60**(8 Suppl): p. 2035-41.

17. Fader, A.N., D. Boruta, A.B. Olawaiye, and P.A. Gehrig, *Uterine papillary serous carcinoma: epidemiology, pathogenesis and management.* Curr Opin Obstet Gynecol, 2010. **22**(1): p. 21-9.

18. Cirisano, F.D., Jr., S.J. Robboy, R.K. Dodge, R.C. Bentley, H.R. Krigman, I.S. Synan, J.T. Soper, and D.L. Clarke-Pearson, *Epidemiologic and surgicopathologic findings of papillary serous and clear cell endometrial cancers when compared to endometrioid carcinoma.* Gynecol Oncol, 1999. **74**(3): p. 385-94.

19. Goff, B.A., D. Kato, R.A. Schmidt, M. Ek, J.A. Ferry, H.G. Muntz, J.M. Cain, H.K. Tamimi, D.C. Figge, and B.E. Greer, *Uterine papillary serous carcinoma: patterns of metastatic spread.* Gynecol Oncol, 1994. **54**(3): p. 264-8.

20. Carcangiu, M.L., L.K. Tan, and J.T. Chambers, *Stage IA uterine serous carcinoma: a study of 13 cases.* Am J Surg Pathol, 1997. **21**(12): p. 1507-14.

21. Wheeler, D.T., K.A. Bell, R.J. Kurman, and M.E. Sherman, *Minimal uterine serous carcinoma: diagnosis and clinicopathologic correlation.* Am J Surg Pathol, 2000. **24**(6): p. 797-806.

22. Fader, A.N., A.D. Santin, and P.A. Gehrig, *Early stage uterine serous carcinoma: management updates and genomic advances.* Gynecol Oncol, 2013. **129**(1): p. 244-50.

23. Pol, F., D. Allen, R. Bekkers, P. Grant, and S. Hyde, *Adjuvant treatment, tumour recurrence and the survival rate of uterine serous carcinomas: a single-institution review of 62 women.* Southern African Journal of Gynaecological Oncology, 2015. **7**(1): p. 14-20.

24. Fader, A.N., R.D. Drake, D.M. O'Malley, H.E. Gibbons, W.K. Huh, L.J. Havrilesky, P.A. Gehrig, E. Tuller, A.E. Axtell, K.M. Zanotti, and C. Uterine Papillary Serous Carcinoma, *Platinum/taxane-based chemotherapy with or without radiation therapy favorably impacts survival outcomes in stage I uterine papillary serous carcinoma.* Cancer, 2009. **115**(10): p. 2119-27.

25. Maxwell, G.L., J.I. Risinger, C. Gumbs, H. Shaw, R.C. Bentley, J.C. Barrett, A. Berchuck, and P.A. Futreal, *Mutation of the PTEN tumor suppressor gene in endometrial hyperplasias.* Cancer Res, 1998. **58**(12): p. 2500-3.

26. Levine, R.L., C.B. Cargile, M.S. Blazes, B. van Rees, R.J. Kurman, and L.H. Ellenson, *PTEN mutations and microsatellite instability in complex atypical hyperplasia, a precursor lesion to uterine endometrioid carcinoma.* Cancer Res, 1998. **58**(15): p. 3254-8.

27. Tantbirojn, P., S. Triratanachat, P. Trivijitsilp, and S. Niruthisard, *Detection of PTEN immunoreactivity in endometrial hyperplasia and adenocarcinoma.* J Med Assoc Thai, 2008. **91**(8): p. 1161-5.

28. McConechy, M.K., J. Ding, M.C. Cheang, K.C. Wiegand, J. Senz, A.A. Tone, W. Yang, L.M. Prentice, K. Tse, T. Zeng, H. McDonald, A.P. Schmidt, D.G. Mutch, J.N. McAlpine, M.

Hirst, S.P. Shah, C.H. Lee, P.J. Goodfellow, C.B. Gilks, and D.G. Huntsman, *Use of mutation profiles to refine the classification of endometrial carcinomas.* J Pathol, 2012. **228**(1): p. 20-30.

29.   Zighelboim, I., P.J. Goodfellow, F. Gao, R.K. Gibb, M.A. Powell, J.S. Rader, and D.G. Mutch, *Microsatellite instability and epigenetic inactivation of MLH1 and outcome of patients with endometrial carcinomas of the endometrioid type.* J Clin Oncol, 2007. **25**(15): p. 2042-8.

30.   Scholten, A.N., C.L. Creutzberg, L.J. van den Broek, E.M. Noordijk, and V.T. Smit, *Nuclear beta-catenin is a molecular feature of type I endometrial carcinoma.* J Pathol, 2003. **201**(3): p. 460-5.

31.   Slomovitz, B.M., T.W. Burke, P.J. Eifel, L.M. Ramondetta, E.G. Silva, A. Jhingran, J.C. Oh, E.N. Atkinson, R.R. Broaddus, D.M. Gershenson, and K.H. Lu, *Uterine papillary serous carcinoma (UPSC): a single institution review of 129 cases.* Gynecol Oncol, 2003. **91**(3): p. 463-9.

32.   Ambros, R.A., M.E. Sherman, C.M. Zahn, P. Bitterman, and R.J. Kurman, *Endometrial intraepithelial carcinoma: a distinctive lesion specifically associated with tumors displaying serous differentiation.* Hum Pathol, 1995. **26**(11): p. 1260-7.

33.   Carcangiu, M.L. and J.T. Chambers, *Uterine papillary serous carcinoma: a study on 108 cases with emphasis on the prognostic significance of associated endometrioid carcinoma, absence of invasion, and concomitant ovarian carcinoma.* Gynecol Oncol, 1992. **47**(3): p. 298-305.

34.   Emons, G., G. Fleckenstein, B. Hinney, A. Huschmand, and W. Heyl, *Hormonal interactions in endometrial cancer.* Endocr Relat Cancer, 2000. **7**(4): p. 227-42.

35.   Yi, X. and W. Zheng, *Endometrial glandular dysplasia and endometrial intraepithelial neoplasia.* Curr Opin Obstet Gynecol, 2008. **20**(1): p. 20-5.

36.   Zheng, W., S.X. Liang, X. Yi, E.C. Ulukus, J.R. Davis, and S.K. Chambers, *Occurrence of endometrial glandular dysplasia precedes uterine papillary serous carcinoma.* Int J Gynecol Pathol, 2007. **26**(1): p. 38-52.

37.   Liang, S.X., S.K. Chambers, L. Cheng, S. Zhang, Y. Zhou, and W. Zheng, *Endometrial glandular dysplasia: a putative precursor lesion of uterine papillary serous carcinoma. Part II: molecular features.* Int J Surg Pathol, 2004. **12**(4): p. 319-31.

38.   Sherman, M.E., P. Bitterman, N.B. Rosenshein, G. Delgado, and R.J. Kurman, *Uterine serous carcinoma. A morphologically diverse neoplasm with unifying clinicopathologic features.* Am J Surg Pathol, 1992. **16**(6): p. 600-10.

39.   Gehrig, P.A., P.A. Groben, W.C. Fowler, Jr., L.A. Walton, and L. Van Le, *Noninvasive papillary serous carcinoma of the endometrium.* Obstet Gynecol, 2001. **97**(1): p. 153-7.

40.   Sherman, M.E., M.E. Bur, and R.J. Kurman, *p53 in endometrial cancer and its putative precursors: evidence for diverse pathways of tumorigenesis.* Hum Pathol, 1995. **26**(11): p. 1268-74.

41.   Tashiro, H., C. Isacson, R. Levine, R.J. Kurman, K.R. Cho, and L. Hedrick, *p53 gene mutations are common in uterine serous carcinoma and occur early in their pathogenesis.* Am J Pathol, 1997. **150**(1): p. 177-85.

42.   Kuhn, E., R.C. Wu, B. Guan, G. Wu, J. Zhang, Y. Wang, L. Song, X. Yuan, L. Wei, R.B. Roden, K.T. Kuo, K. Nakayama, B. Clarke, P. Shaw, N. Olvera, R.J. Kurman, D.A. Levine, T.L. Wang, and M. Shih Ie, *Identification of molecular pathway aberrations in uterine serous carcinoma by genome-wide analyses.* J Natl Cancer Inst, 2012. **104**(19): p. 1503-13.

43.   Rosenberg, P., S. Wingren, E. Simonsen, O. Stal, B. Risberg, and B. Nordenskjold, *Flow cytometric measurements of DNA index and S-phase on paraffin-embedded early stage endometrial cancer: an important prognostic indicator.* Gynecol Oncol, 1989. **35**(1): p. 50-4.

44.   Pradhan, M., V.M. Abeler, H.E. Danielsen, C.G. Trope, and B.A. Risberg, *Image cytometry DNA ploidy correlates with histological subtypes in endometrial carcinomas.* Mod Pathol, 2006. **19**(9): p. 1227-35.

45.   Santin, A.D., S. Bellone, S. Van Stedum, W. Bushen, M. Palmieri, E.R. Siegel, L.E. De Las Casas, J.J. Roman, A. Burnett, and S. Pecorelli, *Amplification of c-erbB2 oncogene: a major prognostic indicator in uterine serous papillary carcinoma.* Cancer, 2005. **104**(7): p. 1391-7.

46.   Odicino, F.E., E. Bignotti, E. Rossi, B. Pasinetti, R.A. Tassi, C. Donzelli, M. Falchetti, P. Fontana, P.G. Grigolato, and S. Pecorelli, *HER-2/neu overexpression and amplification in uterine serous papillary carcinoma: comparative analysis of immunohistochemistry, real-time reverse transcription-polymerase chain reaction, and fluorescence in situ hybridization.* Int J Gynecol Cancer, 2008. **18**(1): p. 14-21.

47.   Xu, M., P. Schwartz, T. Rutherford, M. Azodi, A. Santin, D. Silasi, M. Martel, and P. Hui, *HER-2/neu receptor gene status in endometrial carcinomas: a tissue microarray study.* Histopathology, 2010. **56**(2): p. 269-73.

48.   Villella, J.A., S. Cohen, D.H. Smith, H. Hibshoosh, and D. Hershman, *HER-2/neu overexpression in uterine papillary serous cancers and its possible therapeutic implications.* Int J Gynecol Cancer, 2006. **16**(5): p. 1897-902.

49.   Slomovitz, B.M., R.R. Broaddus, T.W. Burke, N. Sneige, P.T. Soliman, W. Wu, C.C. Sun, M.F. Munsell, D.M. Gershenson, and K.H. Lu, *Her-2/neu overexpression and amplification in uterine papillary serous carcinoma.* J Clin Oncol, 2004. **22**(15): p. 3126-32.

50.   Singh, P., C.L. Smith, G. Cheetham, T.J. Dodd, and M.L. Davy, *Serous carcinoma of the uterus-determination of HER-2/neu status using immunohistochemistry, chromogenic in situ hybridization, and quantitative polymerase chain reaction techniques: its significance and clinical correlation.* Int J Gynecol Cancer, 2008. **18**(6): p. 1344-51.

51.   Buza, N., D.P. English, A.D. Santin, and P. Hui, *Toward standard HER2 testing of endometrial serous carcinoma: 4-year experience at a large academic center and recommendations for clinical practice.* Mod Pathol, 2013. **26**(12): p. 1605-12.

52.   Santin, A.D., S. Bellone, S. Van Stedum, W. Bushen, L.E. De Las Casas, S. Korourian, E. Tian, J.J. Roman, A. Burnett, and S. Pecorelli, *Determination of HER2/neu status in uterine serous papillary carcinoma: Comparative analysis of immunohistochemistry and fluorescence in situ hybridization.* Gynecol Oncol, 2005. **98**(1): p. 24-30.

53.   Holcomb, K., R. Delatorre, B. Pedemonte, C. McLeod, L. Anderson, and J. Chambers, *E-cadherin expression in endometrioid, papillary serous, and clear cell carcinoma of the endometrium.* Obstet Gynecol, 2002. **100**(6): p. 1290-5.

54.   Mell, L.K., J.J. Meyer, M. Tretiakova, A. Khramtsov, C. Gong, S.D. Yamada, A.G. Montag, and A.J. Mundt, *Prognostic significance of E-cadherin protein expression in pathological stage I-III endometrial cancer.* Clin Cancer Res, 2004. **10**(16): p. 5546-53.

55.   Konecny, G.E., R. Agarwal, G.A. Keeney, B. Winterhoff, M.B. Jones, A. Mariani, D. Riehle, C. Neuper, S.C. Dowdy, H.J. Wang, P.J. Morin, and K.C. Podratz, *Claudin-3 and claudin-4 expression in serous papillary, clear-cell, and endometrioid endometrial cancer.* Gynecol Oncol, 2008. **109**(2): p. 263-9.

56.   Reid-Nicholson, M., P. Iyengar, A.J. Hummer, I. Linkov, M. Asher, and R.A. Soslow, *Immunophenotypic diversity of endometrial adenocarcinomas: implications for differential diagnosis.* Mod Pathol, 2006. **19**(8): p. 1091-100.

57.   Chiesa-Vottero, A.G., A. Malpica, M.T. Deavers, R. Broaddus, G.J. Nuovo, and E.G. Silva, *Immunohistochemical overexpression of p16 and p53 in uterine serous carcinoma and ovarian high-grade serous carcinoma.* Int J Gynecol Pathol, 2007. **26**(3): p. 328-33.

58.   Yoon, G., C. Won Koh, N. Yoon, J.Y. Kim, and H.S. Kim, *Stromal p16 expression is significantly increased in endometrial carcinoma.* Oncotarget, 2016.

59.   Zhao, S., M. Choi, J.D. Overton, S. Bellone, D.M. Roque, E. Cocco, F. Guzzo, D.P. English, J. Varughese, S. Gasparrini, I. Bortolomai, N. Buza, P. Hui, M. Abu-Khalaf, A. Ravaggi, E. Bignotti, E. Bandiera, C. Romani, P. Todeschini, R. Tassi, L. Zanotti, L. Carrara, S. Pecorelli, D.A. Silasi, E. Ratner, M. Azodi, P.E. Schwartz, T.J. Rutherford, A.L. Stiegler, S. Mane, T.J. Boggon, J. Schlessinger, R.P. Lifton, and A.D. Santin, *Landscape of somatic single-nucleotide and copy-number mutations in uterine serous carcinoma.* Proc Natl Acad Sci U S A, 2013. **110**(8): p. 2916-21.

60.   Matias-Guiu, X., L. Catasus, E. Bussaglia, H. Lagarda, A. Garcia, C. Pons, J. Munoz, R. Arguelles, P. Machin, and J. Prat, *Molecular pathology of endometrial hyperplasia and carcinoma.* Hum Pathol, 2001. **32**(6): p. 569-77.

61.   Sherman, M.E., *Theories of endometrial carcinogenesis: a multidisciplinary approach.* Mod Pathol, 2000. **13**(3): p. 295-308.

62.   Merritt, M.A. and D.W. Cramer, *Molecular pathogenesis of endometrial and ovarian cancer.* Cancer Biomark, 2010. **9**(1-6): p. 287-305.

63.   Roelofsen, T., M.A. van Ham, J.M. Wiersma van Tilburg, S.F. Zomer, M. Bol, L.F. Massuger, and J. Bulten, *Pure compared with mixed serous endometrial carcinoma: two different entities?* Obstet Gynecol, 2012. **120**(6): p. 1371-81.

64.   Alektiar, K.M., A. McKee, O. Lin, E. Venkatraman, M.J. Zelefsky, B. McKee, W.J. Hoskins, and R.R. Barakat, *Is there a difference in outcome between stage I-II endometrial cancer of papillary serous/clear cell and endometrioid FIGO Grade 3 cancer?* Int J Radiat Oncol Biol Phys, 2002. **54**(1): p. 79-85.

65.   Ayeni, T.A., J.N. Bakkum-Gamez, A. Mariani, M.E. McGree, A.L. Weaver, M.G. Haddock, G.L. Keeney, H.J. Long, 3rd, S.C. Dowdy, and K.C. Podratz, *Comparative outcomes assessment of uterine grade 3 endometrioid, serous, and clear cell carcinomas.* Gynecol Oncol, 2013. **129**(3): p. 478-85.

66. Alkushi, A., M. Köbel, S.E. Kalloger, and C.B. Gilks, *High-grade endometrial carcinoma: serous and grade 3 endometrioid carcinomas have different immunophenotypes and outcomes.* Int J Gynecol Pathol, 2010. **29**(4): p. 343-50.

67. Boruta, D.M., 2nd, P.A. Gehrig, P.A. Groben, V. Bae-Jump, J.F. Boggess, W.C. Fowler, Jr., and L. Van Le, *Uterine serous and grade 3 endometrioid carcinomas: is there a survival difference?* Cancer, 2004. **101**(10): p. 2214-21.

68. Hamilton, C.A., M.K. Cheung, K. Osann, L. Chen, N.N. Teng, T.A. Longacre, M.A. Powell, M.R. Hendrickson, D.S. Kapp, and J.K. Chan, *Uterine papillary serous and clear cell carcinomas predict for poorer survival compared to grade 3 endometrioid corpus cancers.* Br J Cancer, 2006. **94**(5): p. 642-6.

69. Kim, H.J., T.J. Kim, Y.Y. Lee, C.H. Choi, J.W. Lee, D.S. Bae, and B.G. Kim, *A comparison of uterine papillary serous, clear cell carcinomas, and grade 3 endometrioid corpus cancers using 2009 FIGO staging system.* J Gynecol Oncol, 2013. **24**(2): p. 120-7.

70. Talhouk, A., M.K. McConechy, S. Leung, H.H. Li-Chang, J.S. Kwon, N. Melnyk, W. Yang, J. Senz, N. Boyd, A.N. Karnezis, D.G. Huntsman, C.B. Gilks, and J.N. McAlpine, *A clinically applicable molecular-based classification for endometrial cancers.* Br J Cancer, 2015. **113**(2): p. 299-310.

71. Wei, J.J., A. Paintal, and P. Keh, *Histologic and immunohistochemical analyses of endometrial carcinomas: experiences from endometrial biopsies in 358 consultation cases.* Arch Pathol Lab Med, 2013. **137**(11): p. 1574-83.

72. Cancer Genome Atlas Research Network, C. Kandoth, N. Schultz, A.D. Cherniack, R. Akbani, Y. Liu, H. Shen, A.G. Robertson, I. Pashtan, R. Shen, C.C. Benz, C. Yau, P.W. Laird, L. Ding, W. Zhang, G.B. Mills, R. Kucherlapati, E.R. Mardis, and D.A. Levine, *Integrated genomic characterization of endometrial carcinoma.* Nature, 2013. **497**(7447): p. 67-73.

73.   Hui, P., M. Kelly, D.M. O'Malley, F. Tavassoli, and P.E. Schwartz, *Minimal uterine serous carcinoma: a clinicopathological study of 40 cases.* Mod Pathol, 2005. **18**(1): p. 75-82.

74.   Zheng, W. and P.E. Schwartz, *Serous EIC as an early form of uterine papillary serous carcinoma: recent progress in understanding its pathogenesis and current opinions regarding pathologic and clinical management.* Gynecol Oncol, 2005. **96**(3): p. 579-82.

75.   Snyder, M.J., R. Bentley, and S.J. Robboy, *Transtubal spread of serous adenocarcinoma of the endometrium: an underrecognized mechanism of metastasis.* Int J Gynecol Pathol, 2006. **25**(2): p. 155-60.

76.   Ayeni, T.A., J.N. Bakkum-Gamez, A. Mariani, M.E. McGree, A.L. Weaver, M.M. Alhilli, J.R. Martin, G.L. Keeney, S.C. Dowdy, and K.C. Podratz, *Impact of tubal ligation on routes of dissemination and overall survival in uterine serous carcinoma.* Gynecol Oncol, 2013. **128**(1): p. 71-6.

77.   Group, S.G.O.C.P.E.C.W., W.M. Burke, J. Orr, M. Leitao, E. Salom, P. Gehrig, A.B. Olawaiye, M. Brewer, D. Boruta, J. Villella, T. Herzog, F. Abu Shahin, and C. Society of Gynecologic Oncology Clinical Practice, *Endometrial cancer: a review and current management strategies: part I.* Gynecol Oncol, 2014. **134**(2): p. 385-92.

78.   del Carmen, M.G., M. Birrer, and J.O. Schorge, *Uterine papillary serous cancer: a review of the literature.* Gynecol Oncol, 2012. **127**(3): p. 651-61.

79.   Rauh-Hain, J.A., W.B. Growdon, J.O. Schorge, A.K. Goodman, D.M. Boruta, C. McCann, N.S. Horowitz, and M.G. del Carmen, *Prognostic determinants in patients with stage IIIC and IV uterine papillary serous carcinoma.* Gynecol Oncol, 2010. **119**(2): p. 299-304.

80.   S. G. O. Clinical Practice Endometrial Cancer Working Group, W.M. Burke, J. Orr, M. Leitao, E. Salom, P. Gehrig, A.B. Olawaiye, M. Brewer, D. Boruta, T.J. Herzog, F.A. Shahin, and C. Society of Gynecologic Oncology Clinical Practice, *Endometrial cancer: a review and current management strategies: part II.* Gynecol Oncol, 2014. **134**(2): p. 393-402.

81. Sovak, M.A., M.L. Hensley, J. Dupont, N. Ishill, K.M. Alektiar, N. Abu-Rustum, R. Barakat, D.S. Chi, P. Sabbatini, D.R. Spriggs, and C. Aghajanian, *Paclitaxel and carboplatin in the adjuvant treatment of patients with high-risk stage III and IV endometrial cancer: a retrospective study.* Gynecol Oncol, 2006. **103**(2): p. 451-7.

82. Vaidya, A.P., R. Littell, C. Krasner, and L.R. Duska, *Treatment of uterine papillary serous carcinoma with platinum-based chemotherapy and paclitaxel.* Int J Gynecol Cancer, 2006. **16 Suppl 1**: p. 267-72.

83. Miller, K.D., R.L. Siegel, C.C. Lin, A.B. Mariotto, J.L. Kramer, J.H. Rowland, K.D. Stein, R. Alteri, and A. Jemal, *Cancer treatment and survivorship statistics, 2016.* CA Cancer J Clin, 2016. **66**(4): p. 271-89.

84. Sagr, E.R., D. Denschlag, A. Kerim-Dikeni, G. Stanimir, G. Gitsch, and L. Gilbert, *Prognostic factors and treatment-related outcome in patients with uterine papillary serous carcinoma.* Anticancer Res, 2007. **27**(2): p. 1213-7.

85. Creasman, W.T., F. Odicino, P. Maisonneuve, M.A. Quinn, U. Beller, J.L. Benedet, A.P. Heintz, H.Y. Ngan, and S. Pecorelli, *Carcinoma of the corpus uteri. FIGO 26th Annual Report on the Results of Treatment in Gynecological Cancer.* Int J Gynaecol Obstet, 2006. **95 Suppl 1**: p. S105-43.

86. Baselga, J., *Treatment of HER2-overexpressing breast cancer.* Ann Oncol, 2010. **21 Suppl 7**: p. vii36-40.

87. Arnould, L., M. Gelly, F. Penault-Llorca, L. Benoit, F. Bonnetain, C. Migeon, V. Cabaret, V. Fermeaux, P. Bertheau, J. Garnier, J.F. Jeannin, and B. Coudert, *Trastuzumab-based treatment of HER2-positive breast cancer: an antibody-dependent cellular cytotoxicity mechanism?* Br J Cancer, 2006. **94**(2): p. 259-67.

88. Dungo, R.T. and G.M. Keating, *Afatinib: first global approval.* Drugs, 2013. **73**(13): p. 1503-15.

89.   Wynn, P. *FDA approves GILOTRIFTM (afatinib) as first-line treatment for metastatic non-small cell lung cancer with common EGFR mutations*. 2013 [cited 2016 December 20]; Available from: https://www.boehringer-ingelheim.us/press-release/fda-approves-gilotrif-afatinib-first-line-treatment-metastatic-non-small-cell-lung.

90.   Soria, J.C., E. Felip, M. Cobo, S. Lu, K. Syrigos, K.H. Lee, E. Goker, V. Georgoulias, W. Li, D. Isla, S.Z. Guclu, A. Morabito, Y.J. Min, A. Ardizzoni, S.M. Gadgeel, B. Wang, V.K. Chand, G.D. Goss, and L.U.-L. Investigators, *Afatinib versus erlotinib as second-line treatment of patients with advanced squamous cell carcinoma of the lung (LUX-Lung 8): an open-label randomised controlled phase 3 trial.* Lancet Oncol, 2015. **16**(8): p. 897-907.

91.   Wynn, P. *FDA approves Gilotrif® (afatinib) as new oral treatment option for patients with squamous cell carcinoma of the lung*. 2016 [cited 2016 December 20]; Available from: https://www.boehringer-ingelheim.us/press-release/fda-approves-gilotrifr-afatinib-new-oral-treatment-option-patients-squamous-cell.

92.   NIH Clinical Trials. *A Phase II Evaluation of Afatinibin Patients With Persistent or Recurrent HER2-positive Uterine Serous Carcinoma (Afatinib)*. 2016/12/08]; Available from: https://clinicaltrials.gov/show/NCT02491099.

93.   Fleming, G.F., M.W. Sill, K.M. Darcy, D.S. McMeekin, J.T. Thigpen, L.M. Adler, J.S. Berek, J.A. Chapman, P.A. DiSilvestro, I.R. Horowitz, and J.V. Fiorica, *Phase II trial of trastuzumab in women with advanced or recurrent, HER2-positive endometrial carcinoma: a Gynecologic Oncology Group study.* Gynecol Oncol, 2010. **116**(1): p. 15-20.

94.   Santin, A.D., *Letter to the Editor referring to the manuscript entitled: "Phase II trial of trastuzumab in women with advanced or recurrent HER-positive endometrial carcinoma: a Gynecologic Oncology Group study" recently reported by Fleming et al., (Gynecol Oncol., 116;15-20;2010).* Gynecol Oncol, 2010. **118**(1): p. 95-6; author reply 96-7.

95.   NIH Clinical Trials. *Evaluation of carboplatin/paclitaxel with and without trastuzumab (Herceptin) in uterine serous cancer.* 2016/12/08]; Available from: https://clinicaltrials.gov/ct2/show/NCT01367002.

96.   Growdon, W.B., J. Groeneweg, V. Byron, C. DiGloria, D.R. Borger, R. Tambouret, R. Foster, A. Chenna, J. Sperinde, J. Winslow, and B.R. Rueda, *HER2 over-expressing high grade endometrial cancer expresses high levels of p95HER2 variant.* Gynecol Oncol, 2015. **137**(1): p. 160-6.

97.   Sperinde, J., X. Jin, J. Banerjee, E. Penuel, A. Saha, G. Diedrich, W. Huang, K. Leitzel, J. Weidler, S.M. Ali, E.M. Fuchs, C.F. Singer, W.J. Kostler, M. Bates, G. Parry, J. Winslow, and A. Lipton, *Quantitation of p95HER2 in paraffin sections by using a p95-specific antibody and correlation with outcome in a cohort of trastuzumab-treated breast cancer patients.* Clin Cancer Res, 2010. **16**(16): p. 4226-35.

98.   Duchnowska, R., J. Sperinde, A. Chenna, M. Haddad, A. Paquet, Y. Lie, J.M. Weidler, W. Huang, J. Winslow, T. Jankowski, B. Czartoryska-Arlukowicz, P.J. Wysocki, M. Foszczynska-Kloda, B. Radecka, M.M. Litwiniuk, J. Zok, M. Wisniewski, D. Zuziak, W. Biernat, and J. Jassem, *Quantitative measurements of tumoral p95HER2 protein expression in metastatic breast cancer patients treated with trastuzumab: independent validation of the p95HER2 clinical cutoff.* Clin Cancer Res, 2014. **20**(10): p. 2805-13.

99.   Menderes, G., M. Clark, and A.D. Santin, *Novel targeted therapies in uterine serous carcinoma, an aggressive variant of endometrial cancer.* Discov Med, 2016. **21**(116): p. 293-303.

100.   Lopez, S., E. Cocco, J. Black, S. Bellone, E. Bonazzoli, F. Predolini, F. Ferrari, C.L. Schwab, D.P. English, E. Ratner, D.A. Silasi, M. Azodi, P.E. Schwartz, C. Terranova, R. Angioli, and A.D. Santin, *Dual HER2/PIK3CA Targeting Overcomes Single-Agent Acquired Resistance in HER2-Amplified Uterine Serous Carcinoma Cell Lines In Vitro and In Vivo.* Mol Cancer Ther, 2015. **14**(11): p. 2519-26.

101. Kamat, A.A., W.M. Merritt, D. Coffey, Y.G. Lin, P.R. Patel, R. Broaddus, E. Nugent, L.Y. Han, C.N. Landen, Jr., W.A. Spannuth, C. Lu, R.L. Coleman, D.M. Gershenson, and A.K. Sood, *Clinical and biological significance of vascular endothelial growth factor in endometrial cancer.* Clin Cancer Res, 2007. **13**(24): p. 7487-95.

102. Hirai, M., A. Nakagawara, T. Oosaki, Y. Hayashi, M. Hirono, and T. Yoshihara, *Expression of vascular endothelial growth factors (VEGF-A/VEGF-1 and VEGF-C/VEGF-2) in postmenopausal uterine endometrial carcinoma.* Gynecol Oncol, 2001. **80**(2): p. 181-8.

103. Aghajanian, C., M.W. Sill, K.M. Darcy, B. Greer, D.S. McMeekin, P.G. Rose, J. Rotmensch, M.N. Barnes, P. Hanjani, and K.K. Leslie, *Phase II trial of bevacizumab in recurrent or persistent endometrial cancer: a Gynecologic Oncology Group study.* J Clin Oncol, 2011. **29**(16): p. 2259-65.

104. NIH Clinical Trials. *Evaluation of carboplatin /paclitaxel /bevacizumab in the treatment of advanced stage endometrial carcinoma*. 2016/12/08]; Available from: https://clinicaltrials.gov/ct2/show/NCT00513786.

105. Vilchez, D., I. Saez, and A. Dillin, *The role of protein clearance mechanisms in organismal ageing and age-related diseases.* Nat Commun, 2014. **5**: p. 5659.

106. Hurst-Kennedy, J., L.S. Chin, and L. Li, *Ubiquitin C-terminal hydrolase l1 in tumorigenesis.* Biochem Res Int, 2012. **2012**: p. 123706.

107. Pickart, C.M., *Mechanisms underlying ubiquitination.* Annu Rev Biochem, 2001. **70**: p. 503-33.

108. Li, W. and Y. Ye, *Polyubiquitin chains: functions, structures, and mechanisms.* Cell Mol Life Sci, 2008. **65**(15): p. 2397-406.

109. Komander, D., *The emerging complexity of protein ubiquitination.* Biochem Soc Trans, 2009. **37**(Pt 5): p. 937-53.

110. Pickart, C.M. and I.A. Rose, *Ubiquitin carboxyl-terminal hydrolase acts on ubiquitin carboxyl-terminal amides.* J Biol Chem, 1985. **260**(13): p. 7903-10.

111. Fraile, J.M., V. Quesada, D. Rodriguez, J.M. Freije, and C. Lopez-Otin, *Deubiquitinases in cancer: new functions and therapeutic options.* Oncogene, 2012. **31**(19): p. 2373-88.

112. Caballero, O.L., V. Resto, M. Patturajan, D. Meerzaman, M.Z. Guo, J. Engles, R. Yochem, E. Ratovitski, D. Sidransky, and J. Jen, *Interaction and colocalization of PGP9.5 with JAB1 and p27(Kip1).* Oncogene, 2002. **21**(19): p. 3003-10.

113. Wilkinson, K.D., K.M. Lee, S. Deshpande, P. Duerksen-Hughes, J.M. Boss, and J. Pohl, *The neuron-specific protein PGP 9.5 is a ubiquitin carboxyl-terminal hydrolase.* Science, 1989. **246**(4930): p. 670-3.

114. Case, A. and R.L. Stein, *Mechanistic studies of ubiquitin C-terminal hydrolase L1.* Biochemistry, 2006. **45**(7): p. 2443-52.

115. Larsen, C.N., J.S. Price, and K.D. Wilkinson, *Substrate binding and catalysis by ubiquitin C-terminal hydrolases: identification of two active site residues.* Biochemistry, 1996. **35**(21): p. 6735-44.

116. Kajimoto, Y., T. Hashimoto, Y. Shirai, N. Nishino, T. Kuno, and C. Tanaka, *cDNA cloning and tissue distribution of a rat ubiquitin carboxyl-terminal hydrolase PGP9.5.* J Biochem, 1992. **112**(1): p. 28-32.

117. Wilson, P.O., P.C. Barber, Q.A. Hamid, B.F. Power, A.P. Dhillon, J. Rode, I.N. Day, R.J. Thompson, and J.M. Polak, *The immunolocalization of protein gene product 9.5 using rabbit polyclonal and mouse monoclonal antibodies.* Br J Exp Pathol, 1988. **69**(1): p. 91-104.

118. Leroy, E., R. Boyer, G. Auburger, B. Leube, G. Ulm, E. Mezey, G. Harta, M.J. Brownstein, S. Jonnalagada, T. Chernova, A. Dehejia, C. Lavedan, T. Gasser, P.J. Steinbach, K.D. Wilkinson, and M.H. Polymeropoulos, *The ubiquitin pathway in Parkinson's disease.* Nature, 1998. **395**(6701): p. 451-2.

119. Nishikawa, K., H. Li, R. Kawamura, H. Osaka, Y.L. Wang, Y. Hara, T. Hirokawa, Y. Manago, T. Amano, M. Noda, S. Aoki, and K. Wada, *Alterations of structure and hydrolase*

activity of parkinsonism-associated human ubiquitin carboxyl-terminal hydrolase L1 variants. Biochem Biophys Res Commun, 2003. **304**(1): p. 176-83.

120.   Bonazzi, V.F., D.J. Nancarrow, M.S. Stark, R.J. Moser, G.M. Boyle, L.G. Aoude, C. Schmidt, and N.K. Hayward, *Cross-platform array screening identifies COL1A2, THBS1, TNFRSF10D and UCHL1 as genes frequently silenced by methylation in melanoma.* PLoS One, 2011. **6**(10): p. e26121.

121.   Fellenberg, J., B. Lehner, and D. Witte, *Silencing of the UCHL1 gene in giant cell tumors of bone.* Int J Cancer, 2010. **127**(8): p. 1804-12.

122.   Fukutomi, S., N. Seki, K. Koda, and M. Miyazaki, *Identification of methylation-silenced genes in colorectal cancer cell lines: genomic screening using oligonucleotide arrays.* Scand J Gastroenterol, 2007. **42**(12): p. 1486-94.

123.   Kagara, I., H. Enokida, K. Kawakami, R. Matsuda, K. Toki, H. Nishimura, T. Chiyomaru, S. Tatarano, T. Itesako, K. Kawamoto, K. Nishiyama, N. Seki, and M. Nakagawa, *CpG hypermethylation of the UCHL1 gene promoter is associated with pathogenesis and poor prognosis in renal cell carcinoma.* J Urol, 2008. **180**(1): p. 343-51.

124.   Li, L., Q. Tao, H. Jin, A. van Hasselt, F.F. Poon, X. Wang, M.S. Zeng, W.H. Jia, Y.X. Zeng, A.T. Chan, and Y. Cao, *The tumor suppressor UCHL1 forms a complex with p53/MDM2/ARF to promote p53 signaling and is frequently silenced in nasopharyngeal carcinoma.* Clin Cancer Res, 2010. **16**(11): p. 2949-58.

125.   Mitsui, Y., H. Shiina, M. Hiraki, N. Arichi, T. Hiraoka, M. Sumura, S. Honda, H. Yasumoto, and M. Igawa, *Tumor suppressor function of PGP9.5 is associated with epigenetic regulation in prostate cancer--novel predictor of biochemical recurrence after radical surgery.* Cancer Epidemiol Biomarkers Prev, 2012. **21**(3): p. 487-96.

126.   Okochi-Takada, E., K. Nakazawa, M. Wakabayashi, A. Mori, S. Ichimura, T. Yasugi, and T. Ushijima, *Silencing of the UCHL1 gene in human colorectal and ovarian cancers.* Int J Cancer, 2006. **119**(6): p. 1338-44.

127.   Ummanni, R., E. Jost, M. Braig, F. Lohmann, F. Mundt, C. Barett, T. Schlomm, G. Sauter, T. Senff, C. Bokemeyer, H. Sultmann, C. Meyer-Schwesinger, T.H. Brummendorf, and S. Balabanov, *Ubiquitin carboxyl-terminal hydrolase 1 (UCHL1) is a potential tumour suppressor in prostate cancer and is frequently silenced by promoter methylation.* Molecular Cancer, 2011. **10**.

128.   Lee, Y.M., J.Y. Lee, M.J. Kim, H.I. Bae, J.Y. Park, S.G. Kim, and D.S. Kim, *Hypomethylation of the protein gene product 9.5 promoter region in gallbladder cancer and its relationship with clinicopathological features.* Cancer Sci, 2006. **97**(11): p. 1205-10.

129.   Leiblich, A., S.S. Cross, J.W. Catto, G. Pesce, F.C. Hamdy, and I. Rehman, *Human prostate cancer cells express neuroendocrine cell markers PGP 9.5 and chromogranin A.* Prostate, 2007. **67**(16): p. 1761-9.

130.   Mizukami, H., T. Goto, Y. Kitamura, M. Sakata, M. Saito, K. Ishibashi, G. Kigawa, H. Nemoto, Y. Sanada, and K. Hibi, *PGP9.5 was less frequently methylated in advanced gastric carcinoma.* Hepatogastroenterology, 2009. **56**(94-95): p. 1576-9.

131.   Mizukami, H., A. Shirahata, T. Goto, M. Sakata, M. Saito, K. Ishibashi, G. Kigawa, H. Nemoto, Y. Sanada, and K. Hibi, *PGP9.5 methylation as a marker for metastatic colorectal cancer.* Anticancer Res, 2008. **28**(5A): p. 2697-700.

132.   Hussain, S., O. Foreman, S.L. Perkins, T.E. Witzig, R.R. Miles, J. van Deursen, and P.J. Galardy, *The de-ubiquitinase UCH-L1 is an oncogene that drives the development of lymphoma in vivo by deregulating PHLPP1 and Akt signaling.* Leukemia, 2010. **24**(9): p. 1641-55.

133.   Carrieri, C., L. Cimatti, M. Biagioli, A. Beugnet, S. Zucchelli, S. Fedele, E. Pesce, I. Ferrer, L. Collavin, C. Santoro, A.R. Forrest, P. Carninci, S. Biffo, E. Stupka, and S. Gustincich, *Long non-coding antisense RNA controls Uchl1 translation through an embedded SINEB2 repeat.* Nature, 2012. **491**(7424): p. 454-7.

134.   McKeon, J.E., D. Sha, L. Li, and L.S. Chin, *Parkin-mediated K63-polyubiquitination targets ubiquitin C-terminal hydrolase L1 for degradation by the autophagy-lysosome system.* Cell Mol Life Sci, 2015. **72**(9): p. 1811-24.

135.   Xu, L., D.C. Lin, D. Yin, and H.P. Koeffler, *An emerging role of PARK2 in cancer.* J Mol Med (Berl), 2014. **92**(1): p. 31-42.

136.   Tezel, E., K. Hibi, T. Nagasaka, and A. Nakao, *PGP9.5 as a prognostic factor in pancreatic cancer.* Clin Cancer Res, 2000. **6**(12): p. 4764-7.

137.   Miyoshi, Y., S. Nakayama, Y. Torikoshi, S. Tanaka, H. Ishihara, T. Taguchi, Y. Tamaki, and S. Noguchi, *High expression of ubiquitin carboxy-terminal hydrolase-L1 and -L3 mRNA predicts early recurrence in patients with invasive breast cancer.* Cancer Sci, 2006. **97**(6): p. 523-9.

138.   Akishima-Fukasawa, Y., Y. Ino, Y. Nakanishi, A. Miura, Y. Moriya, T. Kondo, Y. Kanai, and S. Hirohashi, *Significance of PGP9.5 expression in cancer-associated fibroblasts for prognosis of colorectal carcinoma.* Am J Clin Pathol, 2010. **134**(1): p. 71-9.

139.   Goto, Y., L. Zeng, C.J. Yeom, Y. Zhu, A. Morinibu, K. Shinomiya, M. Kobayashi, K. Hirota, S. Itasaka, M. Yoshimura, K. Tanimoto, M. Torii, T. Sowa, T. Menju, M. Sonobe, H. Kakeya, M. Toi, H. Date, E.M. Hammond, M. Hiraoka, and H. Harada, *UCHL1 provides diagnostic and antimetastatic strategies due to its deubiquitinating effect on HIF-1alpha.* Nat Commun, 2015. **6**: p. 6153.

140.   Ma, Y., M. Zhao, J. Zhong, L. Shi, Q. Luo, J. Liu, J. Wang, X. Yuan, and C. Huang, *Proteomic profiling of proteins associated with lymph node metastasis in colorectal cancer.* J Cell Biochem, 2010. **110**(6): p. 1512-9.

141.   Kim, H.J., Y.M. Kim, S. Lim, Y.K. Nam, J. Jeong, and K.J. Lee, *Ubiquitin C-terminal hydrolase-L1 is a key regulator of tumor cell invasion and metastasis.* Oncogene, 2009. **28**(1): p. 117-27.

142.   Jang, M.J., S.H. Baek, and J.H. Kim, *UCH-L1 promotes cancer metastasis in prostate cancer cells through EMT induction.* Cancer Lett, 2011. **302**(2): p. 128-35.

143.   Xiang, T., L. Li, X. Yin, C. Yuan, C. Tan, X. Su, L. Xiong, T.C. Putti, M. Oberst, K. Kelly, G. Ren, and Q. Tao, *The ubiquitin peptidase UCHL1 induces G0/G1 cell cycle arrest and apoptosis through stabilizing p53 and is frequently silenced in breast cancer.* PLoS One, 2012. **7**(1): p. e29783.

144.   Yu, J., Q. Tao, K.F. Cheung, H. Jin, F.F. Poon, X. Wang, H. Li, Y.Y. Cheng, C. Rocken, M.P. Ebert, A.T. Chan, and J.J. Sung, *Epigenetic identification of ubiquitin carboxyl-terminal hydrolase L1 as a functional tumor suppressor and biomarker for hepatocellular carcinoma and other digestive tumors.* Hepatology, 2008. **48**(2): p. 508-18.

145.   Li, J., K. Wang, X. Chen, H. Meng, M. Song, Y. Wang, X. Xu, and Y. Bai, *Transcriptional activation of microRNA-34a by NF-kappa B in human esophageal cancer cells.* BMC Mol Biol, 2012. **13**: p. 4.

146.   Chu, I.M., L. Hengst, and J.M. Slingerland, *The Cdk inhibitor p27 in human cancer: prognostic potential and relevance to anticancer therapy.* Nat Rev Cancer, 2008. **8**(4): p. 253-67.

147.   Kabuta, T., T. Mitsui, M. Takahashi, Y. Fujiwara, C. Kabuta, C. Konya, Y. Tsuchiya, Y. Hatanaka, K. Uchida, H. Hohjoh, and K. Wada, *Ubiquitin C-terminal hydrolase L1 (UCH-L1) acts as a novel potentiator of cyclin-dependent kinases to enhance cell proliferation independently of its hydrolase activity.* J Biol Chem, 2013. **288**(18): p. 12615-26.

148.   Hussain, S., A.L. Feldman, C. Das, S.C. Ziesmer, S.M. Ansell, and P.J. Galardy, *Ubiquitin hydrolase UCH-L1 destabilizes mTOR complex 1 by antagonizing DDB1-CUL4-mediated ubiquitination of raptor.* Mol Cell Biol, 2013. **33**(6): p. 1188-97.

149.   Bheda, A., W. Yue, A. Gullapalli, C. Whitehurst, R. Liu, J.S. Pagano, and J. Shackelford, *Positive reciprocal regulation of ubiquitin C-terminal hydrolase L1 and beta-catenin/TCF signaling.* PLoS One, 2009. **4**(6): p. e5955.

150. Zhong, J., M. Zhao, Y. Ma, Q. Luo, J. Liu, J. Wang, X. Yuan, J. Sang, and C. Huang, *UCHL1 acts as a colorectal cancer oncogene via activation of the beta-catenin/TCF pathway through its deubiquitinating activity.* Int J Mol Med, 2012. **30**(2): p. 430-6.

151. Liu, Y., L. Fallon, H.A. Lashuel, Z. Liu, and P.T. Lansbury, Jr., *The UCH-L1 gene encodes two opposing enzymatic activities that affect alpha-synuclein degradation and Parkinson's disease susceptibility.* Cell, 2002. **111**(2): p. 209-18.

152. Karim, R., B. Tummers, C. Meyers, J.L. Biryukov, S. Alam, C. Backendorf, V. Jha, R. Offringa, G.J. van Ommen, C.J. Melief, D. Guardavaccaro, J.M. Boer, and S.H. van der Burg, *Human papillomavirus (HPV) upregulates the cellular deubiquitinase UCHL1 to suppress the keratinocyte's innate immune response.* PLoS Pathog, 2013. **9**(5): p. e1003384.

153. Vermeulen, K., D.R. Van Bockstaele, and Z.N. Berneman, *The cell cycle: a review of regulation, deregulation and therapeutic targets in cancer.* Cell Prolif, 2003. **36**(3): p. 131-49.

154. Grana, X. and E.P. Reddy, *Cell cycle control in mammalian cells: role of cyclins, cyclin dependent kinases (CDKs), growth suppressor genes and cyclin-dependent kinase inhibitors (CKIs).* Oncogene, 1995. **11**(2): p. 211-9.

155. Schafer, K.A., *The cell cycle: a review.* Vet Pathol, 1998. **35**(6): p. 461-78.

156. Guacci, V., E. Hogan, and D. Koshland, *Chromosome condensation and sister chromatid pairing in budding yeast.* J Cell Biol, 1994. **125**(3): p. 517-30.

157. Guacci, V., D. Koshland, and A. Strunnikov, *A direct link between sister chromatid cohesion and chromosome condensation revealed through the analysis of MCD1 in S. cerevisiae.* Cell, 1997. **91**(1): p. 47-57.

158. Hirano, T., *Chromosome cohesion, condensation, and separation.* Annu Rev Biochem, 2000. **69**: p. 115-44.

159. Dultz, E., E. Zanin, C. Wurzenberger, M. Braun, G. Rabut, L. Sironi, and J. Ellenberg, *Systematic kinetic analysis of mitotic dis- and reassembly of the nuclear pore in living cells.* J Cell Biol, 2008. **180**(5): p. 857-65.

160. Katsani, K.R., R.E. Karess, N. Dostatni, and V. Doye, *In vivo dynamics of Drosophila nuclear envelope components.* Mol Biol Cell, 2008. **19**(9): p. 3652-66.

161. Gerace, L. and G. Blobel, *The nuclear envelope lamina is reversibly depolymerized during mitosis.* Cell, 1980. **19**(1): p. 277-87.

162. Yang, L., T. Guan, and L. Gerace, *Integral membrane proteins of the nuclear envelope are dispersed throughout the endoplasmic reticulum during mitosis.* J Cell Biol, 1997. **137**(6): p. 1199-210.

163. Ellenberg, J., E.D. Siggia, J.E. Moreira, C.L. Smith, J.F. Presley, H.J. Worman, and J. Lippincott-Schwartz, *Nuclear membrane dynamics and reassembly in living cells: targeting of an inner nuclear membrane protein in interphase and mitosis.* J Cell Biol, 1997. **138**(6): p. 1193-206.

164. Mitchison, T.J. and E.D. Salmon, *Mitosis: a history of division.* Nat Cell Biol, 2001. **3**(1): p. E17-21.

165. Civelekoglu-Scholey, G. and D. Cimini, *Modelling chromosome dynamics in mitosis: a historical perspective on models of metaphase and anaphase in eukaryotic cells.* Interface Focus, 2014. **4**(3): p. 20130073.

166. Hagstrom, K.A. and B.J. Meyer, *Condensin and cohesin: more than chromosome compactor and glue.* Nat Rev Genet, 2003. **4**(7): p. 520-34.

167. Lapenna, S. and A. Giordano, *Cell cycle kinases as therapeutic targets for cancer.* Nat Rev Drug Discov, 2009. **8**(7): p. 547-66.

168. Hochegger, H., A. Klotzbucher, J. Kirk, M. Howell, K. le Guellec, K. Fletcher, T. Duncan, M. Sohail, and T. Hunt, *New B-type cyclin synthesis is required between meiosis I and II during Xenopus oocyte maturation.* Development, 2001. **128**(19): p. 3795-807.

169.   Jackman, M., M. Firth, and J. Pines, *Human cyclins B1 and B2 are localized to strikingly different structures: B1 to microtubules, B2 primarily to the Golgi apparatus.* EMBO J, 1995. **14**(8): p. 1646-54.

170.   Minshull, J., R. Golsteyn, C.S. Hill, and T. Hunt, *The A- and B-type cyclin associated cdc2 kinases in Xenopus turn on and off at different times in the cell cycle.* EMBO J, 1990. **9**(9): p. 2865-75.

171.   Draviam, V.M., S. Orrechia, M. Lowe, R. Pardi, and J. Pines, *The localization of human cyclins B1 and B2 determines CDK1 substrate specificity and neither enzyme requires MEK to disassemble the Golgi apparatus.* J Cell Biol, 2001. **152**(5): p. 945-58.

172.   Brandeis, M., I. Rosewell, M. Carrington, T. Crompton, M.A. Jacobs, J. Kirk, J. Gannon, and T. Hunt, *Cyclin B2-null mice develop normally and are fertile whereas cyclin B1-null mice die in utero.* Proc Natl Acad Sci U S A, 1998. **95**(8): p. 4344-9.

173.   Nguyen, T.B., K. Manova, P. Capodieci, C. Lindon, S. Bottega, X.Y. Wang, J. Refik-Rogers, J. Pines, D.J. Wolgemuth, and A. Koff, *Characterization and expression of mammalian cyclin b3, a prepachytene meiotic cyclin.* J Biol Chem, 2002. **277**(44): p. 41960-9.

174.   Hwang, A., A. Maity, W.G. McKenna, and R.J. Muschel, *Cell cycle-dependent regulation of the cyclin B1 promoter.* J Biol Chem, 1995. **270**(47): p. 28419-24.

175.   Pines, J. and T. Hunter, *Isolation of a human cyclin cDNA: evidence for cyclin mRNA and protein regulation in the cell cycle and for interaction with p34cdc2.* Cell, 1989. **58**(5): p. 833-46.

176.   Pines, J. and T. Hunter, *Human cyclins A and B1 are differentially located in the cell and undergo cell cycle-dependent nuclear transport.* J Cell Biol, 1991. **115**(1): p. 1-17.

177.   Clute, P. and J. Pines, *Temporal and spatial control of cyclin B1 destruction in metaphase.* Nat Cell Biol, 1999. **1**(2): p. 82-7.

178.   Lukas, C., C.S. Sorensen, E. Kramer, E. Santoni-Rugiu, C. Lindeneg, J.M. Peters, J. Bartek, and J. Lukas, *Accumulation of cyclin B1 requires E2F and cyclin-A-dependent rearrangement of the anaphase-promoting complex.* Nature, 1999. **401**(6755): p. 815-8.

179.   Hsu, J.Y., J.D. Reimann, C.S. Sorensen, J. Lukas, and P.K. Jackson, *E2F-dependent accumulation of hEmi1 regulates S phase entry by inhibiting APC(Cdh1).* Nat Cell Biol, 2002. **4**(5): p. 358-66.

180.   Matsumoto, M.L., K.E. Wickliffe, K.C. Dong, C. Yu, I. Bosanac, D. Bustos, L. Phu, D.S. Kirkpatrick, S.G. Hymowitz, M. Rape, R.F. Kelley, and V.M. Dixit, *K11-linked polyubiquitination in cell cycle control revealed by a K11 linkage-specific antibody.* Mol Cell, 2010. **39**(3): p. 477-84.

181.   Kirkpatrick, D.S., N.A. Hathaway, J. Hanna, S. Elsasser, J. Rush, D. Finley, R.W. King, and S.P. Gygi, *Quantitative analysis of in vitro ubiquitinated cyclin B1 reveals complex chain topology.* Nat Cell Biol, 2006. **8**(7): p. 700-10.

182.   Dimova, N.V., N.A. Hathaway, B.H. Lee, D.S. Kirkpatrick, M.L. Berkowitz, S.P. Gygi, D. Finley, and R.W. King, *APC/C-mediated multiple monoubiquitylation provides an alternative degradation signal for cyclin B1.* Nat Cell Biol, 2012. **14**(2): p. 168-76.

183.   Porter, L.A. and D.J. Donoghue, *Cyclin B1 and CDK1: nuclear localization and upstream regulators.* Prog Cell Cycle Res, 2003. **5**: p. 335-47.

184.   Lees, E.M. and E. Harlow, *Sequences within the conserved cyclin box of human cyclin A are sufficient for binding to and activation of cdc2 kinase.* Mol Cell Biol, 1993. **13**(2): p. 1194-201.

185.   Parker, L.L. and H. Piwnica-Worms, *Inactivation of the p34cdc2-cyclin B complex by the human WEE1 tyrosine kinase.* Science, 1992. **257**(5078): p. 1955-7.

186.   Baldin, V. and B. Ducommun, *Subcellular localisation of human wee1 kinase is regulated during the cell cycle.* J Cell Sci, 1995. **108 (Pt 6)**: p. 2425-32.

187.   Liu, F., J.J. Stanton, Z. Wu, and H. Piwnica-Worms, *The human Myt1 kinase preferentially phosphorylates Cdc2 on threonine 14 and localizes to the endoplasmic reticulum and Golgi complex.* Mol Cell Biol, 1997. **17**(2): p. 571-83.

188.   Mueller, P.R., T.R. Coleman, A. Kumagai, and W.G. Dunphy, *Myt1: a membrane-associated inhibitory kinase that phosphorylates Cdc2 on both threonine-14 and tyrosine-15.* Science, 1995. **270**(5233): p. 86-90.

189.   Potapova, T.A., J.R. Daum, K.S. Byrd, and G.J. Gorbsky, *Fine tuning the cell cycle: activation of the Cdk1 inhibitory phosphorylation pathway during mitotic exit.* Mol Biol Cell, 2009. **20**(6): p. 1737-48.

190.   Solomon, M.J., T. Lee, and M.W. Kirschner, *Role of phosphorylation in p34cdc2 activation: identification of an activating kinase.* Mol Biol Cell, 1992. **3**(1): p. 13-27.

191.   Fisher, R.P. and D.O. Morgan, *A novel cyclin associates with MO15/CDK7 to form the CDK-activating kinase.* Cell, 1994. **78**(4): p. 713-24.

192.   Lolli, G. and L.N. Johnson, *CAK-Cyclin-dependent Activating Kinase: a key kinase in cell cycle control and a target for drugs?* Cell Cycle, 2005. **4**(4): p. 572-7.

193.   Solomon, M.J., M. Glotzer, T.H. Lee, M. Philippe, and M.W. Kirschner, *Cyclin activation of p34cdc2.* Cell, 1990. **63**(5): p. 1013-24.

194.   Pomerening, J.R., S.Y. Kim, and J.E. Ferrell, Jr., *Systems-level dissection of the cell-cycle oscillator: bypassing positive feedback produces damped oscillations.* Cell, 2005. **122**(4): p. 565-78.

195.   Murray, A.W., M.J. Solomon, and M.W. Kirschner, *The role of cyclin synthesis and degradation in the control of maturation promoting factor activity.* Nature, 1989. **339**(6222): p. 280-6.

196.   Yang, J., E.S. Bardes, J.D. Moore, J. Brennan, M.A. Powers, and S. Kornbluth, *Control of cyclin B1 localization through regulated binding of the nuclear export factor CRM1.* Genes Dev, 1998. **12**(14): p. 2131-43.

197.   Hutten, S. and R.H. Kehlenbach, *CRM1-mediated nuclear export: to the pore and beyond.* Trends Cell Biol, 2007. **17**(4): p. 193-201.

198.   Hagting, A., C. Karlsson, P. Clute, M. Jackman, and J. Pines, *MPF localization is controlled by nuclear export.* EMBO J, 1998. **17**(14): p. 4127-38.

199.   Hagting, A., M. Jackman, K. Simpson, and J. Pines, *Translocation of cyclin B1 to the nucleus at prophase requires a phosphorylation-dependent nuclear import signal.* Curr Biol, 1999. **9**(13): p. 680-9.

200.   Lindqvist, A., W. van Zon, C. Karlsson Rosenthal, and R.M. Wolthuis, *Cyclin B1-Cdk1 activation continues after centrosome separation to control mitotic progression.* PLoS Biol, 2007. **5**(5): p. e123.

201.   Wang, Z., M. Fan, D. Candas, T.Q. Zhang, L. Qin, A. Eldridge, S. Wachsmann-Hogiu, K.M. Ahmed, B.A. Chromy, D. Nantajit, N. Duru, F. He, M. Chen, T. Finkel, L.S. Weinstein, and J.J. Li, *Cyclin B1/Cdk1 coordinates mitochondrial respiration for cell-cycle G2/M progression.* Dev Cell, 2014. **29**(2): p. 217-32.

202.   Bailly, E., J. Pines, T. Hunter, and M. Bornens, *Cytoplasmic accumulation of cyclin B1 in human cells: association with a detergent-resistant compartment and with the centrosome.* J Cell Sci, 1992. **101 (Pt 3)**: p. 529-45.

203.   Chen, Q., X. Zhang, Q. Jiang, P.R. Clarke, and C. Zhang, *Cyclin B1 is localized to unattached kinetochores and contributes to efficient microtubule attachment and proper chromosome alignment during mitosis.* Cell Res, 2008. **18**(2): p. 268-80.

204.   Songyang, Z., S. Blechner, N. Hoagland, M.F. Hoekstra, H. Piwnica-Worms, and L.C. Cantley, *Use of an oriented peptide library to determine the optimal substrates of protein kinases.* Curr Biol, 1994. **4**(11): p. 973-82.

205.   Errico, A., K. Deshmukh, Y. Tanaka, A. Pozniakovsky, and T. Hunt, *Identification of substrates for cyclin dependent kinases.* Adv Enzyme Regul, 2010. **50**(1): p. 375-99.

206. Holt, L.J., B.B. Tuch, J. Villen, A.D. Johnson, S.P. Gygi, and D.O. Morgan, *Global analysis of Cdk1 substrate phosphorylation sites provides insights into evolution.* Science, 2009. **325**(5948): p. 1682-6.

207. Petrone, A., M.E. Adamo, C. Cheng, and A.N. Kettenbach, *Identification of Candidate Cyclin-dependent kinase 1 (Cdk1) Substrates in Mitosis by Quantitative Phosphoproteomics.* Mol Cell Proteomics, 2016. **15**(7): p. 2448-61.

208. Ohta, S., M. Kimura, S. Takagi, I. Toramoto, and Y. Ishihama, *Identification of Mitosis-Specific Phosphorylation in Mitotic Chromosome-Associated Proteins.* J Proteome Res, 2016. **15**(9): p. 3331-41.

209. Bradbury, E.M., R.J. Inglis, and H.R. Matthews, *Control of cell division by very lysine rich histone (F1) phosphorylation.* Nature, 1974. **247**(5439): p. 257-61.

210. Gurley, L.R., J.G. Valdez, and J.S. Buchanan, *Characterization of the mitotic specific phosphorylation site of histone H1. Absence of a consensus sequence for the p34cdc2/cyclin B kinase.* J Biol Chem, 1995. **270**(46): p. 27653-60.

211. Kimura, K., M. Hirano, R. Kobayashi, and T. Hirano, *Phosphorylation and activation of 13S condensin by Cdc2 in vitro.* Science, 1998. **282**(5388): p. 487-90.

212. Abe, S., K. Nagasaka, Y. Hirayama, H. Kozuka-Hata, M. Oyama, Y. Aoyagi, C. Obuse, and T. Hirota, *The initial phase of chromosome condensation requires Cdk1-mediated phosphorylation of the CAP-D3 subunit of condensin II.* Genes Dev, 2011. **25**(8): p. 863-74.

213. Macaulay, C., E. Meier, and D.J. Forbes, *Differential mitotic phosphorylation of proteins of the nuclear pore complex.* J Biol Chem, 1995. **270**(1): p. 254-62.

214. Cai, Y., Y. Gao, Q. Sheng, S. Miao, X. Cui, L. Wang, S. Zong, and S.S. Koide, *Characterization and potential function of a novel testis-specific nucleoporin BS-63.* Mol Reprod Dev, 2002. **61**(1): p. 126-34.

215. Rajanala, K., A. Sarkar, G.D. Jhingan, R. Priyadarshini, M. Jalan, S. Sengupta, and V.K. Nandicoori, *Phosphorylation of nucleoporin Tpr governs its differential localization and is required for its mitotic function.* J Cell Sci, 2014. **127**(Pt 16): p. 3505-20.

216. Lusk, C.P., D.D. Waller, T. Makhnevych, A. Dienemann, M. Whiteway, D.Y. Thomas, and R.W. Wozniak, *Nup53p is a target of two mitotic kinases, Cdk1p and Hrr25p.* Traffic, 2007. **8**(6): p. 647-60.

217. Heald, R. and F. McKeon, *Mutations of phosphorylation sites in lamin A that prevent nuclear lamina disassembly in mitosis.* Cell, 1990. **61**(4): p. 579-89.

218. Peter, M., J. Nakagawa, M. Doree, J.C. Labbe, and E.A. Nigg, *In vitro disassembly of the nuclear lamina and M phase-specific phosphorylation of lamins by cdc2 kinase.* Cell, 1990. **61**(4): p. 591-602.

219. Fourest-Lieuvin, A., L. Peris, V. Gache, I. Garcia-Saez, C. Juillan-Binard, V. Lantez, and D. Job, *Microtubule regulation in mitosis: tubulin phosphorylation by the cyclin-dependent kinase Cdk1.* Mol Biol Cell, 2006. **17**(3): p. 1041-50.

220. Ookata, K., S. Hisanaga, M. Sugita, A. Okuyama, H. Murofushi, H. Kitazawa, S. Chari, J.C. Bulinski, and T. Kishimoto, *MAP4 is the in vivo substrate for CDC2 kinase in HeLa cells: identification of an M-phase specific and a cell cycle-independent phosphorylation site in MAP4.* Biochemistry, 1997. **36**(50): p. 15873-83.

221. Vasquez, R.J., D.L. Gard, and L. Cassimeris, *Phosphorylation by CDK1 regulates XMAP215 function in vitro.* Cell Motil Cytoskeleton, 1999. **43**(4): p. 310-21.

222. Shen, M., Y. Feng, C. Gao, D. Tao, J. Hu, E. Reed, Q.Q. Li, and J. Gong, *Detection of cyclin b1 expression in g(1)-phase cancer cell lines and cancer tissues by postsorting Western blot analysis.* Cancer Res, 2004. **64**(5): p. 1607-10.

223. Viallard, J.F., F. Lacombe, M. Dupouy, H. Ferry, F. Belloc, and J. Reiffers, *Flow cytometry study of human cyclin B1 and cyclin E expression in leukemic cell lines: cell cycle kinetics and cell localization.* Exp Cell Res, 1999. **247**(1): p. 208-19.

224. Gong, J., F. Traganos, and Z. Darzynkiewicz, *Discrimination of G2 and mitotic cells by flow cytometry based on different expression of cyclins A and B1.* Exp Cell Res, 1995. **220**(1): p. 226-31.

225. Wang, A., N. Yoshimi, N. Ino, T. Tanaka, and H. Mori, *Overexpression of cyclin B1 in human colorectal cancers.* J Cancer Res Clin Oncol, 1997. **123**(2): p. 124-7.

226. Suzuki, T., T. Urano, Y. Miki, T. Moriya, J. Akahira, T. Ishida, K. Horie, S. Inoue, and H. Sasano, *Nuclear cyclin B1 in human breast carcinoma as a potent prognostic factor.* Cancer Sci, 2007. **98**(5): p. 644-51.

227. Allan, K., R.C. Jordan, L.C. Ang, M. Taylor, and B. Young, *Overexpression of cyclin A and cyclin B1 proteins in astrocytomas.* Arch Pathol Lab Med, 2000. **124**(2): p. 216-20.

228. Rudolph, P., H. Kuhling, P. Alm, M. Ferno, B. Baldetorp, H. Olsson, and R. Parwaresch, *Differential prognostic impact of the cyclins E and B in premenopausal and postmenopausal women with lymph node-negative breast cancer.* Int J Cancer, 2003. **105**(5): p. 674-80.

229. Santala, S., A. Talvensaari-Mattila, Y. Soini, and M. Santala, *Prognostic value of cyclin B in endometrial endometrioid adenocarcinoma.* Tumour Biol, 2015. **36**(2): p. 953-7.

230. Hartley, R.S., R.E. Rempel, and J.L. Maller, *In vivo regulation of the early embryonic cell cycle in Xenopus.* Dev Biol, 1996. **173**(2): p. 408-19.

231. Taylor, W.R., S.E. DePrimo, A. Agarwal, M.L. Agarwal, A.H. Schonthal, K.S. Katula, and G.R. Stark, *Mechanisms of G2 arrest in response to overexpression of p53.* Mol Biol Cell, 1999. **10**(11): p. 3607-22.

232. Kao, G.D., W.G. McKenna, A. Maity, K. Blank, and R.J. Muschel, *Cyclin B1 availability is a rate-limiting component of the radiation-induced G2 delay in HeLa cells.* Cancer Res, 1997. **57**(4): p. 753-8.

233. Wahl, G.M. and A.M. Carr, *The evolution of diverse biological responses to DNA damage: insights from yeast and p53.* Nat Cell Biol, 2001. **3**(12): p. E277-86.

234. Deng, C., P. Zhang, J.W. Harper, S.J. Elledge, and P. Leder, *Mice lacking p21CIP1/WAF1 undergo normal development, but are defective in G1 checkpoint control.* Cell, 1995. **82**(4): p. 675-84.

235. Kastan, M.B. and J. Bartek, *Cell-cycle checkpoints and cancer.* Nature, 2004. **432**(7015): p. 316-23.

236. Bulavin, D.V., Y. Higashimoto, I.J. Popoff, W.A. Gaarde, V. Basrur, O. Potapova, E. Appella, and A.J. Fornace, Jr., *Initiation of a G2/M checkpoint after ultraviolet radiation requires p38 kinase.* Nature, 2001. **411**(6833): p. 102-7.

237. Chung, J.H. and F. Bunz, *Cdk2 is required for p53-independent G2/M checkpoint control.* PLoS Genet, 2010. **6**(2): p. e1000863.

238. Mailand, N., A.V. Podtelejnikov, A. Groth, M. Mann, J. Bartek, and J. Lukas, *Regulation of G(2)/M events by Cdc25A through phosphorylation-dependent modulation of its stability.* EMBO J, 2002. **21**(21): p. 5911-20.

239. Kastan, M.B., O. Onyekwere, D. Sidransky, B. Vogelstein, and R.W. Craig, *Participation of p53 protein in the cellular response to DNA damage.* Cancer Res, 1991. **51**(23 Pt 1): p. 6304-11.

240. Passalaris, T.M., J.A. Benanti, L. Gewin, T. Kiyono, and D.A. Galloway, *The G(2) checkpoint is maintained by redundant pathways.* Mol Cell Biol, 1999. **19**(9): p. 5872-81.

241. Innocente, S.A., J.L. Abrahamson, J.P. Cogswell, and J.M. Lee, *p53 regulates a G2 checkpoint through cyclin B1.* Proc Natl Acad Sci U S A, 1999. **96**(5): p. 2147-52.

242. Bharadwaj, R. and H. Yu, *The spindle checkpoint, aneuploidy, and cancer.* Oncogene, 2004. **23**(11): p. 2016-27.

243. Barford, D., *Structure, function and mechanism of the anaphase promoting complex (APC/C).* Q Rev Biophys, 2011. **44**(2): p. 153-90.

244. Castro, A., C. Bernis, S. Vigneron, J.C. Labbe, and T. Lorca, *The anaphase-promoting complex: a key factor in the regulation of cell cycle.* Oncogene, 2005. **24**(3): p. 314-25.

245. Acquaviva, C., F. Herzog, C. Kraft, and J. Pines, *The anaphase promoting complex/cyclosome is recruited to centromeres by the spindle assembly checkpoint.* Nat Cell Biol, 2004. **6**(9): p. 892-8.

246. Glotzer, M., A.W. Murray, and M.W. Kirschner, *Cyclin is degraded by the ubiquitin pathway.* Nature, 1991. **349**(6305): p. 132-8.

247. Pfleger, C.M. and M.W. Kirschner, *The KEN box: an APC recognition signal distinct from the D box targeted by Cdh1.* Genes Dev, 2000. **14**(6): p. 655-65.

248. Peters, J.M., *The anaphase-promoting complex: proteolysis in mitosis and beyond.* Mol Cell, 2002. **9**(5): p. 931-43.

249. Di Fiore, B. and J. Pines, *Defining the role of Emi1 in the DNA replication-segregation cycle.* Chromosoma, 2008. **117**(4): p. 333-8.

250. Song, M.S., S.J. Song, N.G. Ayad, J.S. Chang, J.H. Lee, H.K. Hong, H. Lee, N. Choi, J. Kim, H. Kim, J.W. Kim, E.J. Choi, M.W. Kirschner, and D.S. Lim, *The tumour suppressor RASSF1A regulates mitosis by inhibiting the APC-Cdc20 complex.* Nat Cell Biol, 2004. **6**(2): p. 129-37.

251. Kramer, E.R., N. Scheuringer, A.V. Podtelejnikov, M. Mann, and J.M. Peters, *Mitotic regulation of the APC activator proteins CDC20 and CDH1.* Mol Biol Cell, 2000. **11**(5): p. 1555-69.

252. Patra, D. and W.G. Dunphy, *Xe-p9, a Xenopus Suc1/Cks protein, is essential for the Cdc2-dependent phosphorylation of the anaphase- promoting complex at mitosis.* Genes Dev, 1998. **12**(16): p. 2549-59.

253. Kotani, S., S. Tugendreich, M. Fujii, P.M. Jorgensen, N. Watanabe, C. Hoog, P. Hieter, and K. Todokoro, *PKA and MPF-activated polo-like kinase regulate anaphase-promoting complex activity and mitosis progression.* Mol Cell, 1998. **1**(3): p. 371-80.

254. Hayes, M.J., Y. Kimata, S.L. Wattam, C. Lindon, G. Mao, H. Yamano, and A.M. Fry, *Early mitotic degradation of Nek2A depends on Cdc20-independent interaction with the APC/C.* Nat Cell Biol, 2006. **8**(6): p. 607-14.

255. Sudakin, V., G.K. Chan, and T.J. Yen, *Checkpoint inhibition of the APC/C in HeLa cells is mediated by a complex of BUBR1, BUB3, CDC20, and MAD2.* J Cell Biol, 2001. **154**(5): p. 925-36.

256. Pecorelli, S., *Revised FIGO staging for carcinoma of the vulva, cervix, and endometrium.* Int J Gynaecol Obstet, 2009. **105**(2): p. 103-4.

257. Creasman, W., *Revised FIGO staging for carcinoma of the endometrium.* Int J Gynaecol Obstet, 2009. **105**(2): p. 109.

258. Schemper, M. and T.L. Smith, *A note on quantifying follow-up in studies of failure time.* Control Clin Trials, 1996. **17**(4): p. 343-6.

259. Cancer Genome Atlas Research Network, *Integrated genomic characterization of endometrial carcinoma.* Nature, 2013. **497**(7447): p. 67-73.

260. Tusher, V.G., R. Tibshirani, and G. Chu, *Significance analysis of microarrays applied to the ionizing radiation response.* Proc Natl Acad Sci U S A, 2001. **98**(9): p. 5116-21.

261. Liu, Y., H.A. Lashuel, S. Choi, X. Xing, A. Case, J. Ni, L.A. Yeh, G.D. Cuny, R.L. Stein, and P.T. Lansbury, Jr., *Discovery of inhibitors that elucidate the role of UCH-L1 activity in the H1299 lung cancer cell line.* Chem Biol, 2003. **10**(9): p. 837-46.

262. Peltomaki, P., *DNA mismatch repair and cancer.* Mutat Res, 2001. **488**(1): p. 77-85.

263. Heikkinen, K., K. Rapakko, S.M. Karppinen, H. Erkko, S. Knuutila, T. Lundan, A. Mannermaa, A.L. Borresen-Dale, A. Borg, R.B. Barkardottir, J. Petrini, and R. Winqvist, *RAD50 and NBS1 are breast cancer susceptibility genes associated with genomic instability.* Carcinogenesis, 2006. **27**(8): p. 1593-9.

264. Stracker, T.H., J.W. Theunissen, M. Morales, and J.H. Petrini, *The Mre11 complex and the metabolism of chromosome breaks: the importance of communicating and holding things together.* DNA Repair (Amst), 2004. **3**(8-9): p. 845-54.

265. McCubrey, J.A., L.S. Steelman, F.E. Bertrand, N.M. Davis, M. Sokolosky, S.L. Abrams, G. Montalto, A.B. D'Assoro, M. Libra, F. Nicoletti, R. Maestro, J. Basecke, D. Rakus, A. Gizak, Z.N. Demidenko, L. Cocco, A.M. Martelli, and M. Cervello, *GSK-3 as potential target for therapeutic intervention in cancer.* Oncotarget, 2014. **5**(10): p. 2881-911.

266. Abbas, T. and A. Dutta, *p21 in cancer: intricate networks and multiple activities.* Nat Rev Cancer, 2009. **9**(6): p. 400-14.

267. Risinger, J.I., G.L. Maxwell, G.V. Chandramouli, A. Jazaeri, O. Aprelikova, T. Patterson, A. Berchuck, and J.C. Barrett, *Microarray analysis reveals distinct gene expression profiles among different histologic types of endometrial cancer.* Cancer Res, 2003. **63**(1): p. 6-11.

268. Oliva, E. and R.A. Soslow, *High-Grade Endometrial Carcinomas.* Surg Pathol Clin, 2011. **4**(1): p. 199-241.

269. Zannoni, G.F., V.G. Vellone, V. Arena, M.G. Prisco, G. Scambia, A. Carbone, and D. Gallo, *Does high-grade endometrioid carcinoma (grade 3 FIGO) belong to type I or type II endometrial cancer? A clinical-pathological and immunohistochemical study.* Virchows Arch, 2010. **457**(1): p. 27-34.

270. Mutch, D.M., A. Berger, R. Mansourian, A. Rytz, and M.A. Roberts, *The limit fold change model: a practical approach for selecting differentially expressed genes from microarray data.* BMC Bioinformatics, 2002. **3**: p. 17.

271. Suetsugu, S., H. Miki, and T. Takenawa, *Identification of two human WAVE/SCAR homologues as general actin regulatory molecules which associate with the Arp2/3 complex.* Biochem Biophys Res Commun, 1999. **260**(1): p. 296-302.

272. Suetsugu, S., D. Yamazaki, S. Kurisu, and T. Takenawa, *Differential roles of WAVE1 and WAVE2 in dorsal and peripheral ruffle formation for fibroblast cell migration.* Dev Cell, 2003. **5**(4): p. 595-609.

273. Hoon, J.L., W.K. Wong, and C.G. Koh, *Functions and regulation of circular dorsal ruffles.* Mol Cell Biol, 2012. **32**(21): p. 4246-57.

274. Nagase, T., N. Seki, K. Ishikawa, M. Ohira, Y. Kawarabayasi, O. Ohara, A. Tanaka, H. Kotani, N. Miyajima, and N. Nomura, *Prediction of the coding sequences of unidentified human genes. VI. The coding sequences of 80 new genes (KIAA0201-KIAA0280) deduced by analysis of cDNA clones from cell line KG-1 and brain.* DNA Res, 1996. **3**(5): p. 321-9, 341-54.

275. Zhang, J., L. Tang, L. Shen, S. Zhou, Z. Duan, L. Xiao, Y. Cao, X. Mu, L. Zha, and H. Wang, *High level of WAVE1 expression is associated with tumor aggressiveness and unfavorable prognosis of epithelial ovarian cancer.* Gynecol Oncol, 2012. **127**(1): p. 223-30.

276. Zhang, J., S. Zhou, L. Tang, L. Shen, L. Xiao, Z. Duan, L. Jia, Y. Cao, and X. Mu, *WAVE1 gene silencing via RNA interference reduces ovarian cancer cell invasion, migration and proliferation.* Gynecol Oncol, 2013. **130**(2): p. 354-61.

277. Fernando, H.S., A.J. Sanders, H.G. Kynaston, and W.G. Jiang, *WAVE1 is associated with invasiveness and growth of prostate cancer cells.* J Urol, 2008. **180**(4): p. 1515-21.

278. Griffis, E.R., N. Stuurman, and R.D. Vale, *Spindly, a novel protein essential for silencing the spindle assembly checkpoint, recruits dynein to the kinetochore.* J Cell Biol, 2007. **177**(6): p. 1005-15.

279. Silva, P.M., N. Ribeiro, R.T. Lima, C. Andrade, V. Diogo, J. Teixeira, C. Florindo, A. Tavares, M.H. Vasconcelos, and H. Bousbaa, *Suppression of spindly delays mitotic exit and exacerbates cell death response of cancer cells treated with low doses of paclitaxel.* Cancer Lett, 2017.

280.   Topham, C.H. and S.S. Taylor, *Mitosis and apoptosis: how is the balance set?* Curr Opin Cell Biol, 2013. **25**(6): p. 780-5.

281.   Milas, L., N.R. Hunter, B. Kurdoglu, K.A. Mason, R.E. Meyn, L.C. Stephens, and L.J. Peters, *Kinetics of mitotic arrest and apoptosis in murine mammary and ovarian tumors treated with taxol.* Cancer Chemother Pharmacol, 1995. **35**(4): p. 297-303.

282.   Weaver, B.A., *How Taxol/paclitaxel kills cancer cells.* Mol Biol Cell, 2014. **25**(18): p. 2677-81.

283.   Bekier, M.E., R. Fischbach, J. Lee, and W.R. Taylor, *Length of mitotic arrest induced by microtubule-stabilizing drugs determines cell death after mitotic exit.* Mol Cancer Ther, 2009. **8**(6): p. 1646-54.

284.   Holland, A.J., R.M. Reis, S. Niessen, C. Pereira, D.A. Andres, H.P. Spielmann, D.W. Cleveland, A. Desai, and R. Gassmann, *Preventing farnesylation of the dynein adaptor Spindly contributes to the mitotic defects caused by farnesyltransferase inhibitors.* Mol Biol Cell, 2015. **26**(10): p. 1845-56.

285.   Moudgil, D.K., N. Westcott, J.K. Famulski, K. Patel, D. Macdonald, H. Hang, and G.K. Chan, *A novel role of farnesylation in targeting a mitotic checkpoint protein, human Spindly, to kinetochores.* J Cell Biol, 2015. **208**(7): p. 881-96.

286.   Eiger Biopharmaceuticals. *About Sarasar® (Lonafarnib).* 2017/03/08]; Available from: http://www.eigerbio.com/hepatitis-d/about-lonafarnib/.

287.   Tawarayama, H., Y. Yoshida, F. Suto, K.J. Mitchell, and H. Fujisawa, *Roles of semaphorin-6B and plexin-A2 in lamina-restricted projection of hippocampal mossy fibers.* J Neurosci, 2010. **30**(20): p. 7049-60.

288.   Suto, F., K. Ito, M. Uemura, M. Shimizu, Y. Shinkawa, M. Sanbo, T. Shinoda, M. Tsuboi, S. Takashima, T. Yagi, and H. Fujisawa, *Plexin-a4 mediates axon-repulsive activities of both secreted and transmembrane semaphorins and plays roles in nerve fiber guidance.* J Neurosci, 2005. **25**(14): p. 3628-37.

289.   Xu, X.M., D.A. Fisher, L. Zhou, F.A. White, S. Ng, W.D. Snider, and Y. Luo, *The transmembrane protein semaphorin 6A repels embryonic sympathetic axons.* J Neurosci, 2000. **20**(7): p. 2638-48.

290.   Kigel, B., N. Rabinowicz, A. Varshavsky, O. Kessler, and G. Neufeld, *Plexin-A4 promotes tumor progression and tumor angiogenesis by enhancement of VEGF and bFGF signaling.* Blood, 2011. **118**(15): p. 4285-96.

291.   Balakrishnan, A., J.Y. Penachioni, S. Lamba, F.E. Bleeker, C. Zanon, M. Rodolfo, V. Vallacchi, A. Scarpa, L. Felicioni, M. Buck, A. Marchetti, P.M. Comoglio, A. Bardelli, and L. Tamagnone, *Molecular profiling of the "plexinome" in melanoma and pancreatic cancer.* Hum Mutat, 2009. **30**(8): p. 1167-74.

292.   Poole, C.A., S.F. Wotton, and V.C. Duance, *Localization of type IX collagen in chondrons isolated from porcine articular cartilage and rat chondrosarcoma.* Histochem J, 1988. **20**(10): p. 567-74.

293.   Zhang, P., S.A. Jimenez, and D.G. Stokes, *Regulation of human COL9A1 gene expression. Activation of the proximal promoter region by SOX9.* J Biol Chem, 2003. **278**(1): p. 117-23.

294.   Piotrowski, A., M. Benetkiewicz, U. Menzel, T. Diaz de Stahl, K. Mantripragada, G. Grigelionis, P.G. Buckley, M. Jankowski, J. Hoffman, D. Bala, E. Srutek, R. Laskowski, W. Zegarski, and J.P. Dumanski, *Microarray-based survey of CpG islands identifies concurrent hyper- and hypomethylation patterns in tissues derived from patients with breast cancer.* Genes Chromosomes Cancer, 2006. **45**(7): p. 656-67.

295.   Oktem, G., A. Bilir, R. Uslu, S.V. Inan, S.B. Demiray, H. Atmaca, S. Ayla, O. Sercan, and A. Uysal, *Expression profiling of stem cell signaling alters with spheroid formation in CD133high/CD44high prostate cancer stem cells.* Oncol Lett, 2014. **7**(6): p. 2103-2109.

296.   Tothill, R.W., A.V. Tinker, J. George, R. Brown, S.B. Fox, S. Lade, D.S. Johnson, M.K. Trivett, D. Etemadmoghadam, B. Locandro, N. Traficante, S. Fereday, J.A. Hung, Y.E. Chiew, I. Haviv, G. Australian Ovarian Cancer Study, D. Gertig, A. DeFazio, and D.D.

Bowtell, *Novel molecular subtypes of serous and endometrioid ovarian cancer linked to clinical outcome.* Clin Cancer Res, 2008. **14**(16): p. 5198-208.

297.   Ren, C.E., X. Zhu, J. Li, C. Lyle, S. Dowdy, K.C. Podratz, D. Byck, H.B. Chen, and S.W. Jiang, *Microarray analysis on gene regulation by estrogen, progesterone and tamoxifen in human endometrial stromal cells.* Int J Mol Sci, 2015. **16**(3): p. 5864-85.

298.   Chen, S., W. Wu, J. Li, Q. Wang, Y. Li, Z. Wu, W. Zheng, Q. Wu, C. Wu, F. Zhang, and Y. Li, *Single nucleotide polymorphisms in the FAM167A-BLK gene are associated with polymyositis/dermatomyositis in the Han Chinese population.* Immunol Res, 2015. **62**(2): p. 153-62.

299.   Ito, I., Y. Kawaguchi, A. Kawasaki, M. Hasegawa, J. Ohashi, M. Kawamoto, M. Fujimoto, K. Takehara, S. Sato, M. Hara, and N. Tsuchiya, *Association of the FAM167A-BLK region with systemic sclerosis.* Arthritis Rheum, 2010. **62**(3): p. 890-5.

300.   Sun, F., P. Li, H. Chen, Z. Wu, J. Xu, M. Shen, X. Leng, Q. Shi, W. Zhang, X. Tian, Y. Li, and F. Zhang, *Association studies of TNFSF4, TNFAIP3 and FAM167A-BLK polymorphisms with primary Sjogren's syndrome in Han Chinese.* J Hum Genet, 2013. **58**(7): p. 475-9.

301.   Visse, R. and H. Nagase, *Matrix metalloproteinases and tissue inhibitors of metalloproteinases: structure, function, and biochemistry.* Circ Res, 2003. **92**(8): p. 827-39.

302.   Liu, H., Y. Kato, S.A. Erzinger, G.M. Kiriakova, Y. Qian, D. Palmieri, P.S. Steeg, and J.E. Price, *The role of MMP-1 in breast cancer growth and metastasis to the brain in a xenograft model.* BMC Cancer, 2012. **12**: p. 583.

303.   Lin, C.Y., A. Chao, T.H. Wang, S. Hsueh, Y.S. Lee, T.I. Wu, A.S. Chao, H.J. Huang, H.H. Chou, T.C. Chang, and C.H. Lai, *A dual tyrosine kinase inhibitor lapatinib suppresses overexpression of matrix metallopeptidase 1 (MMP1) in endometrial cancer.* J Mol Med (Berl), 2014. **92**(9): p. 969-81.

304. Madlener, M., C. Mauch, W. Conca, M. Brauchle, W.C. Parks, and S. Werner, *Regulation of the expression of stromelysin-2 by growth factors in keratinocytes: implications for normal and impaired wound healing.* Biochem J, 1996. **320 (Pt 2)**: p. 659-64.

305. Chakraborti, S., M. Mandal, S. Das, A. Mandal, and T. Chakraborti, *Regulation of matrix metalloproteinases: an overview.* Mol Cell Biochem, 2003. **253**(1-2): p. 269-85.

306. Mariya, T., Y. Hirohashi, T. Torigoe, Y. Tabuchi, T. Asano, H. Saijo, T. Kuroda, K. Yasuda, M. Mizuuchi, T. Saito, and N. Sato, *Matrix metalloproteinase-10 regulates stemness of ovarian cancer stem-like cells by activation of canonical Wnt signaling and can be a target of chemotherapy-resistant ovarian cancer.* Oncotarget, 2016. **7**(18): p. 26806-22.

307. Zhang, G., M. Miyake, A. Lawton, S. Goodison, and C.J. Rosser, *Matrix metalloproteinase-10 promotes tumor progression through regulation of angiogenic and apoptotic pathways in cervical tumors.* BMC Cancer, 2014. **14**: p. 310.

308. Gawin, B., A. Niederfuhr, N. Schumacher, H. Hummerich, P.F. Little, and M. Gessler, *A 7.5 Mb sequence-ready PAC contig and gene expression map of human chromosome 11p13-p14.1.* Genome Res, 1999. **9**(11): p. 1074-86.

309. Anderl, S., M. Konig, A. Attarbaschi, and S. Strehl, *PAX5-KIAA1549L: a novel fusion gene in a case of pediatric B-cell precursor acute lymphoblastic leukemia.* Mol Cytogenet, 2015. **8**: p. 48.

310. Abe, A., A. Katsumi, M. Kobayashi, A. Okamoto, M. Tokuda, T. Kanie, Y. Yamamoto, T. Naoe, and N. Emi, *A novel RUNX1-C11orf41 fusion gene in a case of acute myeloid leukemia with a t(11;21)(p14;q22).* Cancer Genet, 2012. **205**(11): p. 608-11.

311. Sciorra, V.A. and A.J. Morris, *Roles for lipid phosphate phosphatases in regulation of cellular signaling.* Biochim Biophys Acta, 2002. **1582**(1-3): p. 45-51.

312. Takeuchi, M., M. Harigai, S. Momohara, E. Ball, J. Abe, K. Furuichi, and N. Kamatani, *Cloning and characterization of DPPL1 and DPPL2, representatives of a novel type of mammalian phosphatidate phosphatase.* Gene, 2007. **399**(2): p. 174-80.

313. Dahl, E., G. Kristiansen, K. Gottlob, I. Klaman, E. Ebner, B. Hinzmann, K. Hermann, C. Pilarsky, M. Durst, M. Klinkhammer-Schalke, H. Blaszyk, R. Knuechel, A. Hartmann, A. Rosenthal, and P.J. Wild, *Molecular profiling of laser-microdissected matched tumor and normal breast tissue identifies karyopherin alpha2 as a potential novel prognostic marker in breast cancer.* Clin Cancer Res, 2006. **12**(13): p. 3950-60.

314. Gorokhova, S., S. Bibert, K. Geering, and N. Heintz, *A novel family of transmembrane proteins interacting with beta subunits of the Na,K-ATPase.* Hum Mol Genet, 2007. **16**(20): p. 2394-410.

315. Chen, D., M. Song, O. Mohamad, and S.P. Yu, *Inhibition of Na+/K+-ATPase induces hybrid cell death and enhanced sensitivity to chemotherapy in human glioblastoma cells.* BMC Cancer, 2014. **14**: p. 716.

316. Rajarao, S.J., V.A. Canfield, M.A. Mohideen, Y.L. Yan, J.H. Postlethwait, K.C. Cheng, and R. Levenson, *The repertoire of Na,K-ATPase alpha and beta subunit genes expressed in the zebrafish, Danio rerio.* Genome Res, 2001. **11**(7): p. 1211-20.

317. Lingrel, J.B., *Na,K-ATPase: isoform structure, function, and expression.* J Bioenerg Biomembr, 1992. **24**(3): p. 263-70.

318. Bocciardi, R., R. Giorda, V. Marigo, P. Zordan, D. Montanaro, S. Gimelli, M. Seri, M. Lerone, R. Ravazzolo, and G. Gimelli, *Molecular characterization of a t(2;6) balanced translocation that is associated with a complex phenotype and leads to truncation of the TCBA1 gene.* Hum Mutat, 2005. **26**(5): p. 426-36.

319. Yue, Y., K. Stout, B. Grossmann, U. Zechner, A. Brinckmann, C. White, D.T. Pilz, and T. Haaf, *Disruption of TCBA1 associated with a de novo t(1;6)(q32.2;q22.3) presenting in a child with developmental delay and recurrent infections.* J Med Genet, 2006. **43**(2): p. 143-7.

320. Romania, P., A. Castellano, C. Surace, A. Citti, M.A. De Ioris, P. Sirleto, M. De Mariano, L. Longo, R. Boldrini, A. Angioni, F. Locatelli, and D. Fruci, *High-resolution array CGH*

profiling identifies Na/K transporting ATPase interacting 2 (NKAIN2) as a predisposing candidate gene in neuroblastoma. PLoS One, 2013. **8**(10): p. e78481.

321.   Rajasekaran, A.K. and S.A. Rajasekaran, *Role of Na-K-ATPase in the assembly of tight junctions.* Am J Physiol Renal Physiol, 2003. **285**(3): p. F388-96.

322.   Li, Z. and Z. Xie, *The Na/K-ATPase/Src complex and cardiotonic steroid-activated protein kinase cascades.* Pflugers Arch, 2009. **457**(3): p. 635-44.

323.   Tian, J. and Z.J. Xie, *The Na-K-ATPase and calcium-signaling microdomains.* Physiology (Bethesda), 2008. **23**: p. 205-11.

324.   Aperia, A., *New roles for an old enzyme: Na,K-ATPase emerges as an interesting drug target.* J Intern Med, 2007. **261**(1): p. 44-52.

325.   Repke, K.R.H., *The Role of the Na+/K+ Pump in Normal and Cancer Cell Proliferation*, in *Biomembranes: Basic and Medical Research*, G. Benga and J.M. Tager, Editors. 1988, Springer Berlin Heidelberg: Berlin, Heidelberg. p. 160-176.

326.   Alevizopoulos, K., T. Calogeropoulou, F. Lang, and C. Stournaras, *Na+/K+ ATPase inhibitors in cancer.* Curr Drug Targets, 2014. **15**(10): p. 988-1000.

327.   Schoner, W. and G. Scheiner-Bobis, *Endogenous and exogenous cardiac glycosides: their roles in hypertension, salt metabolism, and cell growth.* Am J Physiol Cell Physiol, 2007. **293**(2): p. C509-36.

328.   Weidemann, H., *Na/K-ATPase, endogenous digitalis like compounds and cancer development -- a hypothesis.* Front Biosci, 2005. **10**: p. 2165-76.

329.   Kask, K., U. Langel, and T. Bartfai, *Galanin--a neuropeptide with inhibitory actions.* Cell Mol Neurobiol, 1995. **15**(6): p. 653-73.

330.   Tatemoto, K., A. Rokaeus, H. Jornvall, T.J. McDonald, and V. Mutt, *Galanin - a novel biologically active peptide from porcine intestine.* FEBS Lett, 1983. **164**(1): p. 124-8.

331.   Kordower, J.H., H.K. Le, and E.J. Mufson, *Galanin immunoreactivity in the primate central nervous system.* J Comp Neurol, 1992. **319**(4): p. 479-500.

332. Branchek, T.A., K.E. Smith, C. Gerald, and M.W. Walker, *Galanin receptor subtypes.* Trends Pharmacol Sci, 2000. **21**(3): p. 109-17.

333. Crawley, J.N., *Biological actions of galanin.* Regul Pept, 1995. **59**(1): p. 1-16.

334. Kim, K.Y., M.K. Kee, S.A. Chong, and M.J. Nam, *Galanin is up-regulated in colon adenocarcinoma.* Cancer Epidemiol Biomarkers Prev, 2007. **16**(11): p. 2373-8.

335. Nagayoshi, K., T. Ueki, K. Tashiro, Y. Mizuuchi, T. Manabe, H. Araki, Y. Oda, S. Kuhara, and M. Tanaka, *Galanin plays an important role in cancer invasiveness and is associated with poor prognosis in stage II colorectal cancer.* Oncol Rep, 2015. **33**(2): p. 539-46.

336. Kanazawa, T., T. Iwashita, P. Kommareddi, T. Nair, K. Misawa, Y. Misawa, Y. Ueda, T. Tono, and T.E. Carey, *Galanin and galanin receptor type 1 suppress proliferation in squamous carcinoma cells: activation of the extracellular signal regulated kinase pathway and induction of cyclin-dependent kinase inhibitors.* Oncogene, 2007. **26**(39): p. 5762-71.

337. Berger, A., R. Lang, K. Moritz, R. Santic, A. Hermann, W. Sperl, and B. Kofler, *Galanin receptor subtype GalR2 mediates apoptosis in SH-SY5Y neuroblastoma cells.* Endocrinology, 2004. **145**(2): p. 500-7.

338. Henson, B.S., R.R. Neubig, I. Jang, T. Ogawa, Z. Zhang, T.E. Carey, and N.J. D'Silva, *Galanin receptor 1 has anti-proliferative effects in oral squamous cell carcinoma.* J Biol Chem, 2005. **280**(24): p. 22564-71.

339. Doufekas, K., R. Hadwin, R. Kandimalla, A. Jones, T. Mould, S. Crowe, A. Olaitan, N. Macdonald, H. Fiegl, E. Wik, H.B. Salvesen, and M. Widschwendter, *GALR1 methylation in vaginal swabs is highly accurate in identifying women with endometrial cancer.* Int J Gynecol Cancer, 2013. **23**(6): p. 1050-5.

340. Hagenbuch, B. and P.J. Meier, *Organic anion transporting polypeptides of the OATP/ SLC21 family: phylogenetic classification as OATP/ SLCO superfamily, new nomenclature and molecular/functional properties.* Pflugers Arch, 2004. **447**(5): p. 653-65.

341. Mikkaichi, T., T. Suzuki, T. Onogawa, M. Tanemoto, H. Mizutamari, M. Okada, T. Chaki, S. Masuda, T. Tokui, N. Eto, M. Abe, F. Satoh, M. Unno, T. Hishinuma, K. Inui, S. Ito, J. Goto, and T. Abe, *Isolation and characterization of a digoxin transporter and its rat homologue expressed in the kidney.* Proc Natl Acad Sci U S A, 2004. **101**(10): p. 3569-74.

342. Toyohara, T., T. Suzuki, R. Morimoto, Y. Akiyama, T. Souma, H.O. Shiwaku, Y. Takeuchi, E. Mishima, M. Abe, M. Tanemoto, S. Masuda, H. Kawano, K. Maemura, M. Nakayama, H. Sato, T. Mikkaichi, H. Yamaguchi, S. Fukui, Y. Fukumoto, H. Shimokawa, K. Inui, T. Terasaki, J. Goto, S. Ito, T. Hishinuma, I. Rubera, M. Tauc, Y. Fujii-Kuriyama, H. Yabuuchi, Y. Moriyama, T. Soga, and T. Abe, *SLCO4C1 transporter eliminates uremic toxins and attenuates hypertension and renal inflammation.* J Am Soc Nephrol, 2009. **20**(12): p. 2546-55.

343. Chu, X.Y., K. Bleasby, J. Yabut, X. Cai, G.H. Chan, M.J. Hafey, S. Xu, A.J. Bergman, M.P. Braun, D.C. Dean, and R. Evers, *Transport of the dipeptidyl peptidase-4 inhibitor sitagliptin by human organic anion transporter 3, organic anion transporting polypeptide 4C1, and multidrug resistance P-glycoprotein.* J Pharmacol Exp Ther, 2007. **321**(2): p. 673-83.

344. Okabe, M., G. Szakacs, M.A. Reimers, T. Suzuki, M.D. Hall, T. Abe, J.N. Weinstein, and M.M. Gottesman, *Profiling SLCO and SLC22 genes in the NCI-60 cancer cell lines to identify drug uptake transporters.* Mol Cancer Ther, 2008. **7**(9): p. 3081-91.

345. Ziliak, D., P.H. O'Donnell, H.K. Im, E.R. Gamazon, P. Chen, S. Delaney, S. Shukla, S. Das, N.J. Cox, E.E. Vokes, E.E. Cohen, M.E. Dolan, and R.S. Huang, *Germline polymorphisms discovered via a cell-based, genome-wide approach predict platinum response in head and neck cancers.* Transl Res, 2011. **157**(5): p. 265-72.

346. Gamazon, E.R., R.S. Huang, N.J. Cox, and M.E. Dolan, *Chemotherapeutic drug susceptibility associated SNPs are enriched in expression quantitative trait loci.* Proc Natl Acad Sci U S A, 2010. **107**(20): p. 9287-92.

347. Trifa, F., S. Karray-Chouayekh, Z.B. Jmaa, E. Jmal, A. Khabir, T. Sellami-Boudawara, M. Frikha, J. Daoud, and R. Mokdad-Gargouri, *Frequent CpG methylation of ubiquitin carboxyl-terminal hydrolase 1 (UCHL1) in sporadic and hereditary Tunisian breast cancer patients: clinical significance.* Med Oncol, 2013. **30**(1): p. 418.

348. Holliday, D.L. and V. Speirs, *Choosing the right cell line for breast cancer research.* Breast Cancer Res, 2011. **13**(4): p. 215.

349. Kim, T.M., H.J. Jeong, M.Y. Seo, S.C. Kim, G. Cho, C.H. Park, T.S. Kim, K.H. Park, H.C. Chung, and S.Y. Rha, *Determination of genes related to gastrointestinal tract origin cancer cells using a cDNA microarray.* Clin Cancer Res, 2005. **11**(1): p. 79-86.

350. Lien, H.C., C.C. Wang, C.H. Lin, Y.S. Lu, C.S. Huang, L.P. Hsiao, and Y.T. Yao, *Differential expression of ubiquitin carboxy-terminal hydrolase L1 in breast carcinoma and its biological significance.* Hum Pathol, 2013.

351. Maxwell, G.L., G.V. Chandramouli, L. Dainty, T.J. Litzi, A. Berchuck, J.C. Barrett, and J.I. Risinger, *Microarray analysis of endometrial carcinomas and mixed mullerian tumors reveals distinct gene expression profiles associated with different histologic types of uterine cancer.* Clin Cancer Res, 2005. **11**(11): p. 4056-66.

352. Steward, J.P., E.P. Ornellas, K.D. Beernink, and W.H. Northway, *Errors in the technique of intraperitoneal injection of mice.* Appl Microbiol, 1968. **16**(9): p. 1418-9.

353. Gaines Das, R. and D. North, *Implications of experimental technique for analysis and interpretation of data from animal experiments: outliers and increased variability resulting from failure of intraperitoneal injection procedures.* Lab Anim, 2007. **41**(3): p. 312-20.

354. Miner, N.A., J. Koehler, and L. Greenaway, *Intraperitoneal injection of mice.* Appl Microbiol, 1969. **17**(2): p. 250-1.

355. Kuang, Z., Y. Yao, Y. Shi, Z. Gu, Z. Sun, and J. Tso, *Winter hibernation and UCHL1-p34cdc2 association in toad oocyte maturation competence.* PLoS One, 2013. **8**(10): p. e78785.

356. Hanahan, D. and R.A. Weinberg, *Hallmarks of cancer: the next generation.* Cell, 2011. **144**(5): p. 646-74.

357. Al Kushi, A., P. Lim, C. Aquino-Parsons, and C.B. Gilks, *Markers of proliferative activity are predictors of patient outcome for low-grade endometrioid adenocarcinoma but not papillary serous carcinoma of endometrium.* Mod Pathol, 2002. **15**(4): p. 365-71.

358. Sarafan-Vasseur, N., A. Lamy, J. Bourguignon, F. Le Pessot, P. Hieter, R. Sesboue, C. Bastard, T. Frebourg, and J.M. Flaman, *Overexpression of B-type cyclins alters chromosomal segregation.* Oncogene, 2002. **21**(13): p. 2051-7.

359. Nam, H.J. and J.M. van Deursen, *Cyclin B2 and p53 control proper timing of centrosome separation.* Nat Cell Biol, 2014. **16**(6): p. 538-49.

360. Yin, X.Y., L. Grove, N.S. Datta, K. Katula, M.W. Long, and E.V. Prochownik, *Inverse regulation of cyclin B1 by c-Myc and p53 and induction of tetraploidy by cyclin B1 overexpression.* Cancer Res, 2001. **61**(17): p. 6487-93.

361. Price, J.C., L.M. Pollock, M.L. Rudd, S.K. Fogoros, H. Mohamed, C.L. Hanigan, M. Le Gallo, N.I.H.I.S.C.C.S. Program, S. Zhang, P. Cruz, P.F. Cherukuri, N.F. Hansen, K.J. McManus, A.K. Godwin, D.C. Sgroi, J.C. Mullikin, M.J. Merino, P. Hieter, and D.W. Bell, *Sequencing of candidate chromosome instability genes in endometrial cancers reveals somatic mutations in ESCO1, CHTF18, and MRE11A.* PLoS One, 2014. **8**(6): p. e63313.

362. Clijsters, L., W. van Zon, B.T. Riet, E. Voets, M. Boekhout, J. Ogink, C. Rumpf-Kienzl, and R.M. Wolthuis, *Inefficient degradation of cyclin B1 re-activates the spindle checkpoint right after sister chromatid disjunction.* Cell Cycle, 2014. **13**(15): p. 2370-8.

363. Wolf, F., C. Wandke, N. Isenberg, and S. Geley, *Dose-dependent effects of stable cyclin B1 on progression through mitosis in human cells.* EMBO J, 2006. **25**(12): p. 2802-13.

364. Mc Gee, M.M., *Targeting the Mitotic Catastrophe Signaling Pathway in Cancer.* Mediators Inflamm, 2015. **2015**: p. 146282.

365.   Brito, D.A. and C.L. Rieder, *Mitotic checkpoint slippage in humans occurs via cyclin B destruction in the presence of an active checkpoint.* Curr Biol, 2006. **16**(12): p. 1194-200.

366.   Chow, J.P., R.Y. Poon, and H.T. Ma, *Inhibitory phosphorylation of cyclin-dependent kinase 1 as a compensatory mechanism for mitosis exit.* Mol Cell Biol, 2011. **31**(7): p. 1478-91.

367.   Weaver, B.A. and D.W. Cleveland, *Decoding the links between mitosis, cancer, and chemotherapy: The mitotic checkpoint, adaptation, and cell death.* Cancer Cell, 2005. **8**(1): p. 7-12.

368.   Ganem, N.J., Z. Storchova, and D. Pellman, *Tetraploidy, aneuploidy and cancer.* Curr Opin Genet Dev, 2007. **17**(2): p. 157-62.

369.   Galipeau, P.C., D.S. Cowan, C.A. Sanchez, M.T. Barrett, M.J. Emond, D.S. Levine, P.S. Rabinovitch, and B.J. Reid, *17p (p53) allelic losses, 4N (G2/tetraploid) populations, and progression to aneuploidy in Barrett's esophagus.* Proc Natl Acad Sci U S A, 1996. **93**(14): p. 7081-4.

370.   Schnerch, D., M. Follo, J. Felthaus, M. Engelhardt, and R. Wasch, *Studying proteolysis of cyclin B at the single cell level in whole cell populations.* J Vis Exp, 2012(67): p. e4239.

371.   Schnerch, D., M. Follo, J. Krohs, J. Felthaus, M. Engelhardt, and R. Wasch, *Monitoring APC/C activity in the presence of chromosomal misalignment in unperturbed cell populations.* Cell Cycle, 2012. **11**(2): p. 310-21.

372.   Juillerat, A., T. Gronemeyer, A. Keppler, S. Gendreizig, H. Pick, H. Vogel, and K. Johnsson, *Directed evolution of O6-alkylguanine-DNA alkyltransferase for efficient labeling of fusion proteins with small molecules in vivo.* Chem Biol, 2003. **10**(4): p. 313-7.

373.   Crivat, G. and J.W. Taraska, *Imaging proteins inside cells with fluorescent tags.* Trends Biotechnol, 2012. **30**(1): p. 8-16.

374.   Lewandoski, M., *Conditional control of gene expression in the mouse.* Nat Rev Genet, 2001. **2**(10): p. 743-55.

375.   Gonzalez, G., S. Mehra, Y. Wang, H. Akiyama, and R.R. Behringer, *Sox9 overexpression in uterine epithelia induces endometrial gland hyperplasia.* Differentiation, 2016. **92**(4): p. 204-215.

376.   Daikoku, T., Y. Hirota, S. Tranguch, A.R. Joshi, F.J. DeMayo, J.P. Lydon, L.H. Ellenson, and S.K. Dey, *Conditional loss of uterine Pten unfailingly and rapidly induces endometrial cancer in mice.* Cancer Res, 2008. **68**(14): p. 5619-27.

377.   Jeong, J.W., H.S. Lee, H.L. Franco, R.R. Broaddus, M.M. Taketo, S.Y. Tsai, J.P. Lydon, and F.J. DeMayo, *beta-catenin mediates glandular formation and dysregulation of beta-catenin induces hyperplasia formation in the murine uterus.* Oncogene, 2009. **28**(1): p. 31-40.

378.   Soyal, S.M., A. Mukherjee, K.Y. Lee, J. Li, H. Li, F.J. DeMayo, and J.P. Lydon, *Cre-mediated recombination in cell lineages that express the progesterone receptor.* Genesis, 2005. **41**(2): p. 58-66.

379.   Daikoku, T., Y. Ogawa, J. Terakawa, A. Ogawa, T. DeFalco, and S.K. Dey, *Lactoferrin-iCre: a new mouse line to study uterine epithelial gene function.* Endocrinology, 2014. **155**(7): p. 2718-24.

380.   Contreras, C.M., E.A. Akbay, T.D. Gallardo, J.M. Haynie, S. Sharma, O. Tagao, N. Bardeesy, M. Takahashi, J. Settleman, K.K. Wong, and D.H. Castrillon, *Lkb1 inactivation is sufficient to drive endometrial cancers that are aggressive yet highly responsive to mTOR inhibitor monotherapy.* Dis Model Mech, 2010. **3**(3-4): p. 181-93.

381.   Felicio, L.S., J.F. Nelson, and C.E. Finch, *Longitudinal studies of estrous cyclicity in aging C57BL/6J mice: II. Cessation of cyclicity and the duration of persistent vaginal cornification.* Biol Reprod, 1984. **31**(3): p. 446-53.

382.   Nelson, J.F., L.S. Felicio, H.H. Osterburg, and C.E. Finch, *Altered Profiles of Estradiol and Progesterone Associated with Prolonged Estrous Cycles and Persistent Vaginal Cornification in Aging C578L/6J Mice1.* Biology of Reproduction, 1981. **24**(4): p. 784-794.

383. Lohff, J.C., P.J. Christian, S.L. Marion, and P.B. Hoyer, *Effect of duration of dosing on onset of ovarian failure in a chemical-induced mouse model of perimenopause.* Menopause, 2006. **13**(3): p. 482-8.

384. Lohff, J.C., P.J. Christian, S.L. Marion, A. Arrandale, and P.B. Hoyer, *Characterization of cyclicity and hormonal profile with impending ovarian failure in a novel chemical-induced mouse model of perimenopause.* Comp Med, 2005. **55**(6): p. 523-7.

385. Mayer, L.P., P.J. Devine, C.A. Dyer, and P.B. Hoyer, *The follicle-deplete mouse ovary produces androgen.* Biol Reprod, 2004. **71**(1): p. 130-8.

386. Roelofsen, T., L.C. van Kempen, J.A. van der Laak, M.A. van Ham, J. Bulten, and L.F. Massuger, *Concurrent endometrial intraepithelial carcinoma (EIC) and serous ovarian cancer: can EIC be seen as the precursor lesion?* Int J Gynecol Cancer, 2012. **22**(3): p. 457-64.

387. Zheng, W., S.X. Liang, H. Yu, T. Rutherford, S.K. Chambers, and P.E. Schwartz, *Endometrial glandular dysplasia: a newly defined precursor lesion of uterine papillary serous carcinoma. Part I: morphologic features.* Int J Surg Pathol, 2004. **12**(3): p. 207-23.

388. Bocking, A. and V.Q. Nguyen, *Diagnostic and prognostic use of DNA image cytometry in cervical squamous intraepithelial lesions and invasive carcinoma.* Cancer, 2004. **102**(1): p. 41-54.

389. Huang, Q., C. Yu, X. Zhang, and R.K. Goyal, *Comparison of DNA histograms by standard flow cytometry and image cytometry on sections in Barrett's adenocarcinoma.* BMC Clin Pathol, 2008. **8**: p. 5.

390. Yin, X.Y., L. Grove, N.S. Datta, M.W. Long, and E.V. Prochownik, *C-myc overexpression and p53 loss cooperate to promote genomic instability.* Oncogene, 1999. **18**(5): p. 1177-84.

391. Chauhan, D., T. Hideshima, C. Mitsiades, P. Richardson, and K.C. Anderson, *Proteasome inhibitor therapy in multiple myeloma.* Mol Cancer Ther, 2005. **4**(4): p. 686-92.

392. Kortuem, K.M. and A.K. Stewart, *Carfilzomib.* Blood, 2013. **121**(6): p. 893-7.

393. Chauhan, D., L. Catley, G. Li, K. Podar, T. Hideshima, M. Velankar, C. Mitsiades, N. Mitsiades, H. Yasui, A. Letai, H. Ovaa, C. Berkers, B. Nicholson, T.H. Chao, S.T. Neuteboom, P. Richardson, M.A. Palladino, and K.C. Anderson, *A novel orally active proteasome inhibitor induces apoptosis in multiple myeloma cells with mechanisms distinct from Bortezomib.* Cancer Cell, 2005. **8**(5): p. 407-19.

394. Oerlemans, R., N.E. Franke, Y.G. Assaraf, J. Cloos, I. van Zantwijk, C.R. Berkers, G.L. Scheffer, K. Debipersad, K. Vojtekova, C. Lemos, J.W. van der Heijden, B. Ylstra, G.J. Peters, G.L. Kaspers, B.A. Dijkmans, R.J. Scheper, and G. Jansen, *Molecular basis of bortezomib resistance: proteasome subunit beta5 (PSMB5) gene mutation and overexpression of PSMB5 protein.* Blood, 2008. **112**(6): p. 2489-99.

395. Buac, D., M. Shen, S. Schmitt, F.R. Kona, R. Deshmukh, Z. Zhang, C. Neslund-Dudas, B. Mitra, and Q.P. Dou, *From bortezomib to other inhibitors of the proteasome and beyond.* Curr Pharm Des, 2013. **19**(22): p. 4025-38.

396. Wang, H., Y. Yu, Z. Jiang, W.M. Cao, Z. Wang, J. Dou, Y. Zhao, Y. Cui, and H. Zhang, *Next-generation proteasome inhibitor MLN9708 sensitizes breast cancer cells to doxorubicin-induced apoptosis.* Sci Rep, 2016. **6**: p. 26456.

397. Mattern, M.R., J. Wu, and B. Nicholson, *Ubiquitin-based anticancer therapy: carpet bombing with proteasome inhibitors vs surgical strikes with E1, E2, E3, or DUB inhibitors.* Biochim Biophys Acta, 2012. **1823**(11): p. 2014-21.

398. Nicholson, B., J.G. Marblestone, T.R. Butt, and M.R. Mattern, *Deubiquitinating enzymes as novel anticancer targets.* Future Oncol, 2007. **3**(2): p. 191-9.

399. Lim, K.H. and K.H. Baek, *Deubiquitinating enzymes as therapeutic targets in cancer.* Curr Pharm Des, 2013. **19**(22): p. 4039-52.

400. He, M., Z. Zhou, A.A. Shah, H. Zou, J. Tao, Q. Chen, and Y. Wan, *The emerging role of deubiquitinating enzymes in genomic integrity, diseases, and therapeutics.* Cell Biosci, 2016. **6**: p. 62.

401. Kemp, M., *Recent Advances in the Discovery of Deubiquitinating Enzyme Inhibitors.* Prog Med Chem, 2016. **55**: p. 149-92.

402. Wang, X., M. Mazurkiewicz, E.K. Hillert, M.H. Olofsson, S. Pierrou, P. Hillertz, J. Gullbo, K. Selvaraju, A. Paulus, S. Akhtar, F. Bossler, A.C. Khan, S. Linder, and P. D'Arcy, *The proteasome deubiquitinase inhibitor VLX1570 shows selectivity for ubiquitin-specific protease-14 and induces apoptosis of multiple myeloma cells.* Sci Rep, 2016. **6**: p. 26979.

403. Chen, J., T.S. Dexheimer, Y. Ai, Q. Liang, M.A. Villamil, J. Inglese, D.J. Maloney, A. Jadhav, A. Simeonov, and Z. Zhuang, *Selective and cell-active inhibitors of the USP1/ UAF1 deubiquitinase complex reverse cisplatin resistance in non-small cell lung cancer cells.* Chem Biol, 2011. **18**(11): p. 1390-400.

404. Liu, N., H. Huang, Q.P. Dou, and J. Liu, *Inhibition of 19S proteasome-associated deubiquitinases by metal-containing compounds.* Oncoscience, 2015. **2**(5): p. 457-66.

405. Mitsui, T., K. Hirayama, S. Aoki, K. Nishikawa, K. Uchida, T. Matsumoto, T. Kabuta, and K. Wada, *Identification of a novel chemical potentiator and inhibitors of UCH-L1 by in silico drug screening.* Neurochem Int, 2010. **56**(5): p. 679-86.

406. Mermerian, A.H., A. Case, R.L. Stein, and G.D. Cuny, *Structure-activity relationship, kinetic mechanism, and selectivity for a new class of ubiquitin C-terminal hydrolase-L1 (UCH-L1) inhibitors.* Bioorg Med Chem Lett, 2007. **17**(13): p. 3729-32.

407. Jacq, X., N.M. Martin, L. Smith, J. Harrigan, C. Knights, H. Robinson, Y. Ofir-Rosenfeld, A. Cranston, M.I. Kemp, and S.P. Jackson, *Abstract 1728: Discovery of highly selective DUB inhibitors with in vivo pre-clinical anti-tumor activity.* Cancer Research, 2015. **75**(15 Supplement): p. 1728-1728.

408. Sedlacek, H., J. Czech, R. Naik, G. Kaur, P. Worland, M. Losiewicz, B. Parker, B. Carlson, A. Smith, A. Senderowicz, and E. Sausville, *Flavopiridol (L86 8275; NSC 649890), a new kinase inhibitor for tumor therapy.* Int J Oncol, 1996. **9**(6): p. 1143-68.

409.   Senderowicz, A.M., *Flavopiridol: the first cyclin-dependent kinase inhibitor in human clinical trials.* Invest New Drugs, 1999. **17**(3): p. 313-20.

410.   Phelps, M.A., T.S. Lin, A.J. Johnson, E. Hurh, D.M. Rozewski, K.L. Farley, D. Wu, K.A. Blum, B. Fischer, S.M. Mitchell, M.E. Moran, M. Brooker-McEldowney, N.A. Heerema, D. Jarjoura, L.J. Schaaf, J.C. Byrd, M.R. Grever, and J.T. Dalton, *Clinical response and pharmacokinetics from a phase 1 study of an active dosing schedule of flavopiridol in relapsed chronic lymphocytic leukemia.* Blood, 2009. **113**(12): p. 2637-45.

411.   Lin, T.S., K.A. Blum, D.B. Fischer, S.M. Mitchell, A.S. Ruppert, P. Porcu, E.H. Kraut, R.A. Baiocchi, M.E. Moran, A.J. Johnson, L.J. Schaaf, M.R. Grever, and J.C. Byrd, *Flavopiridol, fludarabine, and rituximab in mantle cell lymphoma and indolent B-cell lymphoproliferative disorders.* J Clin Oncol, 2010. **28**(3): p. 418-23.

412.   Kouroukis, C.T., A. Belch, M. Crump, E. Eisenhauer, R.D. Gascoyne, R. Meyer, R. Lohmann, P. Lopez, J. Powers, R. Turner, J.M. Connors, and G. National Cancer Institute of Canada Clinical Trials, *Flavopiridol in untreated or relapsed mantle-cell lymphoma: results of a phase II study of the National Cancer Institute of Canada Clinical Trials Group.* J Clin Oncol, 2003. **21**(9): p. 1740-5.

413.   Byrd, J.C., T.S. Lin, J.T. Dalton, D. Wu, M.A. Phelps, B. Fischer, M. Moran, K.A. Blum, B. Rovin, M. Brooker-McEldowney, S. Broering, L.J. Schaaf, A.J. Johnson, D.M. Lucas, N.A. Heerema, G. Lozanski, D.C. Young, J.R. Suarez, A.D. Colevas, and M.R. Grever, *Flavopiridol administered using a pharmacologically derived schedule is associated with marked clinical efficacy in refractory, genetically high-risk chronic lymphocytic leukemia.* Blood, 2007. **109**(2): p. 399-404.

414.   Ramaswamy, B., M.A. Phelps, R. Baiocchi, T. Bekaii-Saab, W. Ni, J.P. Lai, A. Wolfson, M.E. Lustberg, L. Wei, D. Wilkins, A. Campbell, D. Arbogast, A. Doyle, J.C. Byrd, M.R. Grever, and M.H. Shah, *A dose-finding, pharmacokinetic and pharmacodynamic study of a*

novel schedule of flavopiridol in patients with advanced solid tumors. Invest New Drugs, 2012. **30**(2): p. 629-38.

415.   Rudek, M.A., K.S. Bauer, Jr., R.M. Lush, 3rd, S.F. Stinson, A.M. Senderowicz, D.J. Headlee, S.G. Arbuck, M.C. Cox, A.J. Murgo, E.A. Sausville, and W.D. Figg, *Clinical pharmacology of flavopiridol following a 72-hour continuous infusion.* Ann Pharmacother, 2003. **37**(10): p. 1369-74.

416.   Thomas, J.P., K.D. Tutsch, J.F. Cleary, H.H. Bailey, R. Arzoomanian, D. Alberti, K. Simon, C. Feierabend, K. Binger, R. Marnocha, A. Dresen, and G. Wilding, *Phase I clinical and pharmacokinetic trial of the cyclin-dependent kinase inhibitor flavopiridol.* Cancer Chemother Pharmacol, 2002. **50**(6): p. 465-72.

417.   Innocenti, F., W.M. Stadler, L. Iyer, J. Ramirez, E.E. Vokes, and M.J. Ratain, *Flavopiridol metabolism in cancer patients is associated with the occurrence of diarrhea.* Clin Cancer Res, 2000. **6**(9): p. 3400-5.

418.   Asghar, U., A.K. Witkiewicz, N.C. Turner, and E.S. Knudsen, *The history and future of targeting cyclin-dependent kinases in cancer therapy.* Nat Rev Drug Discov, 2015. **14**(2): p. 130-46.

419.   Fry, D.W., P.J. Harvey, P.R. Keller, W.L. Elliott, M. Meade, E. Trachet, M. Albassam, X. Zheng, W.R. Leopold, N.K. Pryer, and P.L. Toogood, *Specific inhibition of cyclin-dependent kinase 4/6 by PD 0332991 and associated antitumor activity in human tumor xenografts.* Mol Cancer Ther, 2004. **3**(11): p. 1427-38.

420.   Toogood, P.L., P.J. Harvey, J.T. Repine, D.J. Sheehan, S.N. VanderWel, H. Zhou, P.R. Keller, D.J. McNamara, D. Sherry, T. Zhu, J. Brodfuehrer, C. Choi, M.R. Barvian, and D.W. Fry, *Discovery of a potent and selective inhibitor of cyclin-dependent kinase 4/6.* J Med Chem, 2005. **48**(7): p. 2388-406.

421.   Finn, R.S., J.P. Crown, I. Lang, K. Boer, I.M. Bondarenko, S.O. Kulyk, J. Ettl, R. Patel, T. Pinter, M. Schmidt, Y. Shparyk, A.R. Thummala, N.L. Voytko, C. Fowst, X. Huang, S.T.

Kim, S. Randolph, and D.J. Slamon, *The cyclin-dependent kinase 4/6 inhibitor palbociclib in combination with letrozole versus letrozole alone as first-line treatment of oestrogen receptor-positive, HER2-negative, advanced breast cancer (PALOMA-1/TRIO-18): a randomised phase 2 study.* Lancet Oncol, 2015. **16**(1): p. 25-35.

422.   Beaver, J.A., L. Amiri-Kordestani, R. Charlab, W. Chen, T. Palmby, A. Tilley, J.F. Zirkelbach, J. Yu, Q. Liu, L. Zhao, J. Crich, X.H. Chen, M. Hughes, E. Bloomquist, S. Tang, R. Sridhara, P.G. Kluetz, G. Kim, A. Ibrahim, R. Pazdur, and P. Cortazar, *FDA Approval: Palbociclib for the Treatment of Postmenopausal Patients with Estrogen Receptor-Positive, HER2-Negative Metastatic Breast Cancer.* Clin Cancer Res, 2015. **21**(21): p. 4760-6.

423.   Kawakami, M., L.M. Mustachio, J. Rodriguez-Canales, B. Mino, J. Roszik, P. Tong, J. Wang, J.J. Lee, J.H. Myung, J.V. Heymach, F.M. Johnson, S. Hong, L. Zheng, S. Hu, P.A. Villalobos, C. Behrens, I. Wistuba, S. Freemantle, X. Liu, and E. Dmitrovsky, *Next-Generation CDK2/9 Inhibitors and Anaphase Catastrophe in Lung Cancer.* JNCI: Journal of the National Cancer Institute, 2017. **109**(6): p. djw297-djw297.

424.   Scaltriti, M., P.J. Eichhorn, J. Cortes, L. Prudkin, C. Aura, J. Jimenez, S. Chandarlapaty, V. Serra, A. Prat, Y.H. Ibrahim, M. Guzman, M. Gili, O. Rodriguez, S. Rodriguez, J. Perez, S.R. Green, S. Mai, N. Rosen, C. Hudis, and J. Baselga, *Cyclin E amplification/overexpression is a mechanism of trastuzumab resistance in HER2+ breast cancer patients.* Proc Natl Acad Sci U S A, 2011. **108**(9): p. 3761-6.

425.   Cocco, E., S. Lopez, J. Black, S. Bellone, E. Bonazzoli, F. Predolini, F. Ferrari, C.L. Schwab, G. Menderes, L. Zammataro, N. Buza, P. Hui, S. Wong, S. Zhao, Y. Bai, D.L. Rimm, E. Ratner, B. Litkouhi, D.A. Silasi, M. Azodi, P.E. Schwartz, and A.D. Santin, *Dual CCNE1/PIK3CA targeting is synergistic in CCNE1-amplified/PIK3CA-mutated uterine serous carcinomas in vitro and in vivo.* Br J Cancer, 2016. **115**(3): p. 303-11.

426. NIH Clinical Trials. *A Pharmacologic Study of CYC065, a Cyclin Dependent Kinase Inhibitor, in Patients With Advanced Cancers*. 2017/03/12]; Available from: https://www.clinicaltrials.gov/ct2/show/NCT02552953.

427. Zhang, S., Y. Bao, X. Ju, K. Li, H. Shang, L. Ha, Y. Qian, L. Zou, X. Sun, J. Li, Q. Wang, and Q. Fan, *BA-j as a novel CDK1 inhibitor selectively induces apoptosis in cancer cells by regulating ROS*. Sci Rep, 2015. **5**: p. 13626.

428. Guo, H.M., Y.M. Sun, S.X. Zhang, X.L. Ju, A.Y. Xie, J. Li, L. Zou, X.D. Sun, H.L. Li, and Y. Zheng, *Metabolism and pharmacokinetics of 8-hydroxypiperidinylmethyl-baicalein (BA-j) as a novel selective CDK1 inhibitor in monkey*. Fitoterapia, 2015. **107**: p. 36-43.

VITA

Suet Ying Kwan was born in Hong Kong, October 7 1990, to Hoi Shan Kwan and Suk Chun Cheng. She received her secondary school education at Sha Tin College, Hong Kong, and Queenswood School, UK. In 2008, she entered Imperial College London, UK, and received her Bachelor of Science in Biomedical Science in 2011. In August of 2011, she entered The University of Texas MD Anderson Cancer Center UTHealth Graduate School of Biomedical Sciences, Houston, TX, where she conducted her studies under the guidance of Dr. Karen Lu in the Department of Gynecologic Oncology and Reproductive Medicine.